DEPARTMENT OF ELECTRONIC AND ELECTRICAL ENGINEERING
UNIVERSITY OF SHEFFIELD

MODELLING, CONTROL AND SCHEDULING OF HYDRONIC DOMESTIC HEATING SYSTEMS

THESIS SUBMITTED IN PARTIAL FULFILMENT FOR THE OF DEGREE OF PHD

BY

DANIEL JOSEPH ROGERS

SUPERVISED BY DR. MARTIN P. FOSTER AND PROF. CHRIS BINGHAM

APRIL 2014

Summary

This thesis details an investigation to develop an advanced control methodology for domestic heating systems to reduce energy consumption and improve thermal comfort. Based on the recent emergence of Controlled Radiator Valve (CRV) components, this thesis considers the research, development, application and benefits of a modern control methodology to improve the heating efficiency of domestic dwellings using traditional central heating systems.

A novel domestic heating simulation technique using MATLAB/Simulink is introduced and using this simulation method, the suitability of a range of scheduling routines are investigated with the aim of reducing peak energy demand. It is demonstrated that CRVs when used in conjunction with a *Reverse Modulation* (RM) control technique, represent an opportunity for the downscaling in physical size and heat output of domestic heat sources, reducing material cost and cycling losses of the boiler. If such techniques were adopted on a wider scale, the hourly fluctuation of gas demand could be decreased, reducing the strain on the UK's gas storage capability.

In an effort to increase the effectiveness of any proposed scheduling routines, an advanced control method is introduced namely, Model Predictive Control (MPC) which, along with a novel implement, facilitates more complex control without compromising user friendliness. A key contribution of the thesis is the development of an on-line modelling method, which, in contrast to previously reported techniques, requires no prerequisite knowledge of the thermodynamic behaviour of a given controlled zone and a training period of only 48 hours. Moreover, it is shown that excellent performance is obtained without the normal requirements for measurements of site weather or input from other external sources of weather data, thereby reducing system cost and complexity. The proposed techniques are applied in a controlled zone using a BS EN 60335 oil filled heat emitter, whose input power is closely controlled using a Pulse Width Modulating (PWM) power converter within an instrumented test cell, and also in an occupied dwelling. Results demonstrated MPC can be implemented in a dwelling with minimal perquisite modelling and still achieve superior set point tracking when compared to more conventional solutions resulting in an energy saving of up to 22%.

Moreover, it is proven that only a 20% control resolution is required to achieve effective set point tracking in a heated zone.

Following on, the MPC controller is refined for use with low cost thermic CRVs. The ability of the presented control methodologies to maintain superior temperature regulation despite the use of oversized heat emitters is a key contribution of the thesis. A comparison of techniques is included using experimental measurements from both an oversized oil filled heat emitter within a test chamber, and also from BS EN 442 water-filled heat emitters within an occupied dwelling. Results show the proposed methodologies can be realised using more cost-effective thermoelectric valves, whilst providing superior set point tracking.

Following on, a novel scheduled RM-MPC controller is introduced that utilises the quadratic programming formulation of MPC to prioritise the subdivision of energy supply between heat emitters. A comparison of controllers is included and using experimental measurements a central heat source of less than a quarter of the original design specification is able to achieve required thermal comfort levels in designate areas.

In the penultimate chapter a novel pre-emptive hysteresis controller is introduced. This technique was developed to achieve the required 20% control band suitable for PWM operation and provide a suitable method for interfacing the novel scheduling RM-MPC procedure of distributed heat emitters. The controller is proven to be effective, enabling the temperature of heat emitters (and thus their heat output) to be tightly controlled irrespective of their size and operating temperature of the central heat source.

The work is concluded in the final chapter, where a summary of the achievements of this work is provided in the context of current research. Finally the scope for further work is outlined, suggesting beneficial commercial areas of this research and proposes avenues of further research

A notable omission from this report is the extensive work regarding various modelling techniques and construction of hardware that proved flawed. Only ideas that have contributed positively to the investigation are included.

The work presented in this thesis has been exhibited by presentation at international conferences and publication in learned society journals, details of which are stated below.

Gladwin D, Rogers D, Street M, Sheffield S, Bingham C, Stewart P. Building heating simulation design for control analysis. Modelling and Simulation (AfricaMS 2010) Gaborone, Botswana, 2010, pp. 685–040.

Rogers D, Foster MP, Bingham C. Novel Control Techniques for Wet Central Heating Systems in the UK (poster presentation), All Energy 2011, Aberdeen, Scotland, 2011.

Rogers D, Foster MP, Bingham C. Simulation of a scheduling control scheme for domestic central heating systems in the UK. Applied Simulation and Modelling (ASM 2011), Crete, Greece, 2011, pp. 715–045.

Rogers D, Foster MP, Bingham C. Model predictive controlled domestic dwelling heating system, (poster presentation) All Energy 2012, Aberdeen, Scotland, 2012.

Rogers D, Foster MP, Bingham C. A recursive modelling technique applied to the Model Predictive Control of fluid filled heat emitters, Building and Environment 2013;69, pp. 33–44.

Rogers D, Foster MP, Bingham C. Experimental investigation of a Recursive Modelling MPC for space heating in an occupied domestic dwelling, Building and Environment 2014;72, pp. 356-367.

Acknowledgements

Firstly, I would like to thank my supervisors Martin Foster and Chris Bingham for their invaluable guidance and support throughout this work. In particular their persistence while trudging through the mountains of unintelligible material over the last four years and helping me turn it into a coherent body of work.

My thanks also to members of the Electrical Machines and Drives group, in particular Dan Schofield, Dan Gladwin and Chi Tsang who have provided me with a considerable amount of technical help throughout my time at Sheffield.

Also a special thanks to Liuping Wang of the Royal Melbourne Institute of Technology (Australia), who's invaluable help regarding her publications helped formulate some of my principle ideas.

A further acknowledgement must go to the EPSRC for funding this research and their generous financial support.

Finally I wish to thank my wife Thumri, who has provided unfailing support and encouragement while completing this work. I cannot think of anyone who would be as patient while their house was turned into a test rig.

Contents

Nomenclature

Abbreviation	Description
A	State matrix
A_d	State matrix (digital)
A_e	Augmented state matrix (digital)
B	Input matrix
B_d	Input matrix (digital)
B_e	Augmented input matrix (digital)
c	Specific heat capacity of material
C	Output matrix
C_d	Output matrix (digital)
C_e	Augmented output matrix (digital)
CRV	Controllable Radiator Valve
D	Feed-through matrix
DSM	Demand Side Management
f	Accessibility factor of wall
F	Prediction equation matrix (x)
G_{ob}	Observer gain matrix
G_{cont}	Controller gain
H	Quadratic programing matrix
I	Identity matrix
IE	Integral Error
J	Cost function
k	Discrete point in time
K_{em}	Heat emitter heat loss constant
K_{of}	Heat emitter operating factor
m	Mass

M	Matrix reflecting constraints
MAOT	Mean abstract opening time
MACT	Mean abstract closing time
MEC	Mean Energy consumed
ME	Modelling error
MO	Maximum overshoot
MPC	Model predictive control
MTSI	Mean total solar irradiance
N_p	Prediction horizon
N_c	Control Horizon
P	Power (heat)
P_n	n^{th} heat contribution
P_{em}	Heat contribution of heat emitter
PME	Predicted mean error
Q	Energy
Q_n	n^{th} energy contribution
R	Set point vector
RMSE	Root Mean Squared Error
SF	Satisfaction factor
SPTE	Set point tracking error
t	Time
T	Temperature
T_z	Ambient temperature of zone
T_{em}	Mean temperature of heat emitter
T_{sn}	Temperature of n^{th} surface
TRV	Thermostatic Radiator Valve
U	Input vector
X	State vector
Y	Output matrix
V	Quadratic programming vector

λ	Weighting factor
ΔSP	Set point change
β	Thermal resistance
β_{sin}	Equivalent inside resistance of n^{th} surface
β_{son}	Equivalent outside resistance of n^{th} surface
β_{win}	Equivalent resistance of window in test cell
Λ	Area
Λ_{sn}	Area of n^{th} surface
Φ	Prediction equation matrix (ΔU)
Ψ	Heat loss coefficient
Ψ_{isn}	n^{th} inside surface heat loss coefficient
Ψ_{osn}	n^{th} outside surface heat loss coefficient
γ	Constraint limit matrix
ζ	Thermal capacitance
ζ_a	Thermal capacitance of air within test cell

List of figures

List of tables

Chapter 1. Introduction

Central heating transfers heat from a central boiler to a number of heat emitters using a system of water filled pipes. It is currently the most popular way of heating a house in the UK. In 1970 less than a third of houses in the UK had central heating; by 2001 this had risen to 81% [1]. In 2011, carbon dioxide emissions attributed to domestic sources accounted for 13% of total UK carbon dioxide emissions [2]. Considering the UK's current commitment to cutting carbon dioxide emissions by 26% from 1990 levels by 2020 and 80% by 2050 under the Climate Change Act 2008 [3], domestic central heating is a key area where emissions must be cut.

Since 2006 a Standard Assessment Procedure (SAP) or Energy Rating has been required on all new homes. SAP uses figures from Seasonal Efficiency of Domestic Boilers in the UK (SEDBUK) to calculate energy needed for heating and hot water systems and these figures are used by local authorities in the UK to assess the energy efficiency of buildings. From 2007 the Home Information Pack (HIP) became law requiring any house sold to have a log book detailing the characteristics of the property including the heating services. The department for communities and local government's target that all new homes should be net zero carbon by 2016 [2] is yet another reaffirmation of the UK authorities desire to reduce domestic greenhouse gas emissions. The legal obligation to monitor the energy efficiency of dwellings is the first step to control the emissions generated by them.

Despite these incentives, a survey commissioned by the UK government in 2011 [4] determined that, of the 98% of homes with central heating systems only 49% had the full range of basic controls as defined by the Energy Saving Trust. Even more surprising, nearly 400,000 have no controls at all. At present, the majority of homes (with central heating) feature a central heating boiler, radiators and a controller in the form of room thermostat(s) and/or Thermostatic radiator valves (TRVs).

After formally introducing the concept of thermal comfort, the drawbacks of prevalent heating systems will be first discussed in this work. Following on with specific discussions relating to current technologies, state-of-the-art building control and emerging and possibly disruptive technologies his thesis presents a new type of controller.

The proposed method offers the opportunity for achieving superior thermal comfort while retaining the original heating infrastructure of a dwelling. Compared to prevalent methods, such a controller achieved >20% energy savings. Further development of this new controller enabled energy use to be accurately budgeted by constraining energy input. Such a system will allow householders on limited income to ensure areas of within a dwelling are maintained at safe internal temperatures even during severe weather. Moreover, this enabled the use of a central boiler unit rated at an equivalent 25% of the output power of what would conventionally be used. Furthermore, the installation of smaller boilers have further benefits, including reduced cycling losses and less embedded energy overhead of the units (manufacture, transport and maintenance overheads).

This thesis is confined to the dominant method of space heating in the UK [4], namely using a single central boiler and heat emitters throughout a dwelling controlled by remote thermostats, Thermostatic Radiator Valves (TRVs) or a combination of both.

The remainder of the chapter briefly introduces the concept of thermal comfort and satisfaction and subsequently acts as an introduction to the traditional central heating system. Traditional, current state-of-the art and emerging technologies in the field and the main factors that affect occupant comfort, system performance and efficiency are then discussed.

1.1. Thermal comfort

In an effort to limit the scope of research, direct temperature measurement was favoured as the feed -back metric for the control methods developed in this thesis. For completeness, a brief introduction into the concept of thermal comfort is introduced, including a description of the popular Predicted Mean Vote index for thermal comfort.

1.2. Predicted Mean Vote

According to the American Society of Heating Refrigerating and Air conditioning Engineers (ASHRAE) thermal comfort is defined as “that condition of mind which expresses satisfaction with the thermal environment” [5]. Efforts have been made since the 1970s to quantify this metric and use it within heating systems as opposed to direct

ambient temperature measurement.

Fanger [6] concluded that thermal comfort or user satisfaction was dependant on many factors including clothing, humidity and diet. The research led to the Predicted Mean Vote (PMV) index. The PMV index predicts the mean response of a larger group of people according to the ASHRAE thermal sensation guide (Table 1.1) [6].

hot	warm	Slightly warm	neutral	Slightly cool	cool	cold
3	2	1	0	-1	-2	-3

Table 1.1: ASHRAE thermal sensation guide

$$PMV = (0.003e^{-0.036M} + 0.028)L \qquad (1)$$

Using eqn (1) where L is the thermal load and M is the metabolic rate of the occupants, the PMV index for a given building can be defined. The metabolic rate of the occupants is defined by ASHRAE standards [5] for a range of activities ranging from reclining to bricklaying. The thermal load is defined as 'the difference between the internal heat production within the given heating zone and the heat lost to the environment for a person at comfort skin temperature and evaporative heat loss by sweating at the actual activity level'. The predicted percentage dissatisfied index (PPD) is a measure of the thermal comfort of a group of people at a particular thermal environment. Neutral thermal sensation or a score of zero is the target PMV of any system, plotting PMV against PPD (fig. 1) one may observe that even with a PMV of zero the PPD will still be 5%.

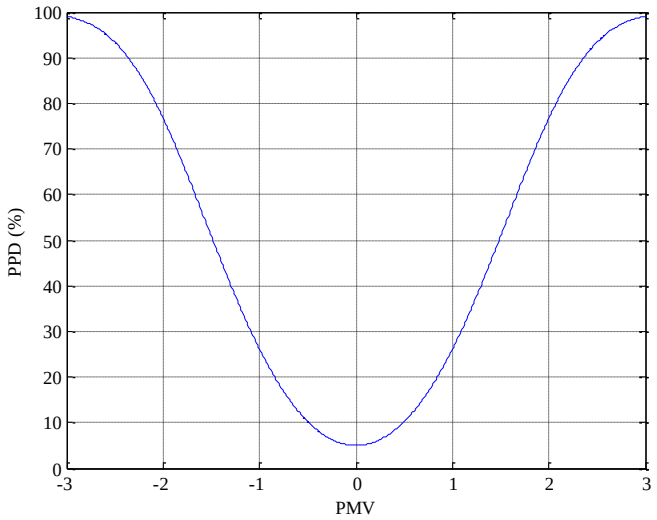

Figure 1.1: Predicted Mean Vote (PMV) vs. Percentage Persons Dissatisfied

There have been attempts at redefining this scale, Van hoof and Hesen [7] found the PMV index was inappropriate for air conditioning systems and promote an Adaptive Thermal Comfort (ATC) measure more suitable for the more moderate climates of the Netherlands (and presumably the UK). Though their measure did not so perform so well when used in combination with a heating system.

Abstract measurement of satisfaction levels such as PMV are becoming more popular for use in gauging thermal comfort particularly in air conditioning controllers [8]. On a smaller scale, such as domestic and smaller commercial premises, ambient temperature is still the principle feedback measurement for central heating systems as demonstrated by the survey in 2011 by the BRE [4]. The following sections introduce the three main subsystems associated with the dominant traditional domestic central heating system topology namely, the control system, the heat emitters and then the boiler or central heat unit.

1.3. Current common control methods

As outlined by Consumer Focus group [9] and further summarised by *theRTK* report commissioned by the DECC in January 2014 [4] there are two typical prevalent heating control devices in the UK. The first is the remote thermostat or roomstat. This consists of a shunted bimetallic strip acting as a switch closing the contacts when the ambient temperature drops below a desired ambient temperature or set point (fig. 1.2a). When

these contacts are closed the heating system (usually the boiler, pumps and valves) are energised. When the zone reaches set point (plus hysteresis band) the contacts are broken, the heating is de-energised and so the zone cools. More recently roomstats that use a temperature sensor and electronic circuit to operate, these do reduce the hysteresis band and are discussed later in this chapter.

Thermostatic Radiator Valves (TRVs) offer localised control within a dwelling. Originally developed by Danfoss in 1943, they control the flow rate into an individual heat emitter and thus the heat output of that heat emitter. This is achieved by a working fluid (liquid or gas) within the head of the valve that expands and contracts over the specific ambient temperature range, pushing a plate or pin, operating the valve. A simplified TRV is shown in (fig. 1.2b).

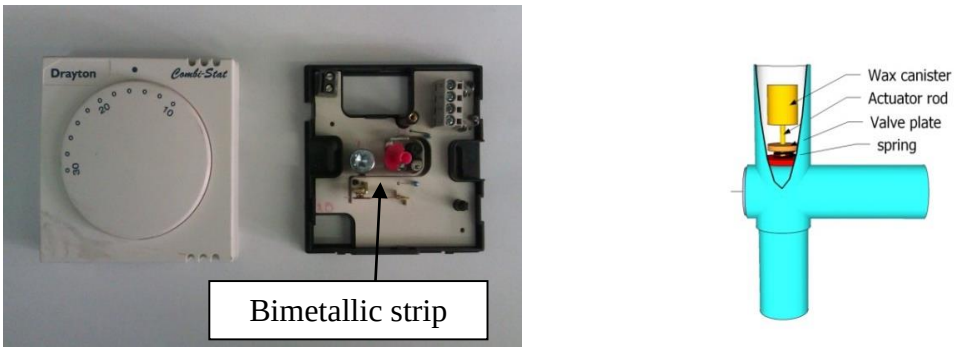

(a) (b)

Figure 1.2: Prevalent heating control (a) BS EN 60730 roomstat (b) Simplified TRV cross-section

The prevailing topology of domestic central heating systems in the UK uses flow and return pipes to every heat emitter, this layout being the statutory instruction for installers [10]. Figures 1.3a and 1.3b illustrate a simplified two heat emitter system using both these roomstat and TRV control topologies that utilise either the roomstat or the TRV.

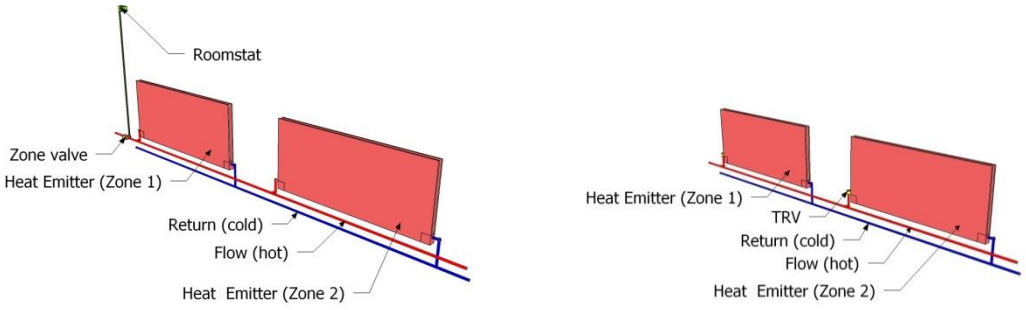

(a) (b)

Figure 1.3: Standard central heating layouts (a) central roomstat (b) individual TRVs

A centrally located roomstat controls a heated zone (fig. 1.3a), operating a valve controlling a group of heat emitters. Using TRVs (fig. 1.3b), each heat emitter is an individual autonomous heat source; if all the TRVs close on the system (at an ambient temperature set point for each zone) the water within the system will not be cooled by the heat emitters (neglecting pipe losses). When the water returns to the boiler at the same temperature as when it left, the boiler's internal thermostat turns the boiler off. The boiler will usually only fire again when an individual TRV opens, cooling the system water.

1.3.1 Limitations of traditional control technologies

The roomstat is usually located in a central location leading to inaccurate temperature control at the extremities of the building. Any regional temperature variations within a house due to extra heating from other sources (solar, electrical devices etc.) or extra temperature loss (due to larger windows, less insulation) are not compensated for leading to overheating (waste of energy) or under heating (poor comfort). Furthermore, they often have a large hysteresis region (often >2°C) in an attempt to avoid the short-cycling of the central boiler unit, however this can lead to unnecessary over-heating [11].

TRVs (particularly the wax based) are essentially a pre-set proportional controller. Considering the enormous variety of physical layout of dwellings such a controller may be miss-tuned for a variety of situations. In particular furniture in close proximity to the TRV may cause a micro-climate leading to misrepresentative feed back and hence poor performance [12].

Research has proved that the localised control offered by TRVs does offer energy savings over the more traditional central thermostat/motorised valve system [13]. TRVs have also gained appeal due to the fact that only a plumber is required to fit the whole system whereas electrical/mechanical control devices require another trade and the associated inconvenience and expense.

The survey conducted by Liao et al [14] found that of all the systems surveyed that used TRVs, 65% of the TRVs were performing poorly. One of the problems is that they failed to reduce the output of the heat emitter when the room was at the desired temperature, as a result the room was over heated and energy was wasted. It became apparent that the occupants did not know how to operate the TRVs. 32% percent of the TRVs were set at "MAX" and more than 65% were found to be set higher than required. It would be valid to state there is less occupancy interest in the energy use of a commercial building as the occupants are not necessarily responsible for energy cost. However it does demonstrate the lack of operational knowledge from building occupants and indicate the possibility that this level of ignorance would carry forth to their own individual dwellings.

1.4. Heat emitters

The heat emitters (more commonly termed radiators) of central heating systems vary in shapes, sizes and mechanical constitution. The heat introduced by the heat emitter to the air within a zone is proportional to the difference between surface temperature of the heat emitter and the zone air (ΔT). The constant of proportionality is the product of the rated output of the emitter and the operating factor. The operating factor compensates for the non-linearity of the heat output characteristic of the heat emitter (fig. 1.4). This operating factor has to be obtained empirically and is stated in the associated literature supplied by the manufacture.

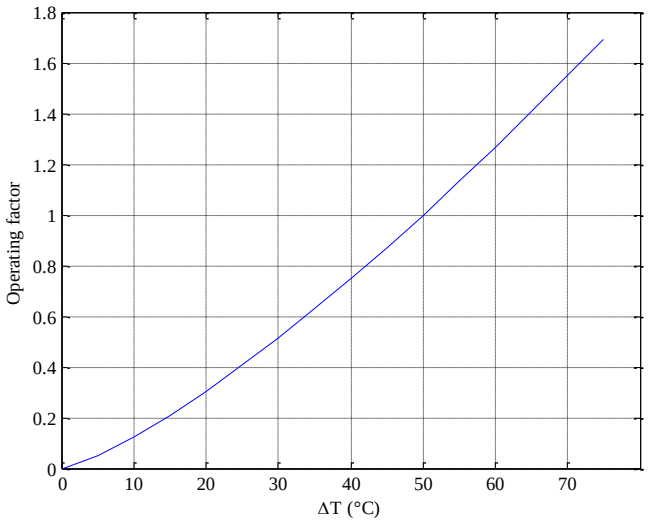

Figure 1.4: Operating factor for the most common steel flat panel heat emitters

The size of a heat emitter is chosen according to predicted heat losses of the zone. Standard heat loss factors for calculating heat losses according building construction that are available from CIBSE/ASHRAE [15] tables are used for predicting these heat requirements.

1.4.1 Limitations of heat emitters

The surveys conducted by Liao et al [14] and Peeters et al [16] determined the size of heat emitter is often selected by evaluating the room size and its use, with no regard for thermal losses. Hence the heat emitter can be oversized if the room has a smaller coefficient of heat loss due to insulation, building fabric etc.

Due to the increased rate of change of ambient zone temperature caused by oversized heat emitters, the ambient temperature profile of the zone oscillates between upper and lower hysteresis bands more frequently. This causes the central heat source to be turned on and off at a greater frequency causing excessive boiler cycling. Excessive boiler cycling leads to greater energy waste associated with frequent starting and stopping of the central heating unit [17].

1.5. Central heat source

The means by which the fluid is heated by the central heat source has certainly progressed and in the 21st century, gas fired central heating boilers dominate the UK heating demography.

1.5.1 Gas central heating boilers

Natural gas is the dominant fuel type used in the UK due to abundant domestic gas reserves from the North Sea in the late 20th century. These are now diminishing, but with so much of the national energy supply infrastructure built around gas supply, and with states such as Norway and Malaysia agreeing to long term contracts to supply the UK [18], gas use for central heating are unlikely to diminish any time soon.

Within the boiler the fuel is burned and the hot gasses are passed through a heat exchanger which heats the circulating fluid being pumped through it. If the rate at which fuel was burned (thus heat output) is controlled the boiler is considered *modulating*, if the boiler has no control over the rate of fuel burned it is a *non-modulating* heat source.

Considering a non-modulating heat source, the circulating fluid temperature (and thus heat emitter output) oscillates according to the heat source thermostat hysteresis band. If the heat supply (from the boiler), is closely matched to heat demand (by the heat emitters), the magnitude of the circulating temperature oscillation will be close to the hysteresis limits of the heat source thermostat. If the heat source is rated at more than the demand (oversized) the circulating fluid's temperature will rise too fast, causing larger oscillations in circulating temperature beyond the hysteresis limits of the heat source thermostat. Such a phenomenon will cause heat emitter temperature to oscillate beyond perceptible comfort levels leading to unnecessary heat output resulting in energy waste.

From 2005 in the UK all new gas fired boilers fitted in domestic (with some minor exceptions) have had to be condensing boilers [10]. These condense the hot waste vapour given off during the combustion process within the heat exchanger to provide additional heat to the circulation fluid. This additional feature contributes to an increase in efficiency that is documented between 10 and 12%.

Modulating boilers offer a method of matching demand to supply. This is now standard on the majority of central heating boilers on the market today and is achieved by adjusting the flow of fuel/air mix that is subsequently burned at the heat exchanger. The majority of domestic condensing boilers adjust this flow by having a variable exhaust speed fan that effectively sucks the fuel/air mix at a variable rate through the combustion chamber for burning. A PID controller is used to enable the fan speed to set the desired circulating fluid temperature, however the rate of burn cannot be turned too low as the stoichiometric (optimum gas air mix) is difficult to maintain at very low fuel/air velocities. The ratio between full rated power output and minimum power output is called the turn down ratio. Commercial units such as the Potterton Sirius (50-100kW) state a turn down ratio of up to 9:1 [19], however for smaller rated domestic boilers (24-32kW) the ratio is nearer 6:1 [20].

Considering a turn down ratio of 6:1 for a typical 24kW boiler unit installed within a typical 3 bedroom house, the minimum power output will be 4kW which in milder weather could still be excessive. On such occasions the boiler will revert to an on/off control method as it is unable to modulate, switching between a hysteresis band to maintain the required circulating fluid temperature. An oversized boiler in non-modulating mode will switch on and off more frequently increasing energy waste attributed to starting and stopping of the heat source. These are termed cycling losses and even on a modern modulating heat source oversizing can lead to a 10-12% increase in energy waste [17]. Moreover, The Johnson boiler company in 2003 [21] found even a boiler with a high turn down ratio will perform worse than one with a low turn down ratio but with an identical output. For example, a 4kW boiler with a 4:1 turn down ration operating at 25% load will perform better than 10kW boiler with a 10% turn down ratio.

Combination boilers exacerbate the oversizing problem as they have to be sized to provide instantaneous hot water which requires a greater output rating (110 % recommended) than is needed to provide heating for the dwelling. Thus the lowest demand a combinational boiler can match is heightened, causing further mismatch between the heat supplied by the boiler and demand from the heat emitters in milder weather.

1.5.2 Oil

Oil fired boiler systems are favoured in areas where the nationwide gas supply network is not present, usually in rural and remote areas. Systems (particularly commercial) that do offer all the same features as gas boilers such as modulating output and condensing heating cycles are available [22]. However, modulating the oil combustion is more difficult due to the associated difficulties in mixing air and oil leading to turn down ratios of less than 4:1. The use of a condensing heat cycle is more difficult too as the condensate from oil combustion are more acidic than from gas requiring the use of more specialised materials within the boiler.

1.5.3 Biomass

Due to environmental concerns and the rise in gas prices, biomass boilers are fast becoming more popular as they offer a renewable heat source. Indeed on a larger scale, the installation of a biomass electricity generation plant at Drax in Yorkshire is key part of the UKs bid to comply with EU renewable sector utilisation laws [23]. In essence they work in principle in an identical fashion to oil and gas fired central heating systems but range in sophistication from a series of water filled pipes that surround an open fire to a modulating, condensing auto feed unit as offered by Windhager [24]. Biomass describes a plethora of fuels including wood logs, pellets, organic sludge, and many more organic materials.

In theory, a basic log burner would have an extremely high turn down ratio as the user can put more or less fuel on as they desire to control the heat output. Unfortunately, this approach to heating control is somewhat labour intensive and for a system of comparable convenience to a gas boiler, wood pellet boilers are usually favoured. With such systems any degree modulation is harder to attain as the fuel is usually in solid form, resulting in low turn down ratios of between 2-3:1 [24]. An alternative of course is to use heavily processed biomass derived fuels that are in fluid form thus increasing efficiency, although their environmental credentials have been called into question by the amount of processing and transportation involved [25].

1.5.4 Heat Pumps

The heat pump is a relatively new technology to the UK but has been widely used mainland Europe, the US and Australasia for more than 20 years and are now being adopted as a central heat source for central heating systems.

The heat pump unit (fig. 1.5) uses a mechanical pump to compress a condensing fluid or refrigerant and so increasing its temperature. The warm refrigerant is then passed through a heat exchanger warming the circulating fluid of the heating system. The refrigerant has now cooled (by exchanging its heat) and becomes a high pressure moderate temperature liquid. After this stage the refrigerant is then decompressed by a metering device (which can be a valve or even a turbine) and passed back to the evaporator (located outside under the ground).

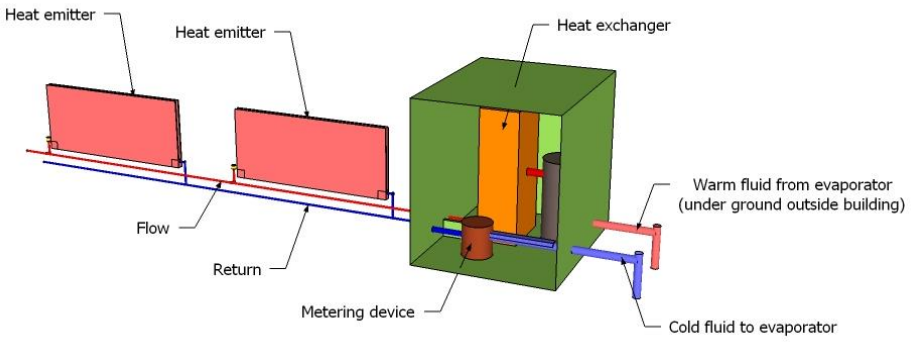

Figure 1.5. Simplified ground source heat pump as central heat source

The heat pump is completely different to other central heat sources as it does not burn a fuel to raise the temperature of the circulating fluid within the heat emitters. Instead the energy input (usually electricity) powers the mechanical pump. The ground source heat pump relies on the principle that ground temperature varies little even in the winter months at depths of around 1-2m in the UK in large parts of the country [26]. In effect, heat from the large amount of fluid at a low level temperature in the evaporator (which is often hundreds of meters long under the ground) is exchanged via the pump and heat exchanger to a small amount of fluid (circulating in the central heating system) at a higher temperature level. The performance of heat pumps is graded by a Coefficient Of

Performance (COP), which is the ratio of heat provided by the system and the energy put in it (mainly powering the pump). A COP figures quoted from leading manufactures such as Mitsubishi and Siemens range between 6-3:1 for ground source heat pumps.

Heat pumps are usually more suited to underfloor heating systems that only require moderate temperatures within their circulating fluid (<50°C). However, if heat emitters are oversized, it has been found that they can be an effective central heat source for a traditional central heating system [27]. As a retro fit device in urban areas ground source heat pumps are somewhat impractical as they need substantial attached land to locate the evaporator. Air source heat pumps that have the evaporator in open air external to the building do solve this problem. Unfortunately, they do not offer the same levels of COP as to raise the cooler outside air to moderate temperatures suitable for heating the circulating fluid requires more energy input to the pump.

1.5.5 Limitations of central heat sources

Research by L.Peeters et al [16] found that boilers are on average oversized by a factor of 50% [16]. By retro fitting insulation, the margin by which the boiler is oversized is further increased. Worst of all the boiler size is relatively unimportant to the installer and is found that the same size boiler is installed in a multitude of buildings regardless of size often for the convenience of the construction company. One of the main design criteria is cost of appliance which varies little between sizes of boiler and whether the system will work. Over sizing is a very primitive (and very inefficient) way of ensuring the system achieves minimum specified performance.

1.5.6 Summary of the traditional central heating system

Clearly, the majority of traditional central hydronic central heating systems in the UK have seen little improvement in their operation over the last 30-40 years. Boiler technology has advanced significantly and condensing boilers with high turn down ratios are in widespread use. Unfortunately the control of the heat emitters themselves in the majority of cases has seen little improvement. Moreover, the uptake of alternative fuel sources is hampered by the lack of development, as gas is still the fuel of choice due to many external factors such as mature infrastructure and plentiful installation and

maintenance support.

The next section addresses current control technology that is available on the open market that offers to improve the traditional central heating system and in particular the control of heat emitters.

1.6. Advanced commercial products

Within the last ten years a multitude of new products suitable for the domestic hydronic central heating systems have been launched. This section summarises the most advanced commercially available hardware designed for the domestic heating system market in the UK.

1.6.1 Programmable thermostats

In essence a programmable thermostat is roomstat with a clock. The user may then program set schedules into the clock according to a set occupancy pattern. Thus the heating is only activated when the building is occupied, preventing unnecessary heating and the wasting of energy. The occupancy schedules are estimated by the user according to his/her habits. Such devices were promoted as energy saving, particularly in the USA. However, more recent work by Malinick el al [28] has found they can use more energy and indeed the U.S. Environmental Protection Agency (EPA) rescinded their EnergyStar© rating in 2009. The EPA has concluded that users were now switching on and off their systems manually when they arrived home to save energy (and money), as opposed to leaving the heating or cooling system on permanently as before. The previous assumed behavioural pattern gave a false high benchmark, thus accentuating any proposed savings.

1.6.2 NEST and other 'learning' thermostats

Nest™ is one of a new breed of 'learning' thermostats (EcoBee™ and BayWeb™ offer others). Using built in motion sensors, Nest™ acquires the occupancy habits of the user(s). After several days 'training' the controller activates the heating system according to these

learnt schedules. Although this system has attracted much publicity in the United States and in Europe [29], the evidence for its energy savings is unclear. Perhaps Nest's most interesting feature is the ability to operate by a vote system of occupant satisfaction as opposed to direct temperature monitoring. Such a scheme enables the heating (or cooling) system to ensure actual thermal comfort as opposed to maintaining a physical measure of ambient temperature.

The Nest's ability to be linked to the user's mobile phone makes the possibility of implementing a predictive occupancy system as proposed by Gupta et al [30]. Nest™ also has Zigbee communications ability (as yet unused), possibly for further integration into other domestic utilities such as lighting. EcoBee™ and BayWeb™ also offer similar capabilities. More recently British Gas have launched their own remote programmable thermostat, HIVE™. At present, no automated occupancy driven control is available with this device.

PreHeat was a system developed and trialled as part of a Microsoft research project [31]. Using a far more comprehensive sensor network around 11 test dwellings in the UK and the USA in 2011, Preheat aimed to predict and learn occupancy levels and adjust schedules accordingly. Furthermore, Preheat used a predictive heating method that forecast the time an HVAC system takes to heat the zone to set point. The measure of the predictive heating method used was called MissTime (defined as total occupied time not at set point) and across two UK homes tested MissTime was reduced by half and also reduced gas usage by up to 18%. Though the authors admit this was more due to preheat being used on a per room basis so it made additional savings by heating rooms individually.

1.6.3 TPI by Siemens

Siemens offer programmable thermostats with the addition of an adaptive PID controller. The method of implementing PID control is by measuring response for each scheduled heating period and tuning the PID controller accordingly. The PID controller modulates the input power level by way of variable duty PWM signal that is sent to the boiler. Such an approach is limited by the maximum cycling rate of the boiler. A cycling rate too frequent (PWM duty cycle too small) will incur excessive wear and start-up losses. However, the PWM duty cycle must be small enough to be analogous to a modulated

power output.

1.6.4 Dataterm™ by Warmworld

The Dataterm™ controller is perhaps the most well know of the new breed of fuzzy logic central heating controllers (PassivEnergy™ and Danfoss™ TP75 are others). The Dataterm™ system can be considered as an advanced programmable roomstat, enabling the user to program the time at which the room is required to be at set point as opposed to setting the times at which the heating is to be activated. Using a conventional programmable thermostat, a fixed *setback* or *preheating* time is chosen manually. *Setback* can be defined as *the period of time in advance at which the heating needs to activate to reach the set point required at the start of the heating schedule*. During extreme cold weather conditions, the heating may take longer to reach set point thus requiring a longer setback time. In more moderate weather the heating would need to be activated much later to achieve the same set point at a given time.

Dataterm™ uses fuzzy logic to 'learn' the heating characteristics of a house and the trends in localised weather conditions. This is achieved by measuring and assessing room temperature and outside temperature during a heating cycle. After a period of 'learning' the system will be able to apply heat for different setback periods before the heating cycle time depending on the outside temperature thus reducing overheating in more moderate conditions and increasing comfort levels in more extreme cold conditions (this is often termed 'weather compensation'). According to the manufacturers it offers up to 25% energy savings [32].

This system is best suited to updating single thermostat dwellings or updating systems with individual zones. However the system does rely on extensive and complicated plumbing (for individual zone control) and requires initial extensive user/installer programming. As noted in the surveys conducted by Liao and later by Peeters [14], [33], most users and installers take little interest in operating and programming heating controls correctly and effectively.

1.6.5 EnergyMaster™ by Total Energy Controls

The Energy Master is another weather compensating central heating programmer incorporating a further innovative feature. Electronic sensors are fitted to the flow and the return pipes of the central heating system, enabling the accurate monitoring of the actual system water temperature, the manufacturer calls this system Variable Thermal Response or VTR. Using this real time data it can *vary the water temperature according to the demand imposed* [34]. The manufacturer claims the extra monitoring and feedback system *reduces the fuel wastage caused through temperature overshoot, heat saturation of the heat exchanger, flue losses and unnecessary boiler cycling, whilst improving internal comfort levels and reducing* CO_2 *emissions*.

The Energy Master is connected in parallel with the switch wires of the roomstat, effectively being able to override the present control system. By monitoring the speed at which the boiler reaches boiler thermostat set point, the unit can assess the demand imposed on the boiler. After a predetermined number of heating cycles the unit will override the roomstat, turning off the boiler at a pre-programmed time (correlated through the measured speed of heating) before demand is reached resulting in reduced overshoot during the heating cycle

1.6.6 The House Heat™ by HouseTech Solutions

The House Heat system is a whole system rather than just a 'bolt on' fuzzy controller. It is a wireless integrated domestic central heating control system that has been available in Germany and Scandinavia since the year 2000 and has recently come on to the market in the UK (probably due to the expiry of a UK patent in 2008). Designed to be installed in conjunction with existing systems that use TRV's it allows easy modification of many traditional heating domestic heating installations.

The House Heat consists of wireless valve actuator heads that can easily replace existing TRV heads. These contain a transmitter receiver unit and an electrically operated drive mechanism that will operate the existing valve and are very similar to systems developed by Honeywell [35]. Within each zone a remote temperature sensor is installed and another

external to the house (measuring outside temperature). Each system component communicates with a central controller. The central controller evaluates the difference between ambient temperature within the zone and the set point, using this deficit an algorithm can be implemented to match heating demand to requirement.

Even if the central heat source is supplying circulating fluid at a fixed temperature the controllable actuator heads can control the flow of circulating fluid through a heat emitter. This allows the heat emitter to operate at a range of temperatures not directly dependant on the heat source output temperature. As a result more sophisticated methods such as PID (which House Heat and the Honeywell version use) are possible. Indeed the Honeywell HR80 valve controllers use a fuzzy logic controller to learn the heating characteristics and apply it as a PWM routine with the valve aiding it to maintain a set point error of within 0.7°C.

It even offers a remote monitoring option where the central controller can be replaced with a PC, enabling remote monitoring and programming.

The advantages of PID over bang-bang control are well known, and the manufactures claim a saving of up to 30% over traditional TRV systems [36], though the specifics of such a comparison test are not revealed. The multi zone control, remote monitoring and programming, and the ease of updating an existing system make the House Heat and other wireless CRV systems a significant advance. However, there are many more advanced methods of control than PID, which have been shown to offer greater efficiency in similar situations (discussed in further chapters). The House Heat in particular requires substantial initial user programming and there is no allowance for priority programming or scheduling of zones.

1.7. Summary of advanced commercial products

So far, the latest control techniques for conventional hydronic central heating systems available on the open market have been examined and discussed. Primarily the focus of improvement has been in enabling more specific operation of individual areas within a dwelling in line with occupancy, with less attention on the actual set point tracking of the actual controllers. Moreover, little regard has been paid to the addressing some of the

largest issues facing existing central heating systems namely, heat source and heat emitter oversizing.

1.8. Current state-of-the-art Heating Ventilation Air Conditioning (HVAC) control research

The pace of HVAC research has quickened in the last two decades due to the economic and environmental drivers mentioned at the start of this chapter. Furthermore with the dramatic increase in processing power available while in parallel its decreasing cost, sophisticated methods and hardware that were the preserve of heavy industry have now become an economic reality on small scale systems.

In particular control methods have become a key area where research is being directed. Dounis and, C. Caraiscos have produced an excellent review of advances in environmental control systems [37]. They conclude adaptability of any advanced control system is the main priority due to the variations of the mechanical make up of building structures and thus their thermal behaviour. Various hybrid fuzzy controllers are proposed as the most practical way of improving heating control when used in conjunction with a Multi Agent Control Scheme (MACS). However, opinion differs across the research community so the main current topics are discussed here.

1.8.1 Distributed Monitoring

Distributed dynamic monitoring techniques for smaller commercial premises and dwellings have been inherited from the commercial building sector. The 'smart building' is now the norm for office blocks and large commercial premises, using environment monitoring system integrated with other services such as the IT networks and security systems to balance environmental conditions with occupancy levels. The opportunities that have arisen from the advent of Wireless Sensor Networks (WSNs) have only multiplied the level of building automation [38]. The smooth integration of such systems still remains one of the main topics of investigation due to the large amount of conflicting products and communication protocols. Using predetermined programs or 'intelligent controllers' that 'learn' the behaviour, a more dynamic approach to HVAC control can be

utilised, only maintaining a habitable environment when necessary and utilising more advanced control methods. Boonsawat et al [39] have designed and installed a temperature monitoring system using the popular now Zigbee IEEE 802.15.4 standard and Baoit et al [40] have proposed an integrated system that utilises distributed sensors within a domestic heating control system. Such a system achieved energy savings of up to 14%.

1.8.2 Fuzzy Logic

As previously discussed basic domestic heating fuzzy controllers are now commercially available and research into different methods of application are on-going. The fundamental parts of any fuzzy logic controller are the rule base and inference mechanism, earlier fuzzy logic controllers (and one would suspect the commercially available products) use a fixed or 'static' rule base. Current research revolves around methods of adapting these two parameters to the very unpredictable conditions within a heated space. Fuzzy logic's ability to handle non-linear systems coupled with the large thermal inertia which are inherent in any HVAC control system make it ideal candidate. Moreover, Fuzzy logic can operate from a rule base, which makes it ideal for integrating to a Predicted Mean Vote (PMV) or satisfaction scale as opposed to a direct control target or set point.

Miriel and Fermanual [41] implemented a fuzzy thermostat in conjunction with a conventional gas fired boiler/valve operated central heating system. The system improved thermal comfort considerably halving the average temperature variation inside the test house, from 2°C to 1°C when compared to conventional bang-bang thermostat control. Sedano et al [42] have designed a fuzzy control scheme for domestic (electric) heaters. The system consists of a central control unit that by using two fuzzy rule sets determines which of the distributed agents (heaters) should be activated. The aim is to achieve thermal comfort while keeping the total power consumption below the Contracted Power Limit (CPL) set by the utility company. Simulation results indicated that the system reduced energy consumption and avoided total power consumption exceeding the CPL for the majority of house layouts investigated. However the system has yet to be tested in hardware form and their research is on-going. Gouda et al [43] have implemented a quasi-adaptive fuzzy heating controller (QUAFLC) that negates the need for the lengthy set up and commissioning procedure for advanced heating systems. A feed-forward neural

network is used to predict indoor temperature and the fuzzy controller evaluates the difference between the predicted indoor temperature and the measured indoor temperature. The real-time implementation of the QUAFLC were compared to simulations of a PI controlled system resulting in reduced overheating of the test room, thus improving thermal comfort and reducing energy consumption. Kolokotsia et al [44] have studied an Integrated Indoor Energy Management System (IEEMS) that uses a set of distributed sensors together with a fuzzy controller. Comparing the fuzzy controller and simple ON/OFF control, the fuzzy controller returned almost 38% energy savings.

More recently Homod et al [45], proposed and simulated an auto tuned HVAC system utilising a Takagi-Sugeno Fuzzy Forward (TSFF) network. This system uses the Fanger PMV/PPD rule base as a feed back mechanism [6]. Using an initial model gained from assessing the mechanical make up of the system, the TSFF is steadily tuned online using a gradient algorithm to enhance the stability of the system. In simulations this scheme achieved a mean PMV of 0.0254 as opposed to 0.1979 offered by the conventional cascaded PID controller. A further variation on this work [46] uses occupancy rates to update the TSFF and implements the system in a simulated residence. Navale et al [47] have used a genetic algorithm to adaptively tune a fuzzy logic controller (AFLC) controlling an educational facility's cooling plant. The AFLC reduced energy consumption by 2-2.5% when compared to the existing PID control system. Soyeguder et al [48] proposed, and simulated, a similar system for tuning parameters of a PID compensation scheme for dampers within a HVAC system, to the effect that negligible steady state error and settling time were achieved.

1.8.3 Artificial Neural Networks

Modelled on the workings of neurons and synapses in the human brain, the artificial neural network combines the weighted influences of inputs to a system via an activation function to give the required output. The measure of influence (or *weight*) of each input is tuned to give the required outputs using a set of predetermined correct inputs and outputs for a set amount of time. The period of time and the data set used for learning is termed the *learning method.* ANNs have found popularity when used in conjunction with energy systems due to their ability to perform well with missing or incomplete input data

during operation. In a practical application such as a heating control system within a dwelling the learning method could be implemented by having a predetermined output requirement (room set point temperature, set by user) and the ANN could record the measured inputs (heat emitter output, neighbouring room temperatures etc.) which satisfy the output requirement. After the period of learning the ANN would have built up a satisfaction model of what input influences and by what weights satisfy the user.

Arigiriou et al [49] tested a Neural Network controller that could be installed in parallel on an existing on/off heating control system, with encouraging results. Overheating caused by solar effects in particular was reduced thus saving 7.5% energy use within their test cell. Within the last decade, research using pure Neural Control in conjunction with heating systems seems to have become less popular. However Jassar et al [50] have incorporated the learning abilities of a neural network and the vagueness interpretation capabilities of fuzzy logic creating a hybrid sensor/modelling device. By using validated simulation the model proved to be exceptionally accurate (0.22°C overall error) and the authors suggest it could be used to create a so-called 'soft sensor' using the boiler parameters to estimate the zone temperature, negating the need for distributed temperature sensors located around the building being heated.

1.8.4 Model Predictive Control

The fastest growing area of research regarding the control of HVAC systems is the use of Model Predictive Control (MPC). The need for individual zone controls due to varying thermal performance throughout a building together with the continuous process nature of the heating problem make MPC the ideal candidate. As a response to this, and other advantages, MPC based strategies are steadily finding favour due to them being able to readily incorporate performance constraints whilst providing optimal (constrained) performance.

Since 2003 there has been over a 10 fold increase in the amount of publications regarding HVAC Model Predictive Control (HVACMPC) within the leading literature. However research related to MPC and the modification of the traditional wet central heating system remains somewhat limited.

Kolokotsa et al [51] have designed and implemented an MPC controller integrated with an existing Building Energy Management System (BEMS). This controller not only operates the heating but other environmental controls such as lighting, and air conditioning. Although the system does prove effective, the paper is vague about any amounts of energy saved by such a system.

Lui et al [52] used an 'intelligent step change in flow-rate' to control the heat output of distributed heat emitters to maintain steadier ambient temperatures when compared to traditional TRV control. Considering a TRV operated heating zone, the proportion of off time to on time gives a measure of the heating demand. Each TRV installed within the system has wireless position sensor communicating with a central control unit. By installing a flow control valve between the boiler unit and the TRV controlled heat emitters, the flow to that zone (and thus the heat supplied to it) can be fully controlled. The opening of the flow control valve is adjusted by the output of a MPC algorithm using the simulation model proposed and the heat demand given by the proportion of on time to off time of the TRV's. A state-space simulation model is needed to predict the likely demand owing to outside temperature and thermal inertia of the building. The results from experimental trials showed that using such a system improved temperature variation (user comfort) by maintaining the ambient temperature within 0.5°C of set point under a range of different weather conditions.

Liao and Dexter [53] have published the development of a control scheme that uses a simplified physical model to estimate air temperature within the zone to predict the optimum amount of heat supplied to the heating system. The control system has three embedded control loops. An inner control loop that is simple ON/OFF control of the boiler according to the difference between its temperature and the set point. An intermediate control loop that uses a conventional PI controller determines the water temperature set point from an estimate of heating system output and the desired heat output. The third and outermost loop uses a discrete time model to estimate room temperature and to predict the output of the heating system needed to maintain the room at set point. By monitoring the temperature of the building for five days, the discrete time model could be 'trained' (the PI controller was tuned using the Ziegler–Nichols method). Even for what could be considered an up to date heating system (TRV controlled heat

emitters and a condensing boiler) the system still achieved a 14% energy saving during real time trials. However the authors conclude the cost of training and tuning the controller is prohibitive for small scale heating such as domestic use.

More recent research focuses on the modelling and algorithms used by the MPC controller, with an emphasis on the real-time identification of system thermal behaviour. In contrast to black box techniques, the heat transfer surfaces within a building structure are represented in terms of a set of physical heat equations. This strategy unfortunately yields a model that can contain many hundreds of states, resulting in requirements for high computational effort for subsequent control purposes. Some progress has been made to incorporate model order reduction, resulting in lumped parameter equivalents [54], [55], though their structure is required to be defined prior to commissioning, which is often considered impractical.

Research by Privara et al has already demonstrated the effectiveness of MPC for HVAC. Their first experience with a real world implementation of an MPC controller [56] applied to an existing heating system within the Czech Technical Institute returned energy savings of between 17% and 24%. The crucial part of the system was the model identification scheme which used subspace methods, i.e. using oblique projections to find the Karman state sequence and then use least squares method to obtain the system matrices. More recently the research group has focused on the acquisition of useful models of buildings on line, Zacekova and Ferkl [57] using a multi-step ahead error minimization approach to model the building. The system achieved a 30% energy saving over the classical rule based controller already in use. Balan et al [58] propose an algorithm that allows the direct use of a non-linear model, in simulations recording a better behavioural temperature profile when compared to classical PID.

Molina et al [59] proposed and simulated a system that incorporated the fluctuation of energy prices into the MPC algorithm (an actual ‘cost’ function!). A genetic algorithm was used to tune the controller to achieve an acceptable trade between energy consumption/cost and thermal comfort. Thermal comfort was defined in terms of PMV/PPD. The system recording significantly lower energy consumption when the MPC algorithm was optimised with cost. When optimised in terms of thermal comfort there was identical energy usage but a significantly higher level of occupant satisfaction.

Most recently, using a traditional central heating system Short [60] proposes a ‘plug and play’ scheme which offers a practical MPC implementation under realistic circumstances (minimal commissioning expertise required). However, although the feasibility of the system is proven, its effectiveness with regards to energy savings and set tracking is unclear. Finally using distributed electrical heaters, Lefort [61] has demonstrated in simulation a hierarchal MPC energy management system enables the cost of electricity use to be halved by the optimisation of the user schedule.

1.9. Summary

The overwhelming majority of domestic and small commercial heating systems use water filled heat emitters. The common theme of the limitations of current systems is over sizing of heat source and emitters and their associated energy waste. As over 80% of homes in the UK have central heating systems using a boiler and water filled heat emitters it would be impractical to suggest a whole new heating method or mechanical system. The aim of this investigation is to implement a system that improves the efficiency of domestic central heating making use of the existing mechanical services.

Within the last decade commercial products have advanced considerably. The gradual progression away from reliance on hysteresis control and towards established superior methods such as PID and Fuzzy Logic has achieved some considerable energy savings and functional performance advancement, though specific figures and analysis substantiating their claims is brief at best. Furthermore, there is no commercial control product that addresses boiler/emitter oversizing which according to surveys [16] is extremely common and extremely wasteful.

From a control perspective, academic research institutions lead the way, implementing a variety of control methodologies achieving documented energy savings of over 30%. In particular, there has been an almost meteoric rise within the last 10 years regarding MPC. Most encouragingly the recent work by Privara et al [62]–[64] and Liao et al [53] demonstrate that energy saving control solutions are possible whilst preserving the main mechanical components of an HVAC system that is nearly 50 years old! However,

research regarding the control of HVAC systems with the aim of reducing the oversizing of boiler is limited.

CRV's have already been proven as an ideal method for interfacing advanced control techniques to existing central heating systems [34]–[36]. Considering proven advanced control methods suitable for older HVAC systems and the lack of research regarding heat source oversizing compensation three key aims evolve. The first is to reduce the effects of central heat source (boiler) oversizing to save used and embedded energy and the second is the implementation of an advanced control algorithm in conjunction with the heat emitters to save further energy. The third is to control heat emitter temperature, allowing the metering of heat supplied to and thus energy used by individual heat emitters. By addressing these three key areas, the efficiency of the ubiquitous central heating system may be dramatically increased in terms of usability and energy consumption.

Following on from the success of the latest research [53], [56], [57], [60], [61], [65]–[71] MPC was chosen as the candidate control method due to its constraint handling properties. In an effort to limit the scope of research and considering the monitoring capabilities of the CRV, direct temperature measurement was favoured as a feedback for all subsequent control methods.

To allow commensurate assessment of subsequent control methods, simulation of proposed methods was deemed essential. There is a plethora of commercial simulation building software packages available, however their ability to allow the user to implement a novel control method within the package can be limited. As the MPC formulation requires a thermal model of the zone it may be controlling, a novel building simulation method using the control package MATLAB/Simulink was devised. Such a novel package would provide insight into the construction of a suitable model for the control algorithm itself as well as being able to assess its performance. The next chapter discusses the merits of available software, current research regarding HVAC simulation and documents the development of a novel simulation method using MATLAB/Simulink.

The format of the thesis is as follows. Chapter 2 details the test equipment used. Chapter 3 details the development of a simulation technique. Furthermore a scheduling scheme that reduced central boiler size requirement is proposed. Chapter 4 introduces a *recursive*

modelling controller and describes its novel application to a test chamber and subsequently an occupied dwelling. Chapter 5 takes the implementation further, incorporating a smith predictor and a refined modelling method to enable the implementation of the controller using inexpensive hardware. Following on, Chapter 6 describes the expansion of the RM-MPC controller that utilises the inherent constraint handling of MPC to implement a priority scheduling method. Finally, chapter 7 details the development of a novel pre-emptive hysteresis controller that aims to operate heat emitters between within a fixed temperature band suitable for low cost thermic valves. Chapter 8 concludes the thesis, providing a summary of the research and indicates the most appropriate direction of further work.

Chapter 2. Experimental test facilities and procedures

2.1. Introduction

This chapter describes the two main experimental test facilities employed throughout the work. The first test facility (test cell) was constructed to enable the validation of a control system developed through simulation proposed in Chapter 3. Subsequently, the test equipment (instrumentation) used within the test cell was expanded to create a flexible monitoring system within an existing dwelling which formed the second test facility. By monitoring an existing occupied dwelling, a more realistic appraisal of the effectiveness of a simulation and subsequent control techniques could be obtained.

This chapter begins by introducing the temperature monitoring and control systems developed as part of this work. Following this a low-cost pyranometer is described that allows solar radiation (insolation) to be measured and accounted for in the experiments. Finally, the test cell and test dwelling on which the experimental work is based are described. This information is provided to give the reader an understanding of the number of measurements required and the complexity of the control systems involved.

2.2. Remote temperature monitoring system

A temperature monitoring system was required to ascertain the performance of proposed control methods in this thesis. In the short term it was required to measure ambient and heat emitter temperature. In later chapters it was to be adapted as a wireless controller too. A wireless temperature monitoring system was chosen from the outset of the testing process. Wireless communication was deemed necessary as the priorities required for future installation within an occupied dwelling (chapters 4-6) were ease of installation, reduced aesthetic penalties and lack physical intrusion within the living space.

Following on from Boonsawat [39], Varchola [72] and numerous commercial examples of ZigBee home sensor applications [73], [74], the XBee wireless modem was chosen as a basis for the majority of data gathering and control devices developed during this work. The main capabilities that make the XBee modem suitable for this application are listed

below:

1) Comprehensive technical support from the manufacture and research communities alike.

2) Ease of integration via a serial port enabling a very flexible approach regarding integration with PC's and various software languages.

3) Ease of configuration for sleep mode thus enabling reduction in power consumption.

4) Microcontroller embedded within the modem module allowing direct measurement of voltage without requiring external microcontroller

5) PWM output capability, enabling the module to act as a wireless controller interface.

The XBee communication protocol is a derivative of the Zigbee/IEEE 802.15.4 standard which is widely used in HVAC automation systems in commercial applications [75]. Indeed, the more advanced (and expensive) XBeeSeries 2® and XBeePRO® modems use the standard Zigbee protocol and can facilitate a mesh network topology, enabling in theory, infinite transmission distances. However, due to the short transmission ranges required within a typical dwelling (<30m) and cost considerations, XBeeSeries 1® modems arranged within a star network was deemed a more suitable network system topology. A functional description of the temperature monitoring transmitter device and receiver/data logger set up is provided in the next section.

2.2.1 Transmitter/temperature sensor

Examining the system suggested by Boonsawat in more detail [39] the use of ancillary microcontroller boards was deemed unnecessary for this particular application. The XBee series 1 modem has an inbuilt Freescale® microcontroller, allowing the modem to have a range of configurable outputs including up to 5, 10bit ADC inputs. With no ancillary microcontroller the unit cost of each transmitter/sensor was substantially reduced. Furthermore, following on from commercial products (for example, the Honeywell CT2700) thermistors were chosen as opposed to thermocouples as the temperature measurement transducer. This decision further reduced the number of ancillaries (i.e. no

requirement for thermocouple amplifier circuit) reducing the cost and complexity of the system. Attached to the central transmitter unit, are removable temperature probes.

Each probe consists of a length of twisted pair (CAT5) cable with the temperature transducer (thermistor) mounted at one end. At the other end of the probe, a JR1822 (2.5mm diameter) male connector plug is mounted, allowing easy removal and storage of the probe. Each transmitter unit can support up to three probes via JR1822 female connectors allowing the simultaneous measurement of three separate temperatures. The transmitter also features power supply socket (JR1821, 2.1mm diameter) allowing connection to a battery or a small DC power supply. The transmitter sends three temperature measurements (10-bits) every two seconds entering sleep mode in between to conserve power. Each transmitter circuit was encased using a standard 87mm x 147mm x 32mm BS 4662 surface mounting socket box. These were chosen as they are impact resistant and aesthetically unobtrusive.

An ASUS EeePC Netbook running Ubuntu/Linux operating system was employed as the data logging system with dedicated Application Programming Interface (API) software reading the serial port and recording the data to a text file. The receiver consists of an XBee modem module installed within an appropriate breakout board and FDTI serial to USB converter cable.

A photograph of the complete temperature monitoring and recording system is shown in fig. 2.1, related circuit diagrams and detailed mechanical specifications of the transmitter units are included in Appendix I.

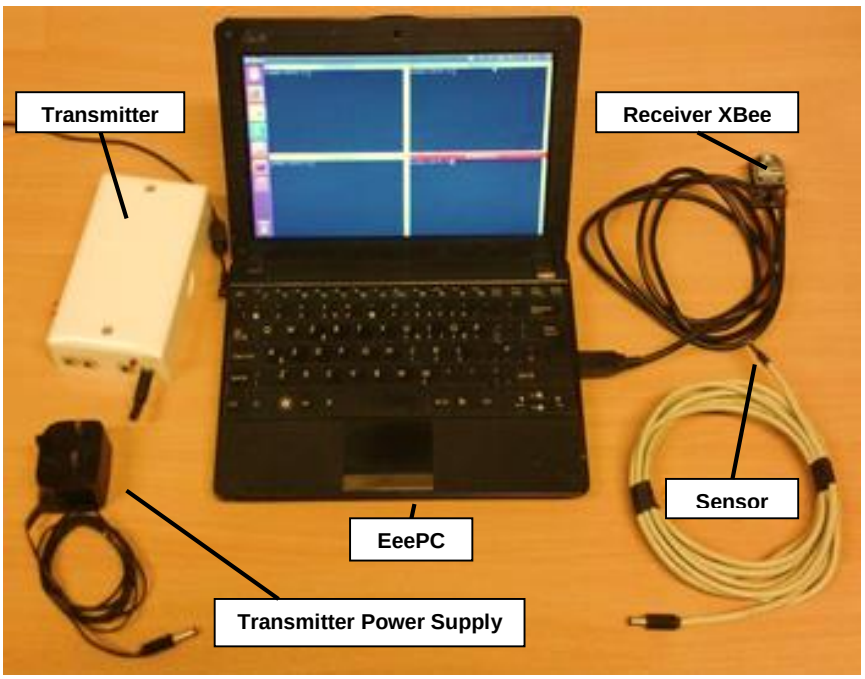

Figure 2.1: XBee based temperature monitoring system

2.3. XBee API

During the development of the remote monitoring system the Series 1 XBee modem's open source Python API [76] was found to be too unreliable and so a bespoke C/C++ XBee API was written. Furthermore, by using C/C++, there was now a future capability for the easy integration of the API within a microcontroller. Such a process would allow the dispensation of the PC in favour of a dedicated embedded system and possibly ease the path of commercialisation of any future controller. Another advantage of C++ is that the serial communication libraries are mature and well tested in commercial applications ensuring reliability of the system.

2.4. Control system framework

The control software framework was developed in a number stages based on a series of sample experiments. For initial monitoring purposes and during the first stages of control system implementation dedicated software would be needed for the recording and display of data. In the medium term this software was adapted for controller implementation. Thus MATLAB or a compliant alternative was needed to enable fast prototyping and implementation of advanced control algorithms. In the long term, once the desired

controller was chosen and tuning parameters and/or methods were known, the whole system could be made in a hardware compatible platform.

The subsequent software framework was largely dictated for the need for a stable and reliable system that could run unmaintained and unattended for several months. Thus, the Ubuntu LTS 10.04 (Long Term Support) operating system was chosen for the short to medium term testing and monitoring. Owing to the nature of this Linux derived operating system the use of MATLAB was deemed unnecessary as the code compliant open source alterative, Octave [77], was freely available that shared much of MATLAB's syntax and functions Henceforth, during the trials detailed in chapter 3,4 5 and 6 it was only necessary to develop the XBee serial class (functions). The operation of the XBee modems could now be operated by Octave software via a 'pipe'. The 'pipe' allowed Octave to operate using data received from the XBee modems but required no further specialised instrument control software to be written specifically for Octave. By separating the basic XBee packet dissemination software and the mathematical/control software, the standard mathematic functionality of Octave could be preserved, simplifying modification and updating of proposed control methods. The software structure developed for this work is shown in fig. 2.2, illustrating the clear distinction between the packet dissemination software (C++) and the mathematical control and recording software (Octave).

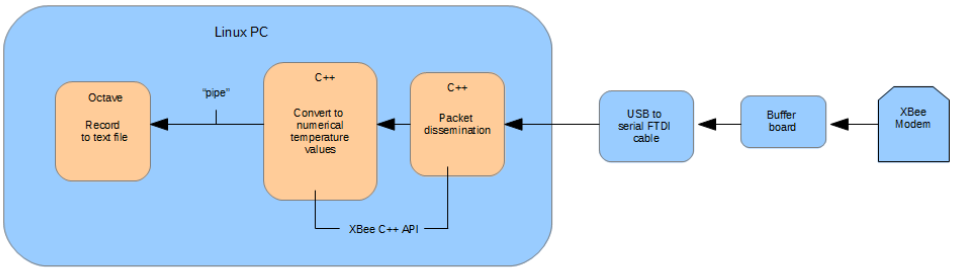

Figure 2.2: XBee software structure

The other associated hardware requirements are also illustrated in Fig. 2.2 namely the FTDI cable and Buffer board. The buffer board is required to enable the Modem to be connected to the FTDI cable, which serves to convert the native RS232 output of the modem to USB communications protocol suitable for the Linux operated PC.

2.5. Wireless controller

Initially only a monitoring and data logging capability was required for the tuning and validation of the simulation models, however, to fully evaluate the proposed heating control algorithms a remote controlled power/heat source was necessary.

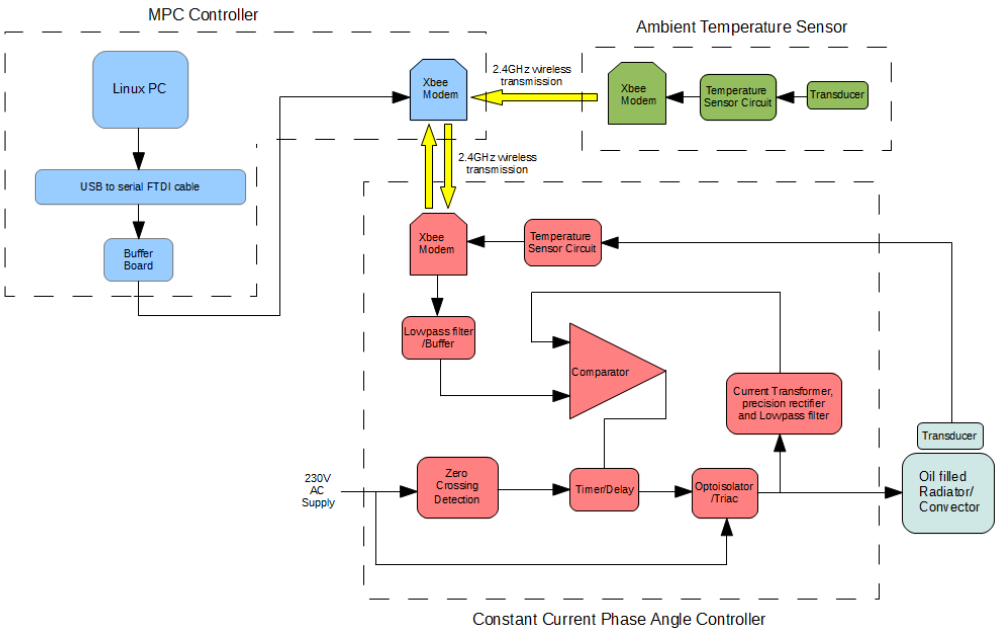

Figure 2.3: Test cell monitoring and control system

A wireless phase angle controller (PAC) circuit was developed to allow the temperature of an oil filled radiator to be accurately controlled. As can be seen from fig. 2.4, the PAC connects to a heating device via a standard 13 amp 3 pin socket and uses a triac circuit to regulate the current through the heater which is sensed using a current transducer. The PAC unit provides additional temperature measure connections for monitoring of ambient temperature too. Furthermore, PAC unit could act as constant current source as it used a comparator circuit to enable the current output to be matched to a pre-calibrated input. A system diagram of the phase controller within the control system as used in the test cell is detailed in fig 2.3 and the complete unit is illustrated in fig. 2.4. The associated circuit diagram of the phase angle controller units is included in Appendix I.

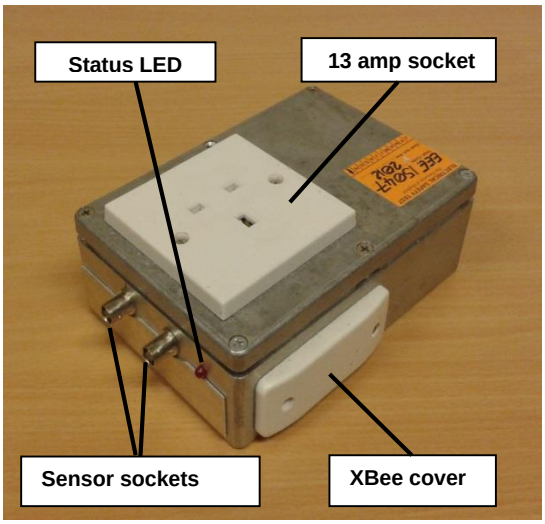

Figure 2.4: XBee operated phase controller

2.6. Microcontroller based wireless control unit

The wireless central control unit controller used consisted of an Arduino MEGA prototyping board with an Arduino Ethernet shield mounted on top. This topology allowed remote access to the recorded data and created a stand-alone data recording system utilising the SD card interface of the Ethernet shield. To save space its XBee Series 1® Modem was mounted on a bespoke break-out board PCB. This method of product development is particularly common using this family of microcontrollers has substantially contributed to the success of the Arduino platform [78]. The prototype microcontroller based datalogger/controller is illustrated in fig 2.5.

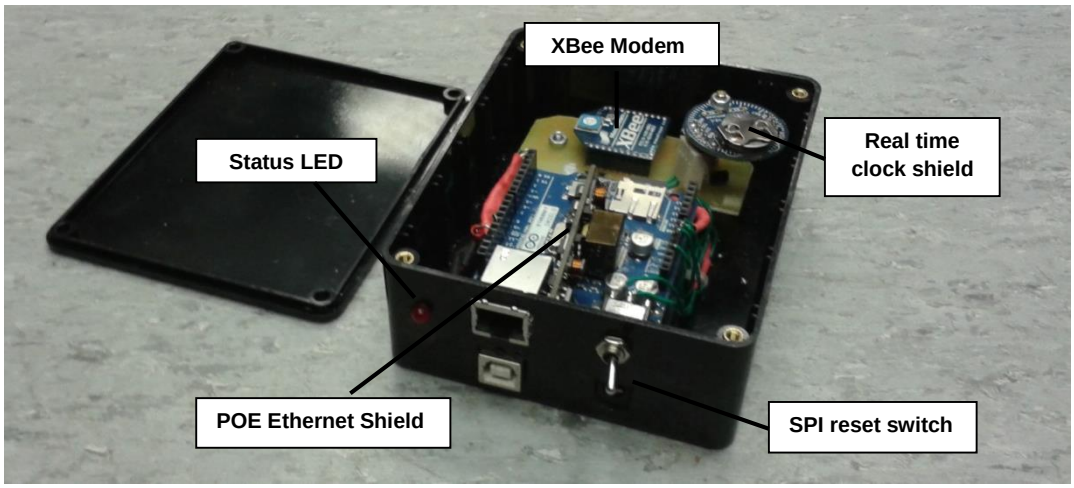

Figure 2.5: Microcontroller based heating controller

2.7. The Low Cost Pyranometer (LPC)

Many advanced HVAC techniques reviewed in chapter 1 rely on measurement of external weather conditions and in particular solar irradiation measuring devices. Within the field of advanced HVAC research solar irradiance is usually only monitored to explain any aberrations in what otherwise would be expected results [43], [69]. Such devices are rarely used to provide a direct contribution to the control system. Thus in line with previous research, only an indication of the prevailing trend of total solar irradiance at a particular time was required for this work.

Traditionally pyranometers use a sensing plate that is constructed from highly thermal conductive material [79]. The plate's temperature is measured and during hours of sunlight the sensing plate absorbs solar radiation warming the plate. The sensing plate is covered by a single or several glass dome(s) is to prevent the effects of convection on the sensing plate. Material composition of the dome, plate and temperature sensors (thermocouples) are chosen as to give a response proportional to thermal irradiance falling on the sensor plate.

More recently, more economical pyranometers have been developed using photodiodes. The sensing element (the photodiode) is easier to interface and the constituent parts do not require such precision manufacture (no glass dome). Indeed one such system by

Martinez et al boasts similar capabilities but at a tenth of the cost of the traditional glass dome type [80]. Sengupta in 2012 produced a comprehensive evaluation of these lower cost devices vs the traditional thermopile based pyranometer [81] determining that regular calibration is required to assimilate the response of both devices. A further important point is that even COTS photodiode based pyranometers still cost hundreds of pounds [80] and although this is a far more proportional cost, an advanced HVAC system having a key part of the system that is disproportionately expensive to other key sensors is far from ideal.

It is known that particular acrylic polymers have a flat spectral transmission between 300 and 2800 nm, which is the requirement (ISO 9060) for the types of glass usually used for COTS equipment that rely on the heating plate principle [79]. Such UV degradation-resistant acrylic is now widely available. Considering the greater ease of machining and polishing of this thermoplastic material, acrylic as opposed to a glass dome was chosen for the inexpensive pyranometer.

2.7.1 Inexpensive pyranometer construction

Following on from traditional pyranometer construction [79] but using more economically viable materials, a dome and sensor plate topology was chosen. The dome was formed from acrylic and measured 100mm in diameter. The thermal sensor consists of a circular copper plate that is machined to 70mm in diameter, 0.5mm thick thermally bonded to a thermistor. This size is the largest the plate can be without excessive diffusion of incident radiation on the plate caused by the ‘misted’ edges of the dome at low angles of sunlight. The plate also has to have of a diameter as great as possible (to capture maximum solar radiation) and be as thin as possible (to have the fastest rate of change of temperature in reaction to solar heating). To allow successful bonding of a thermally reactive device there is also a minimum thickness requirement.

This bead thermistor also defined the thickness of the copper plate as after several trials 0.5mm was the thinnest plate to be successfully bonded thermally to the thermistor without distorting the plate. The plate was sprayed matt black to enable maximum solar energy absorption.

The same Vishay NTC 4K7Ω thermistor as used for the wireless temperature monitoring system described in section 2.2 was bonded to the copper plate for temperature sensing. This allowed the use of identical pseudo-C software to determine temperature of the plate using an ATMEL328 based microcontroller prototyping board. The pyranometer is illustrated in figure 2.6.

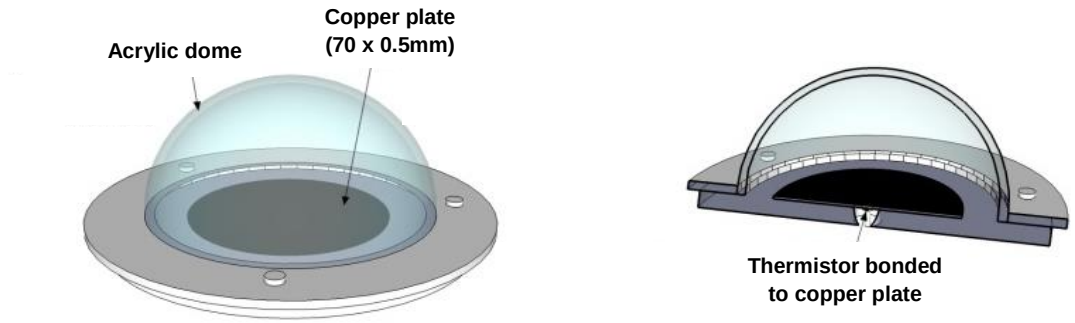

Figure 2.6: Low cost pyranometer

Before the proposed low-cost pyranometer could be used, it was calibrated against a commercial COTS Delta T SPN-1 mounted on the roof of Hicks building, University of Sheffield. Using the relationship between the two, the insolation at a different location (Sir Frederick Mappin Building, University of Sheffield) can be inferred. Although the data from the Delta T SPN-1 would possibly give a reasonable approximation of insolation at the location of the Mappin Building, the considerable distance between the two (>500m) could render such approximations inaccurate. Furthermore, the test cell was located in a sheltered location. Thus in the winter months, this location receives inconsistent levels of sunlight due the shading offered by the surrounding Mappin/Broad lane building complex when the sun is at a low level of elevation.

To obtain a measurement representing the elevation in temperature of the copper plate due to solar irradiance, an ambient shade temperature was required. A polycarbonate 100mm diameter tube was mounted below the first pyranometer, where an additional temperature sensing thermistor was mounted out of direct sunlight. The second pyrometer would use the external shade temperatures using a sensor mounted at 1.5m on the North East side of the Test Cell.

2.7.2 Low cost pyranometer modelling/calibration

The following section describes a simple mathematical model to allow calibration of each LPC.

The law of specific heat capacity describes the change in temperature (ΔT) of common materials due to their physical properties and is defined as *the amount of heat required to change a unit mass of a substance by one unit of temperature* [90]. The product of mass and specific heat capacity (mc) is referred to as thermal mass.

$$Q = mc\delta T \tag{2.1}$$

If one divides (2.1) with respect to time (s) passed, (2.1) becomes (2.2) whereby the rate of change of material temperature being heated is represented in terms of power introduced to it.

$$\delta T = \frac{Q_n}{mc} \Rightarrow \frac{\delta T}{dt} = \frac{Q_n}{mcdt} \Rightarrow \frac{\delta T}{dt} = \frac{P_n}{mc} \Rightarrow \frac{dT}{dt} = \frac{P_n}{mc} \tag{2.2}$$

Considering the heated material in terms of gains and losses, the specific heat capacity and mass can be combined to form a single thermal capacitance ζ_{disk}, (2.2) can subsequently be split becoming (2.3).

$$\frac{dT_{disk}}{dt} = \frac{P_{net}}{mc} \Rightarrow \frac{dT_{disk}}{dt} = \frac{P_{solar} - P_{loss}}{\zeta_{disk}} \tag{2.3}$$

Finally, two assumptions are made. The first neglects the thermal effects of the acrylic dome and air within the pyranometer. The second assumes the heat loss of the disk is directly proportional to the difference between its temperature and the air surrounding it (with the constant of proportionality being thermal conductance, U_{disk}). Taking account of these assumptions, the rate of change of temperature of may be considered as a 1st order differential equation as represented by (2.4). Note thermal resistance is represented by $\beta_{disk.}$

$$\frac{dT_{disk}}{dt} = \frac{\overset{Heat\ gain}{P_{solar}} \overset{Heat\ loss}{\overbrace{-U_{disk}(T_{disk} - T_{shade})}}}{\zeta_{disk}} \qquad \text{Where, } U_{disk} = \frac{1}{\beta_{disk}} \qquad (2.4)$$

The solar irradiance can be divided by the area of the disk to obtain a value of actual solar heat introduced to the disk (P_{solar}).

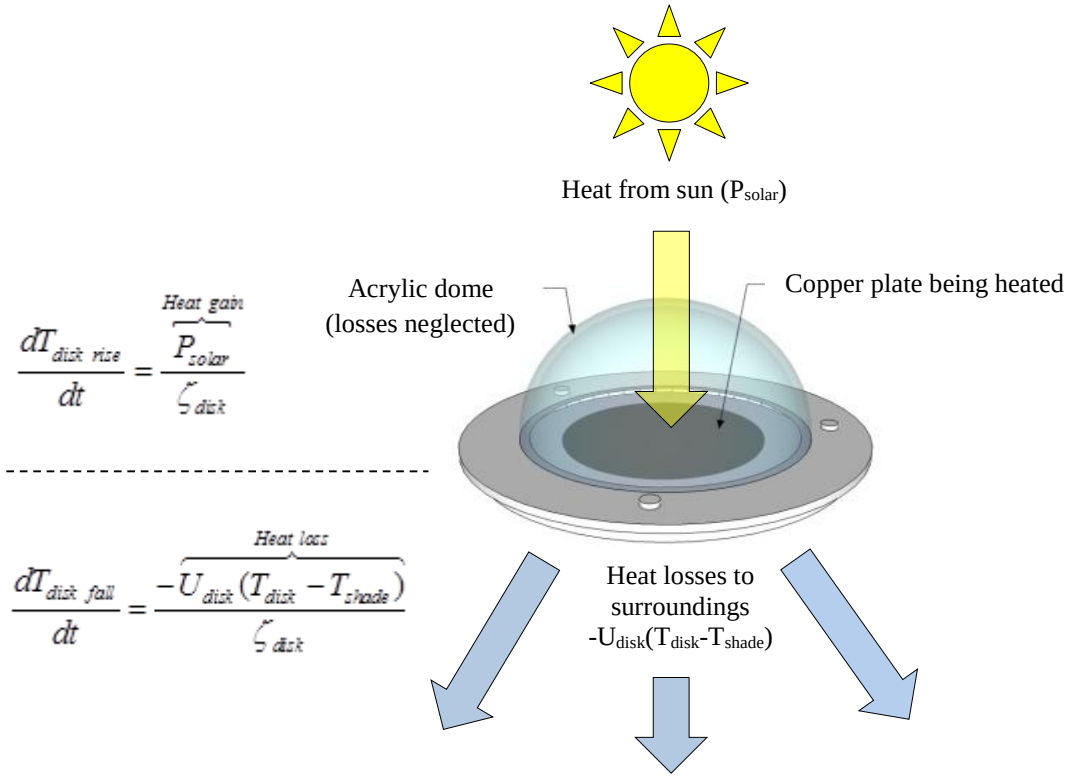

Figure 2.7: LCP in terms of net temperature change

During the week 10/1/12 and 17/1/12 the LCP was calibrated and its performance assessed by assimilating the LCP to the differential equation defined by (4). Using measured temperatures of the metal disk and shade (T_{shade} and T_{disk}) and recorded values of solar irradiance using the DELTA T SPN-1, the values of β_{disk} and ζ_{disk} may be found by employing a modified branching search method described in appendix II.

The values of β_{disk} and ζ_{disk} that returned the lowest Root Mean Square Error (RMSE) between measured and simulated response were β_{disk} = 3.3 $m^2°CW^{-1}$ and ζ_{disk} = 0.7 $J°C^{-1}$. These gave a RMSE of 0.23°C between the response of the LCP and the COTS device (Delta T SPN-1) response is shown in fig. 2.8.

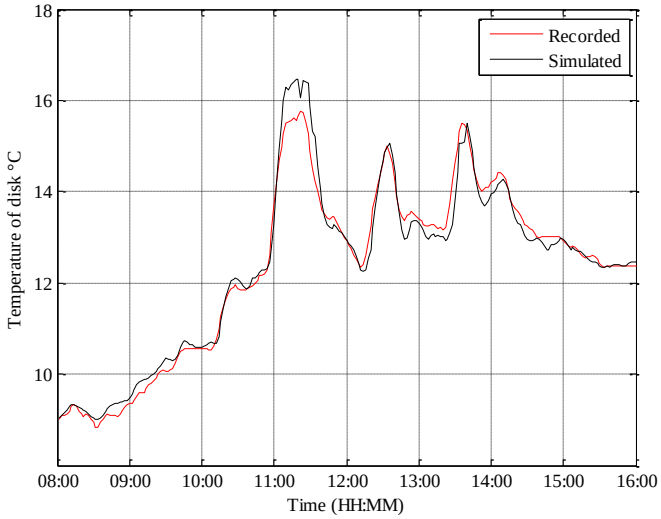

Figure 2.8: Comparison of recorded and calibrated disk temperature (10/02/12)

By feeding these obtained values of β_{disk} , and ζ_{disk} back into the model, the LCP demonstrates commensurate response as shown in fig. 2.9.

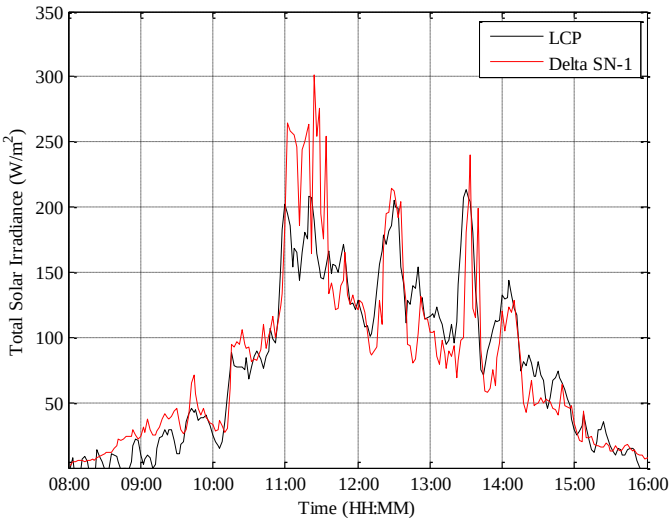

Figure 2.9: Comparison of LCP and COTS pyranometer (10/02/12)

Continuing the calibration process, the pyranometer was monitored for 52 days between the 10/1/12 and 13/3/12. Using these results, the branching algorithm was employed to find appropriate values of β_{disk} and ζ_{disk} for each day. A summary of results is illustrated in fig. 2.10.

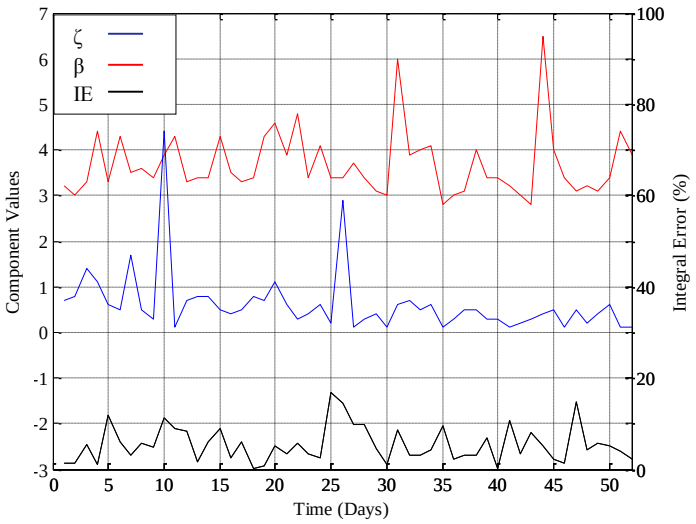

Figure 2.10: Summary of calibration accuracy (10/01/12-13/03/12)

The results illustrated in fig. 2.10 demonstrate that the values of β_{disk} and ζ_{disk} are consistent (β_{disk} between 3 $m^2°CW^{-1}$ and 4 $m^2°CW^{-1}$) and (ζ_{disk} between 0 $J°C^{-1}$ and 2 $J°C^{-1}$) except for 4 distinct points on days 10, 26, 31 and 44. The mean Integral Error (IE) between best fit simulation and recorded results (as in fig. 2.8) was <6% with a standard deviation of 3.9%. The relatively low standard deviation value in comparison to the mean demonstrates the consistency of the 1st order differential equation model and that it offers a valid representation of the pyranometer. If one discounts the extreme points, the mean values of β_{disk} and ζ_{disk} are 3.6 $m^2°CW^{-1}$ and 0.5 $J°C^{-1}$ respectively. The model may be simulated using recorded disk and shade temperatures thus emulating what the LPC could measure if using these calibration values. A summary of these results is illustrated in fig. 2.11, including the RMSE and integral error. The first provides a measure of curve fit or instantaneous accuracy at a given point in time, the second a represents a measure of accuracy regarding an overview of solar irradiance for a given day. The ideal values generated of β_{disk} and ζ_{disk} are illustrated too.

Examining to the extreme RMSE values (instantaneous error) recorded on days 10 and 26, it is clear from fig. 2.10 and fig. 2.11 the 1st order model using the mean values of β_{disk} and ζ_{disk} is still valid for determining the overview of solar irradiance. For each of those days the IE error is still within 15%. On the remaining occasions (days 31 and 44) the cause of extreme values of β_{disk} is due to little (or if any) temperature difference occurring during lower levels of solar irradiance. On such occasions the measurement of

temperature is extremely susceptible to noise given the low cost microcontroller used. However, in this specific situation, such aberrations are not of concern as a low level of solar irradiance presents a situation where little disturbance from solar effects to the heating control system will occur.

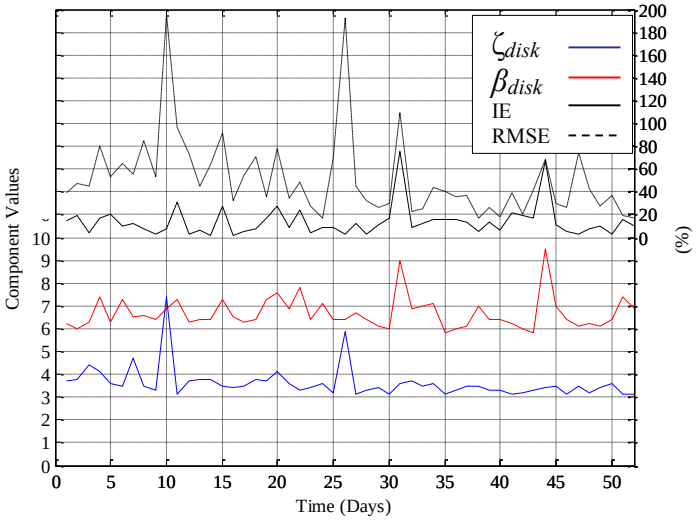

Figure 2.11: Summary of LCP accuracy using mean calibration values (10/01/12-13/03/12)

From a practical point of view, such a device would have an automated calibration process, and it is clear that such extreme (incorrect) values of β_{disk} and ζ_{disk} may be easily identified by their extreme error values generated. For this specialised case (heating control), the days where the mean β_{disk} value is inappropriate (31, 44) readings are not required (very low solar irradiance). An incorrect ζ_{disk} value can be easily identified from its extreme RMISE value, and its value of IE will still be commensurate with a COTS device (fig. 2.11). Indeed, as noted from fig. 2.10 the IE value in both extreme ζ_{disk} cases is <10% which would be expected observing fig. 2.11.

This trial has demonstrated that the LCP may present a simple economic alternative to existing COTS pyranometry solutions. The 1st order equivalent circuit model offers a simple and effective way of calibrating the LCP. Moreover, as demonstrated by the low values of measured IE for 52 days in early 2012, the LCP offers an economical standalone solution for solar irradiance trend assessment. Moreover, future advanced HVAC control

techniques may require solar assessment in large numbers on a housing estate or even within the same conurbation. This low cost pyrometer may offer an economic solution, by using an automated permanent calibration process if one low cost device was mounted next to a traditional COTS device but with the distributed pyranometers of low cost design.

2.8. Test facility 1: 'Luton' bodied truck test cell

A dedicated test cell was located within the rear compartment of a 3.5 tonne 'Luton' bodied truck (see fig. 2.12), giving significant elevation to avoid heat transmission from the ground and providing portability to enable additional control over external influences as required. Additionally, sixteen 600mm x 600mm x 25mm medium-density concrete slabs cover the floor area in close proximity to increase the thermal mass of the floor. Following on from Gouda and Underwood [43], extensive use of fibreglass to insulation to BS EN 13172:2012 and BS1088-1:2003 (marine), timber was used in an attempt to construct a test cell as a fair representation of a single small zone within a dwelling. The mechanical constitution of the test cell is detailed in table 2.1.

Initially, benchmarking tests to acquire thermal resistance values of the test cell wall surfaces were conducted at a location in the heart of Sheffield City Centre UK; 53.38 (north), 1.49 (west). Subsequent long term tests were conducted within 1 mile of the previous test site, at the University of Sheffield Engineering 53.38 (north), 1.48 (west). External environmental (weather) conditions were monitored using a La Crosse WS2300 weather station in conjunction with the proposed low-cost pyranometer manufactured and calibrated against a Delta T SPN 1 pyranometer. The anemometer, pyranometer and a rain gauge are installed on the southern tip of the roof of the test cell. Temperature and humidity sensors are installed at a height of 2m above ground and mounted on the north eastern wall of the test cell, avoiding direct sunlight.

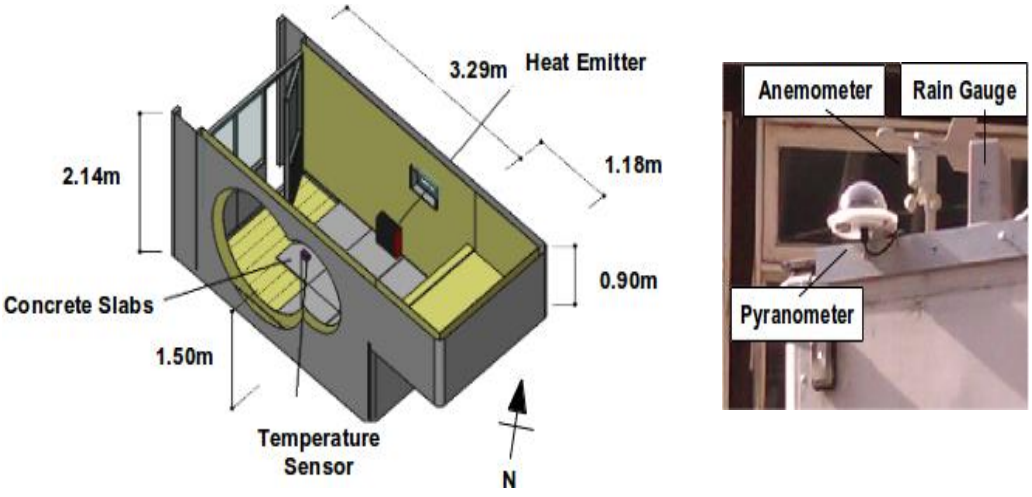

Figure 2.12: Test Cell and environmental measurement

Wall Area (m^2)				Floor (m^2)	Ceiling (m^2)	Window (m^2)	Volume (m^2)
North	East	South	West				
8.04 (1)	4.32 (2)	8.04 (1)	4.22 (1)	9.02 (3)	9.02 (4)	0.23 (5)	34.73

(*) Construction type
All plywood to BS1088-1:2003 (marine), all insulation to BS EN 13172:2012
1) 6mm plywood, 50mm mineral wool insulation, 2mm aluminium sheet
2) 6mm plywood, 50mm mineral wool insulation, 6mm plywood
3) 6mm plywood, 50mm insulation, 25mm plywood
4) 6mm plywood, 50mm insulation, 4mm fibreglass sheet
5) Acrylic air filled double glazing, glazing 3mm thick, 10mm air gap

Table 2.1: Mechanical constitution of test cell

2.9. Test dwelling

After the verification of initial modelling techniques within the test cell, proposed modelling and simulation methods could be expanded to represent a multi zone situation namely, a dwelling or part thereof heated using a conventional water filled heating system. Fig. 2.14 illustrates the 3 semi-detached bedroom dwelling used in this research. The dimensions are outlined in table 2.2. A further La Crosse WS2300 weather station is mounted by the southern apex of the roof and another outside temperature sensor is mounted under the west facing soffit (fig. 2.14) out of the line of direct sunlight. Due to the test dwellings proximity to the Sheffield solar farm [82], the solar irradiance levels

from that installation were deemed suitable for that location.

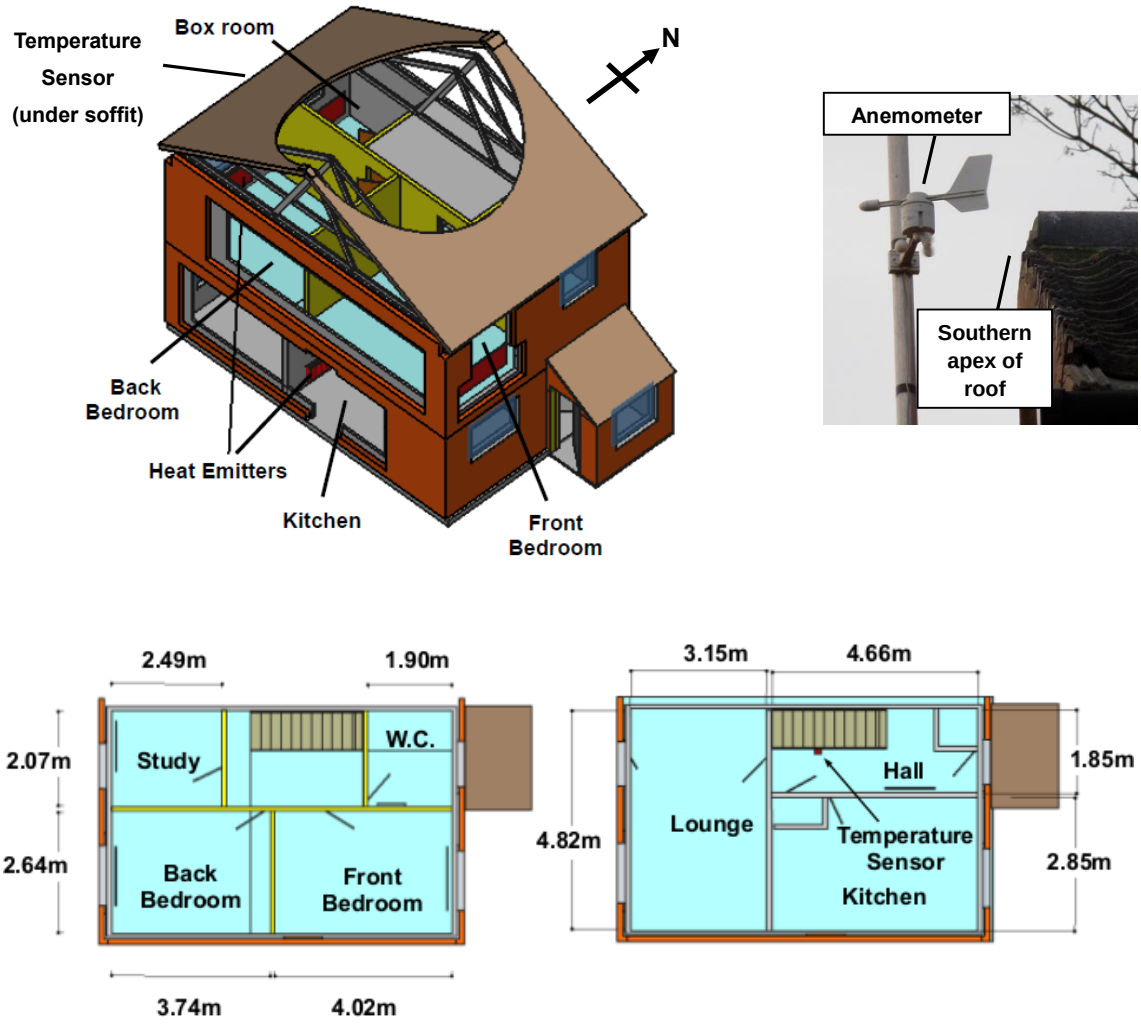

Figure 2.13 Test dwelling

Zone	Wall Area (m^2)				Floor (m^2)	Ceiling (m^2)	Window (m^2)
	North	East	South	West			
1	9.22 (1)	6.07 (2)	9.22 (2)	6.07 (1)	10.61 (5)	10.61 (6)	1.82 (8)
2	8.60 (1)	6.07 (1)	8.60 (2)	6.07 (2)	9.87 (5)	9.87 (6)	1.42 (8)
3	18.00 (4)	8.83 (3)	18.00 (3)	8.83 (3)	8.62 (7)	8.62 (5)	1..53 (8)
4	5.73 (4)	4.77 (1)	5.73 (1)	4.77 (2)	5.15 (5)	5.15 (6)	1.03 (8)
5	7.25 (4)	10.06 (3)	7.25 (2)	10.06 (2)	15.18 (7)	15.18 (5)	n/a
6	4.37 (4)	4.77 (2)	4.37 (1)	4.77 (1)	3.93 (5)	3.93 (6)	1.03 (8)
7	10.25 (4)	6.27 (2)	10.25 (3)	6.27 (3)	13.28 (7)	13.28 (5)	2.40 (8)

(*) Construction type

1) 100mm studwork partition , 450mm stud spacings, 12mm plasterboard, no internal insulation

2) 100mm medium density block work, 50mm retrofit polystyrene filled cavity, 100mm brickwork

3) 100mm block work partition

4) 200mm block work partition

5) 12mm plasterboard, 450mm spaced joists, 20mm tongue/groove floorboards.

6) 12mm plasterboard, 100 mineral wool insulation, loft space

7) 20mm concrete screed, 75mm medium density concrete

8) uPVC/aluminum frame dual glazed windows (10mm air gap)

Table 2.2: Mechanical constitution of test dwelling

2.10. Summary

Bespoke monitoring and control systems specific to the requirements of this research were developed to enable the testing of the control methods developed in this thesis. The following chapter details the development of a simulation method suitable for evaluating different HVAC control techniques applicable to CRVs. Furthermore, using this simulation method, a scheduling method is proposed. Such a technique aims to lower peak heating requirement of a traditional central heating system, reducing the boiler capacity requirement and reduce the occurrence of excessive boiler cycling due to mismatched heat supply and demand.

Chapter 3. Simulation of a scheduled hydronic heating system

3.1. Introduction

With the emergence of CRVs, alternative control strategies for operating heat emitters within a dwelling are now available that were not possible only a few years ago. This chapter examines how CRVs can be employed to improve central heating systems and describes a scheduling control system which has the aim of reducing energy consumption. Simulations are used throughout the investigation to provide a quantitative analysis of the benefits offered. First, this chapter introduces the most popular and capable software available. Due to the limited specification of such software, a Simulink based simulation based method is developed and validated using the test cell. Furthermore, the method is applied to a domestic dwelling, where a simple scheduling routine is trialled to assess any possible benefits of operating distributed heat emitters in such a manner.

3.2. Simulation of heating systems

The computer simulation of dwelling centralised heating systems is approaching its 4th decade [83]. At present hundreds of commercial products are available on the open market, each having attributes according to its purpose and use [84]. Perhaps the greatest step forward in the development of building simulation software was in 1996 when work began to combine two existing programs (DOE-2 and BLAST) that had previously been maintained by the United States Department of Energy. The resulting package, EnergyPlus, has been continuously developed since and is now in its 8th incarnation, offering "a comprehensive and free tool to researcher's architects and engineers alike" [85]. It offers a method of assessing building performance and provides many capabilities including; "time-steps less than an hour, modular systems and plant integrated with heat balance-based zone simulation, multi-zone air flow, thermal comfort, water use, natural ventilation, and photovoltaic systems" [86]. However, its lack of an intuitive CAD based GUI has prohibited its widespread adoption among building services professionals. In response to this, many building energy simulation software packages [86] including the popular Building Research Establishment (BRE) approved package, Design Builder™,

use EnergyPlus as their core engine. There is even a Google Sketch-Up® based bolt-on package, Legacy OpenStudio [87] that enables a complete CAD based simulation package to be created.

Despite the plethora of building heating system simulation software, by 2010 there were no software packages that were available to the industry for the accurate modelling of bespoke heating systems [88]. In particular those with advanced or projected future component technologies and/or intelligent/modern heating control systems were not catered for. Within the research community, only one validated solution existed which was Building Controls Virtual Test Bed (BCVTB). Developed at Berkley [89], BCVTB is based on Ptolemy II, a package that enables multiple software packages to communicate with each other using TCP/IP sockets. Again, the core of BCVTB is EnergyPlus, through which Ptolemy II is able to communicate with software such as MATLAB and Modellica.

Although a prolonged attempt to utilise the BCVTB for the work in this thesis was made, due to the relatively low time step simulation capabilities of EnergyPlus (5 minutes minimum time-step resolution) it was deemed to be of limited use. Instead, following the work of Galdwin [88] and combining with work by Underwood and Gouda, a novel simulation package was developed. Such a package would provide a platform to test heating system performance and possibly aid the formulation of a suitable MPC algorithm.

3.3. Heating system model development

Following on from Gladwin [88], the model is developed using the MATLAB/Simulink environment to allow assessment of a heating scheduling routine. Furthermore, by the use of “lumped parameters” the basic mathematical core of the model can be subsequently developed into a state-space representation suitable for MPC (as is discussed in later chapters).

3.4. Simulation methodology

The following section addresses the construction of a mathematic model that represents the thermal characteristics of building. The model itself consists of the heat source

dynamics that relate the boiler output to the radiator and the zone dynamics that represent the heated zone (i.e. a room).

3.4.1 Introducing a heat source

The rise in ambient air temperature of a heated zone is dependent on the net heat transferred to the air, building fabric and contents of that zone. The net heat transfer is dependent on heat gains (from the heat emitter, inhabitants, solar gain) and the heat losses (ventilation, heat losses through the building fabric of zone).

The law of heat capacity defines the change in temperature (ΔT) of common materials due their physical properties and is defined as *the amount of heat required to change a unit mass of a substance by one unit of temperature* [90]. The product of mass and specific heat capacity (mc) is referred to thermal mass.

$$Q = mc\delta T \tag{3.1}$$

Q = Energy transfer (J)
m = Mass of material (kg)
δT = Temperature change of material (ºC)
c = Specific heat capacity of material ($Jkg^{-1}ºC^{-1}$)

Examining a discrete time interval of 1 second, the temperature change of a material (δT) is equal to the energy supplied during that 1 second divided by the thermal mass of that material. The energy (J) supplied during one second or *per* second is power or heat (Js^{-1} or W). Thus a material's temperature at time t, measured or sampled every second, can be represented by equation (3.2), where P_n is the net power supplied to the material.

$$dT = \frac{Q_n}{mc} \Rightarrow \frac{dT}{dt} = \frac{Q_n}{mcdt} \Rightarrow \frac{dT}{dt} = \frac{P_n}{mc} \tag{3.2}$$

Introducing the component (P_{em}) that equates to the heat expelled to the open air from the heat emitter and combining thermal mass components specific heat capacity (c) and mass

(m) to become thermal capacitance (ζ_{em}), (2) becomes (3). T_{em} represents the surface temperature of the heat emitter.

$$\frac{dT_{em}}{dt} = \frac{P_n}{mc} \Rightarrow \frac{dT_{em}}{dt} = \frac{P_{boiler} - P_{em}}{\zeta_{em}} \tag{3.3}$$

Transforming (3.3) to state space representation where K_{em} is the heat loss constant for that particular heat emitter, forms (3.6). K_{em} can be calculated from a look up table or supplied by the heat emitter manufacturers as the operating factor [91] (K_{of}) combined with the rated power of the heat emitter.

$$\frac{dT_{em}}{dt} = \frac{P_{input} - K_{em}(T_{em} - T_{zone})}{\zeta_{em}} \Rightarrow \frac{dT_{em}}{dt} = \frac{-K_{em}T_{em}}{\zeta_{em}} + \frac{K_{em}T_{zone}}{\zeta_{em}} + \frac{P_{input}}{\zeta_{em}} \tag{3.4}$$

Where,

$$K_{em}(T_{em} - T_{zone}) = P_{rated} \times K_{op} \tag{3.5}$$

$$\overbrace{\begin{bmatrix} \dot{x} \\ \frac{dT_{em}}{dt} \end{bmatrix}}^{\dot{x}} = \overbrace{\frac{-K_{em}}{\zeta_{em}}}^{A} \overbrace{\begin{bmatrix} x \\ T_{em} \end{bmatrix}}^{x} + \overbrace{\begin{bmatrix} \frac{K_{em}}{\zeta_{em}} \\ \frac{1}{\zeta_{em}} \end{bmatrix}}^{B} \overbrace{\begin{bmatrix} T_{zone} & P_{input} \end{bmatrix}}^{u} \tag{3.6}$$

3.5. Zone model

Following on from the previous section, the net heat supplied to the air within the zone has to be determined. The prevalent methods of heating simulation are based on equivalent circuit models [55], [61], [92], [93] are constructed in the form of differential heat balance equations. A contribution from each complete wall construction is combined to allow the simulation of the air temperature within that zone.

3.5.1 Test Cell Model

Returning to (2) it can be surmised the rate of change of temperature of a material can be

determined as the sum of the heat gained minus the heat lost divided by the thermal mass (equal to thermal capacitance) of the material. In the case of a wall surface, the rate of change of temperature of that wall would be determined by heat gained by the warmer side (facing the heated zone) and the heat loss it endures from its colder side. This immediately assumes such a wall surface can be represented by two separate 'halves', one gaining heat and one losing heat. In a heated zone we can refer to each half as 'inner' (facing the zone) and 'outer' (facing the colder area, e.g. unheated areas, outside etc.). It is also known that the heat loss through a wall surface is the product of the surface area, the heat loss coefficient or U-value ($Wm^{-2}°C^{-1}$) and the temperature difference on either side of the wall [15]. To avoid confusion between the U-value and common notation for control input variables (often defined as U), the heat loss coefficient is hereafter known as Ψ. Thus if we consider a single wall surface as two sections 'sandwiched' together, a temperature gaining section and a temperature losing section, then the mean temperature of both can be combined as given by (7). Neglecting external gains, the losing section parameters are represented as Ψ_{os} (outside facing section heat loss coefficient), Λ_{os} (outside facing area), T_s (temperature of surface) and ζ_s (thermal capacitance). The gaining section parameters are represented as Ψ_{is} (inside facing section heat loss coefficient) and Λ_{is} (inside facing area).

$$\frac{dT_s}{dt} = \frac{\overbrace{\Psi_{is}\Lambda_{is}\left(T_{zone} - T_s\right)}^{Gaining\ section}}{\zeta_s} - \frac{\overbrace{\Psi_{os}\Lambda_{os}\left(T_s - T_{ext}\right)}^{Losing\ section}}{\zeta_s} \tag{3.7}$$

Furthermore, since we know that each section of the wall will have the same area $\Lambda_i = \Lambda_o$ and (3.7) becomes (3.8) where Ψ_{is} is the heat loss coefficient of the inner section and Ψ_{os} is the heat loss coefficient of the outer section and A_s is the wall surface area.

$$\frac{dT_s}{dt} = \frac{\overbrace{\Psi_{is}\Lambda_s\left(T_{zone} - T_s\right)}^{Gaining\ section}}{\zeta_s} - \frac{\overbrace{\Psi_{os}\Lambda_s\left(T_s - T_{ext}\right)}^{Losing\ section}}{\zeta_s} \tag{3.8}$$

The determination of Ψ for each inner and outer half is more difficult. Heat loss coefficients are comprehensively defined in both ASHRAE and CIBSE publications [5], [15] for standard wall compositions but only as a complete wall surface. Following on

from Underwood [93] the value of thermal resistance is 'split' after a complete value of resistance is determined from the physical properties of the wall (8). Such a principle can be applied as per (3.9) where Ψ_s is the standard heat loss coefficient for that type of wall composition.

$$\frac{dT_s}{dt} = \frac{\overbrace{\Psi_s \Lambda_s (f-1)(T_{zone} - T_s)}^{Gain}}{\zeta_s} - \frac{\overbrace{\Psi_s \Lambda_s f (T_s - T_{ext})}^{Loss}}{\zeta_s} \tag{3.9}$$

For clarity, (3.9) is depicted pictorially considering a simplified zone (fig. 3.1-3.3).

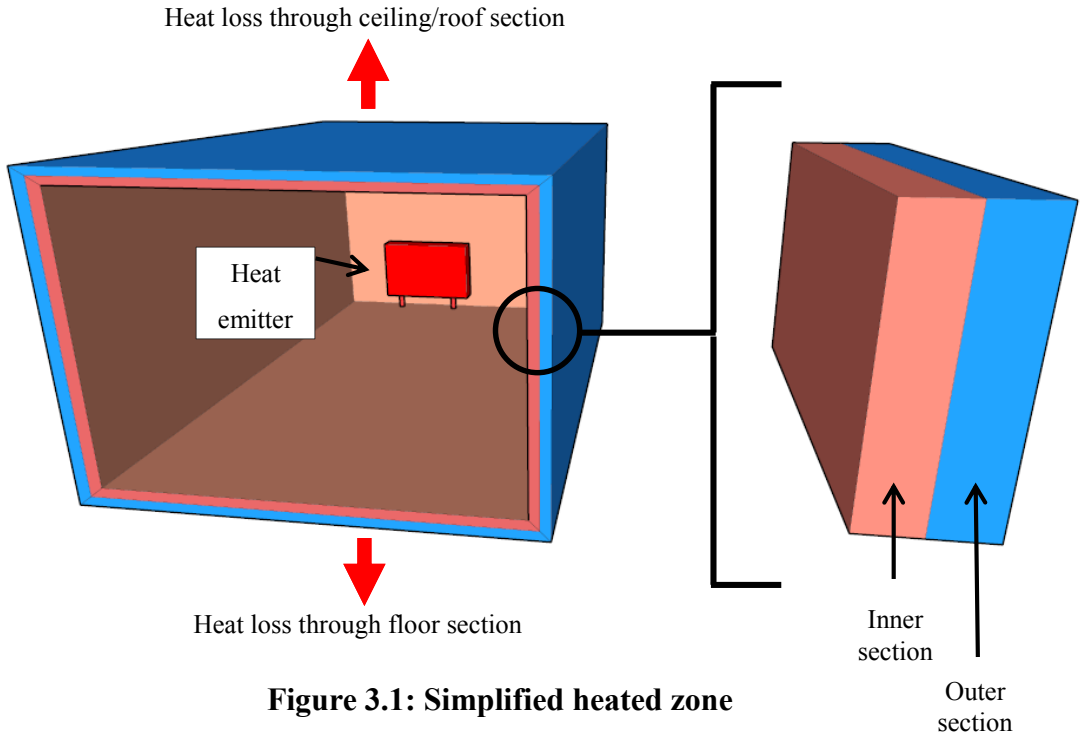

Figure 3.1: Simplified heated zone

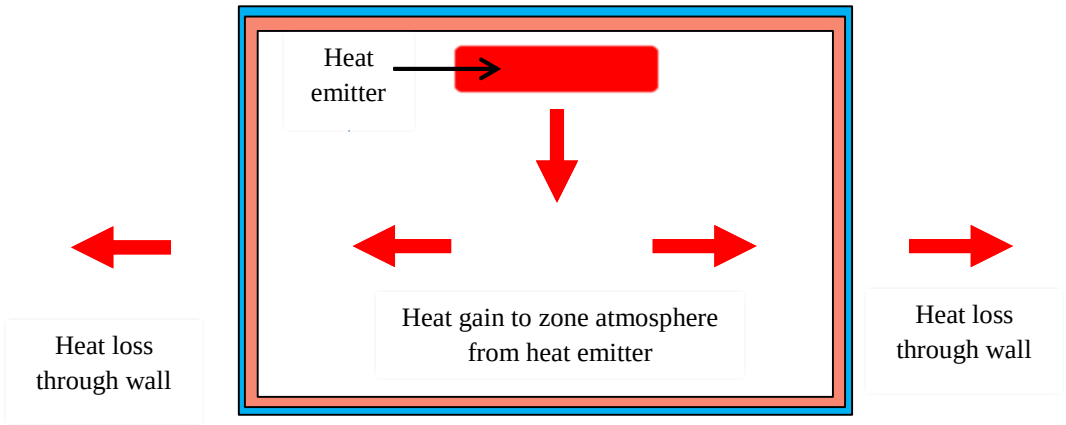

Figure 3.2: Simplified heated zone (plan)

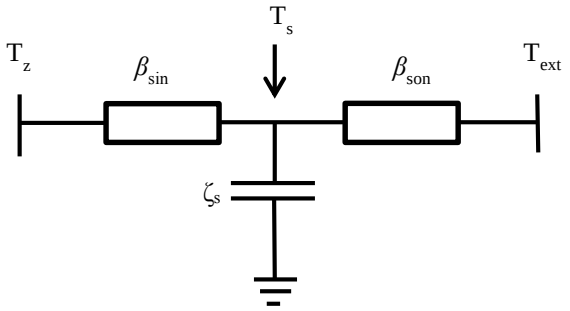

Figure 3.3: Equivalent circuit representation of wall cross -section

The surface area, A_s, accessibility factor, f, and the heat transfer coefficient of each surface Ψ_s gives a total thermal conductance value, the reciprocal of which is the thermal resistance β_s of that surface. A specific surface designated n split into an outer surface and an inner surface (3.10) as each inner section thermal resistance $\beta_{sin} = \Lambda_s \Psi_{s(f-1)}$ and an outer section $\beta_{son} = \Lambda_s \Psi_s f$ where the total thermal resistance of wall n (β_{sn}) is equal to the sum of the inner (R_{sin}) and outer (R_{son}) resistances of wall n.

$$\frac{dT_s}{dt} = \frac{\overbrace{\left(T_{zone} - T_s\right)}^{Gain}}{\beta_{\sin}\zeta_s} - \frac{\overbrace{\left(T_s - T_{ext}\right)}^{Loss}}{\beta_{son}\zeta_s} \tag{3.10}$$

The air temperature (T_a) within the test cell is represented by the sum of all the contributions by n surfaces (11)

$$\frac{dT_a}{dt} = \frac{P_{el}}{\zeta_a} - \frac{\left(T_{z1} - T_{s1}\right)}{\beta_{s1}\zeta_a} + \frac{\left(T_{z2} - T_{s2}\right)}{\beta_{s2}\zeta_a} + \frac{\left(T_{z3} - T_{s3}\right)}{\beta_{s3}\zeta_a} \ldots\ldots\ldots + \frac{\left(T_{zn} - T_{sn}\right)}{\beta_{sn}\zeta_a} \tag{3.11}$$

Neglecting solar and internal gains (occupants, plant etc.) and assuming all wall surfaces are exposed to the same outer surfaces temperature, a complete state space representation of a heated zone (test cell) can be formulated (3.12).

$$\begin{bmatrix} \dot{T}_{s1} \\ \dot{T}_{s2} \\ \cdot \\ \cdot \\ \cdot \\ \cdot \\ \dot{T}_{a} \end{bmatrix} = \begin{bmatrix} \frac{-1}{\beta_{w1}\zeta_{s1}} & 0 & \cdots & 0 & \frac{1}{\beta_{si1}\zeta_{s1}} \\ 0 & \frac{-1}{\beta_{w2}\zeta_{s1}} & \cdots & 0 & \frac{1}{\beta_{si2}\zeta_{s2}} \\ \cdot & \cdot & \cdots & \cdot & \cdot \\ \cdot & \cdot & \cdots & \cdot & \cdot \\ \cdot & \cdot & \cdots & \cdot & \cdot \\ 0 & 0 & \cdots & \frac{-1}{\beta_{wn}\zeta_{s1}} & \frac{1}{\beta_{sin}\zeta_{n}} \\ \frac{-1}{\beta_{si1}\zeta_{s1}} & \frac{-1}{\beta_{si1}\zeta_{s1}} & \cdots & \frac{1}{\beta_{sn}\zeta_{a}} & \frac{\beta_{Total}}{\zeta_{a}} \end{bmatrix} \times \begin{bmatrix} T_{s1} \\ T_{s2} \\ \cdot \\ \cdot \\ \cdot \\ T_{s6} \\ T_{a} \end{bmatrix} + \begin{bmatrix} 0 & \frac{1}{\beta_{so1}\zeta_{1}} \\ 0 & \frac{1}{\beta_{so2}\zeta_{2}} \\ \cdot & \cdot \\ \cdot & \cdot \\ \cdot & \cdot \\ 0 & \frac{1}{\beta_{son}\zeta_{n}} \\ \frac{1}{\zeta_{a}} & \frac{1}{\beta_{win}\zeta_{a}} \end{bmatrix} \times \begin{bmatrix} P_{el} \\ T_{ext} \end{bmatrix}$$

where;

$$\beta_{Total} = \beta_{s1} + \beta_{s2} + ... + \beta_{sn} \tag{3.12}$$

The derivation of thermal capacitance ($J°C^{-1}$) is considered trivial in the literature [55], [92], [93], being the product of mass and specific heat capacity of each constituent part of the each wall summed together. The accessibility factor can be determined by calculation or empirically [93]

3.6. Direct Simulink implementation

Although mathematically succinct, the state space model of a multi zone building may become unwieldy to construct and error prone as the building increases in complexity. A simpler approach has been developed by the author using Simulink, enabling the greater ease of expansion of a proposed simulation model to incorporate multiple zones and heat sources.

Once again considering (3) but at *i* discrete points in time, the current temperature at time *b* of a material represented by the sum of temperature changes at each of those points plus the initial temperature (*I*).

$$T = \sum_{n=0}^{i=b} (T[i] - T[i-1]) + I \tag{3.13}$$

Using Simulink, (3.13) can be thought of a continuous summing arrangement as illustrated in figure 3.4.

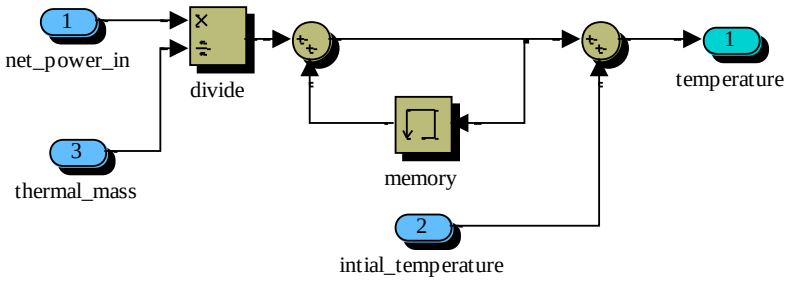

Figure 3.4: Simulink change in material temperature representation

Thus each wall can be considered as in figure 3.4, using the accessibility factor to divide heat contributions to the wall from each side. Considering the complete single zone model previously represented by (13), figure 3.4 is easily duplicated within a Simulink subsystem to make up a complete wall surface (fig. 3.5).

A fluid filled heat emitter can be considered in a similar manner as the wall surfaces. The heat losses are equal to the product of the temperature difference between the zone and heat emitter temperature, the operating factor and the heater rating. The Simulink heat emitter is shown in 3.6. Finally, the net temperature gain or loss of the air within a zone at each discrete point in time, is obtained by summing the all the heat contributions both negative and positive from each wall surface and heat source. The complete test cell Simulink model is shown in fig. 3.7 with the first wall expanded to aid the reader.

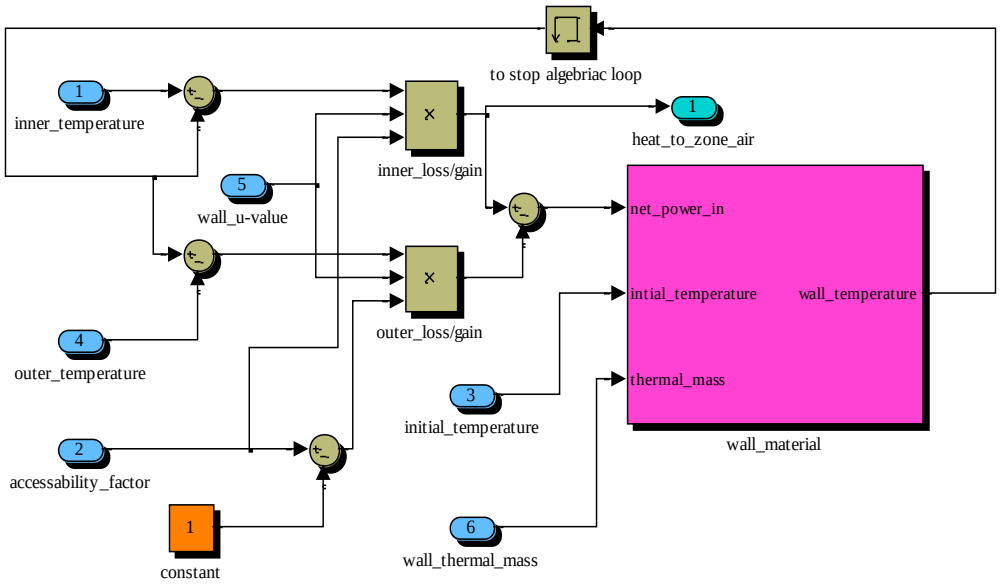

Figure 3.5: Simulink wall surface

The construction parameters such as heat loss coefficient, thermal capacity and thermal resistance may be loaded into the MATLAB workspace using an initialisation script. These can then be called by each 'wall construction' block in turn within any proposed control system.

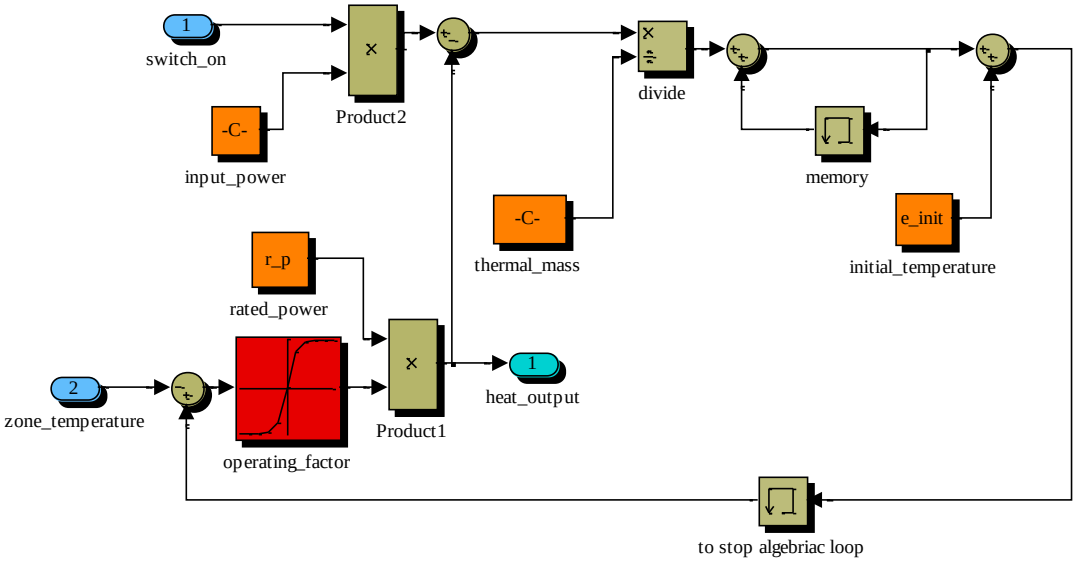

Figure 3.6: Simulink heat emitter model

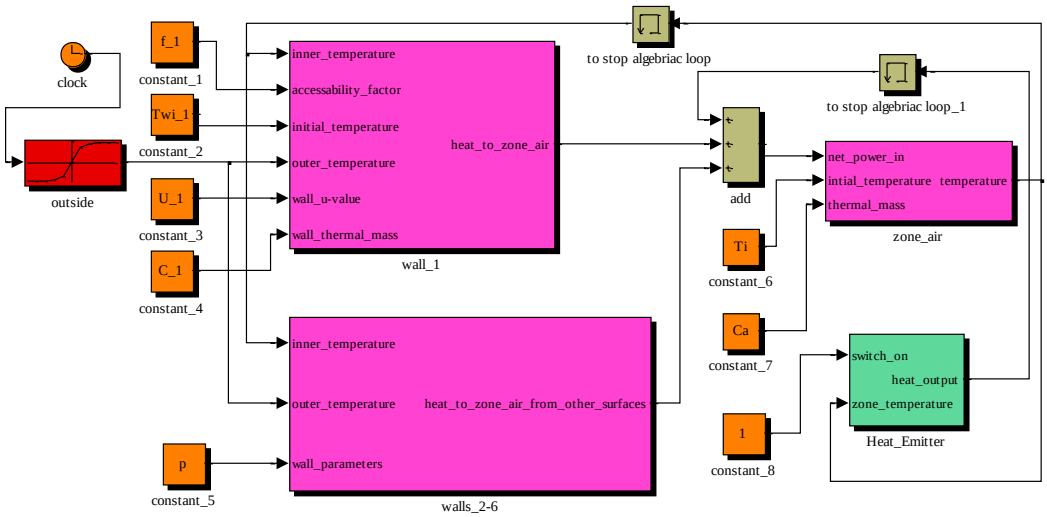

Figure 3.7: Simulink single zone lumped parameter model

3.7. Test Cell model parameter selection

The next stage of formulating the model is determining appropriate values for the accessibility factors (*f*). Recalling (9), the accessibility factor (*f*) determines the abstracted 'split' of thermal capacitance and thermal resistance between the inner and outer wall surfaces. The simplest method of determining these is by empirical calculation. Here, for example, using a recorded temperature profile from the test cell as a benchmark, the proposed model structure can be fed an appropriate range of *f* for each wall surface and simulated of repetitively. The values that result in the closest match between simulated and recorded results are the appropriate values for *f*. However, for this procedure to be correct and valid, the simulation using these derived values of *f* must hold true against subsequently recorded data. Moreover, an appropriate range of candidate values of *f* must be determined for the repetitive simulation to work.

Observing the test cell construction, the number of unknown values of *f* may be reduced by reducing the number of separate wall structures. 'Lumping' the south east upper and lower wall and the upper and lower floors together, a model in the form of (10) is derived with just 6 unknowns. These determine the values of inner and outer surface resistance (β_{so1}-β_{so6} and β_{si1}-β_{si6}).

To reduce the number of unknown values of f further, one may observe that the wall construction of three of the surfaces of the test cell (north east, south east and south west) are virtually identical. If it is assumed the outside temperature is uniform around the test cell, one may assume that their accessibility factors (f) will be identical for each of these surfaces.

As only four unknowns are now to be determined a 'brute force' recursive curve fit approach was employed where approximate values for f were determined via a course parameter space search. A finer scan was employed to refine the values.. Since, the limits of f are always between 0 and 1, a value of 0 for f would state no influence from one 'side' of the wall surface and a value of 1 would state no influence from the other. Observing previous work by Underwood and Gouda [55], bounds of search of 0.1-0.9 in steps of 0.1 for each value of f was initially chosen. This resulted in 6561 simulations to determine each of the four values of f that derive the 12 values of thermal resistance. From this, the process was repeated reducing the bounds of search further around the values found by the initial repetitive simulation process but simulating for an increased resolution of f (in steps of 0.01). The fitness of a parameter set was assessed using the Modelling Error (ME) performance metric, defined as the mean error between the measured temperature response of the system and the simulated temperature response over a heated period. The recorded thermal responses were obtained by operating the heat emitter within the test cell by means of a BS EN 60730 roomstat each day between 6/1/11 to 11/1/11 for the four hour period between 7am and 11am. These times were chosen as a compromise between lack of incident solar irradiance affecting the thermal response of the test cell and available access to the test cell. The first recorded thermal response (6/1/11) was used as the benchmark thermal response with which appropriate values of f could be determined. The whole repetitive simulation process was completed in 16 minutes 38 seconds using a DELL Vostro 200 and MATLAB/Simulink® 2010. The f values that returned the lowest ME value between simulation and the 6/1/11 recorded response are shown in table 3.1. The ME values using those f values for subsequent simulations are also described in table 3.1.

Wall Surface	*f*
NE	0.11
SE	0.11
SW	0.11
NW	0.01
Floor	0.06
Roof+ceiling	0.12

Date	ME (°C)
06/01/2011	0.32
07/01/2011	0.30
08/01/2011	0.48
09/01/2011	0.56
10/01/2011	0.35
11/01/2011	0.47

Table 3.1: Empirically derived accessibility factors and model performance

The experimental thermal transient response and simulated response are depicted in fig. 3.8.

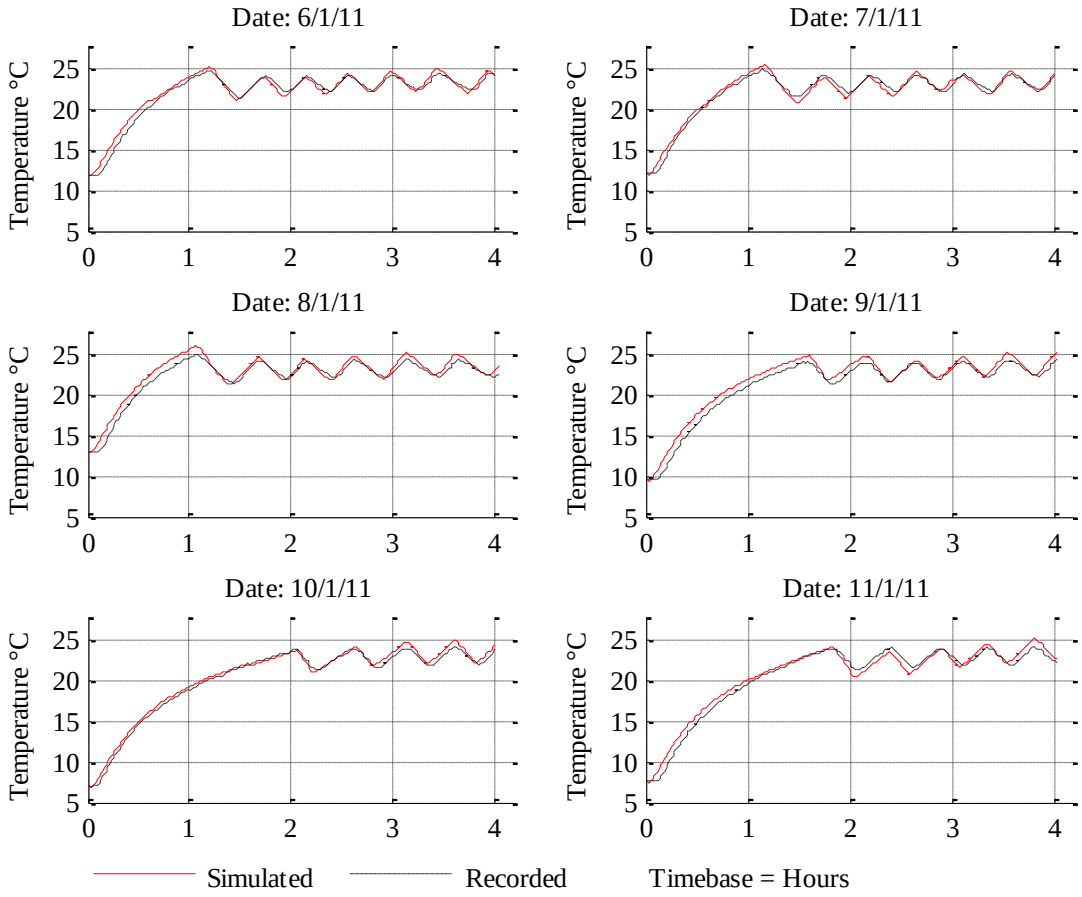

Figure 3.8: Thermal responses of the test cell.

It can be concluded from fig. 3.8 that the curve-fit determined values for *f* (and thus thermal resistance and capacitance values of each wall surface) from one benchmarking

thermal response (6/1/11) provide appropriate values of *f* for all subsequent simulated thermal responses (7-11/11). Thus, the suitability of *f* values gained from one benchmarking thermal response for subsequent response proves the efficacy of the modelling technique. Furthermore, in future one may assume that only one recorded trial for a heated zone would be needed to tune suitable values of thermal resistance in the future (subject to insolation).

As expected, the obtained values for *f* differ between wall surface construction. The less well insulated parts of the structure (in particular the NW facing wall that contained the door and has a large window made of poorly insulating acrylic) have an almost negligible accessibility factor. These particular surfaces possibly could be considered as containing only one element of thermal resistance. The trend is also evident with the floor which although has considerable thermal mass has poor insulating properties and considerable thermal bridging owing to minimal air gaps and insulation between outer and inner surfaces.

The worst ME of all 6 responses was 0.56°C (9/1/11). Considering work by Gouda in 2002 [54] and by Xu and Wang in 2007 [94] where improved simulation methods resulted in 0.58°C at best, this modelling method demonstrates commensurate performance with existing leading simulation techniques. Thus the need for further improvement at the time and a more sophisticated method of obtaining appropriate values of *f* was deemed unnecessary. A summary of the final derived values of thermal capacitance and thermal resistance for the test cell are given in table 3.2.

Surface Facing	Thermal Resistance ($KW^{-1}m$)
North East (outer)	0.0453
North East (inner)	0.3663
South West (outer)	0.0453
South West (inner)	0.3663
South East (outer)	0.0857
South East(inner)	0.6931
North West (outer)	0.0033
North West (inner)	0.3300
Roof (outer)	0.0224
Roof (inner)	0.3505
Floor (outer)	0.0671
Floor (inner)	0.4922
Window	1.7000

Surface Facing	Thermal Capacitance (J°K)
North East	154410
South West	143601
South East	81590
North West	8798
Roof	196640
Floor	655480
Window	n/a
Air+Furnishings	19619

Table 3.2: Derived thermal resistances and capacitances of the test cell

3.8. Simulation of test zones within a dwelling

Having determined suitable values for the lumped thermal resistances and capacitances, the model (fig. 3.7) can now be applied to simulate a single zone within a building and then expanded to represent a multi-zone dwelling.

The lounge area was chosen as a suitable test zone for three reasons:

1. The heat emitter has no TRV control, making the modelling of any heat input from a central source more straightforward.

2. It has no south or east facing windows, thus during periods of minimal occupancy when tests could be conducted, any temperature variations associated with solar gain would be negligible

Following on from Underwood [93], a step input was applied to the heat emitter within the test zone to assess the efficacy of the dwelling simulation. A two and half hour period on the 27/10/10 when the lounge heat emitter temperature and ambient temperature had been previously monitored was chosen since all the doors and windows remained closed

and no occupants were present during this period and thus the response would be dominated by known inputs with no known disturbances. The input power (heat) into the test zone can be deduced from knowledge of the heat emitter surface temperature and its physical dimensions.

For the simulation, thermal resistance values for each surface were derived from standard U-values from CIBSE [15] and the tuning procedure described in the previous section. The thermal capacitance for each surface was derived from first principles by combining mass and specific heat capacities of the constituent materials.

3.8.1 Dwelling model parameter selection

As with the test cell simulation model the thermal capacitances are determined using the recursive curve-fit procedure described previously. The values for the thermal resistances and thermal capacitances for each boundary wall of the zone are summarised in table 3.3. The recorded and simulated response of the test zone is illustrated in fig 3.9.

Surface Facing	Thermal Resistance (KmW^{-1})
North (inner)	0.0436
North (outer)	0.0436
East (1) (inner)	0.0465
East (1) (outer)	0.0465
East (2) (inner)	0.0789
East (2) (outer)	0.0789
South (inner)	0.0493
South (outer)	0.1970
West (inner)	0.0376
West (outer)	0.1504
Ceiling (inner)	0.0242
Ceiling (outer)	0.0242
Floor (inner)	0.0078
Floor (outer)	0.0706
Window	0.1429

Surface Facing	Thermal Capacitance (J°K)
North	883100
East (1)	828200
East (2)	488400
South	259800
West	2916800
Ceiling	46600
Floor	3694600
Window	n/a
Air+Furnishings	527200

Table 3.3: Thermal resistances and capacitances of the test zone (dwelling)

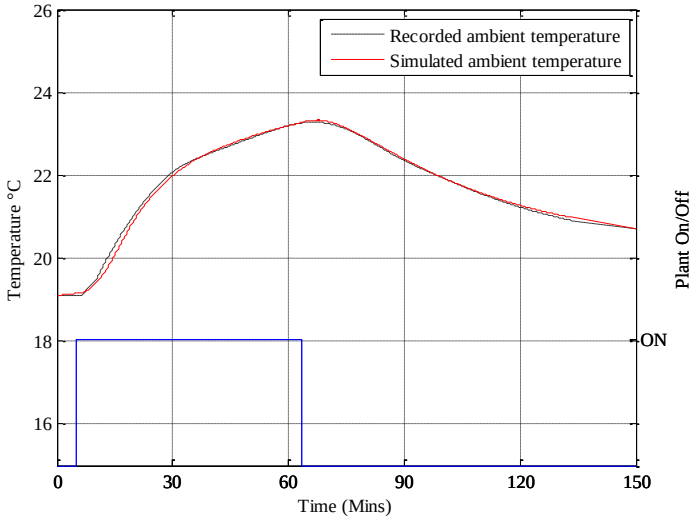

Figure 3.9: Thermal responses of the test zone

The simulation of ambient temperature illustrated in fig. 3.9 demonstrates commensurate performance with an ME of <0.15°C over the 2.5 hour trial. It must be stated that this result is representative of a 'worst possible case scenario' where the heated zones have only the heating system to rely on for maintaining a level of thermal comfort as opposed to occasions where thermal gain from incident solar energy and internal temperature rise attributed to occupants, electrical equipment and cooking.

3.9. Heat emitter simulation

During the test period 27/10/10 the combined heat emitter demand for the whole dwelling was lower than the minimum output (modulation) level of the boiler. At this level of demand the boiler can be considered an unmodulated heat source and so it can be simply modelled as constant heat source controlled by a hysteresis controller (the emulated boiler thermostat).

Using the manufacturer's literature regarding the operating factor, the heat emitter could be simulated using the Simulink model illustrated in fig. 3.6. The results of the simulation are shown in fig. 3.10.

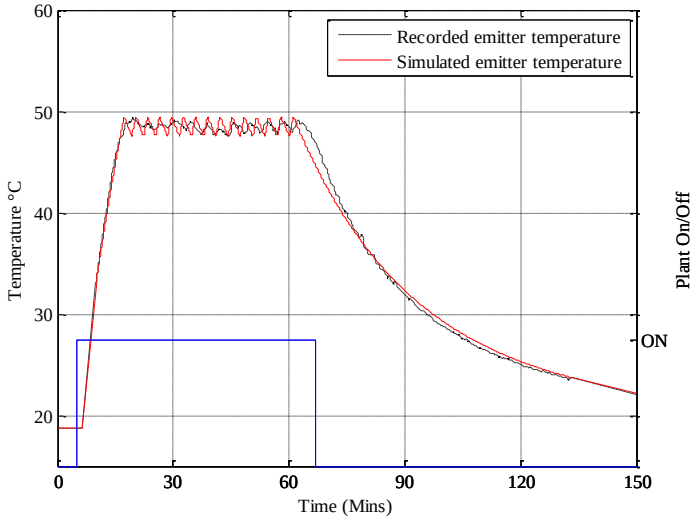

Figure 3.10: Thermal response of the heat emitter.

The ME of the heat emitter simulation is 0.53 °C. There is a notable discrepancy at 65-80 minutes (fig. 3.10). This can be attributed to residual heat in the circulating fluid that remains after the heat source (plant) turned is off, as although the burner is deactivated, the pump has an overrun routine that aims to slow the temperature change of the boiler components to help mitigate wear caused by thermal cycling. In the model, no such routine is accounted for, and for the minimal error its absence caused, was deemed unnecessary.

3.10. Simulation of Novel Control Techniques

The thermal mass of buildings has long been utilised as a method to reduce peak energy demanded by space heating. For example, passive houses [95] relies on this very principle on large internal thermal masses or capacitances (concrete floors and walls) storing thermal energy from direct sunlight in daylight hours to dissipate during the hours of darkness or overcast weather

As stated by Peeters [16] the oversizing of central heating boilers and heat emitters is extremely common. Thus one may assume that central heating systems when considered on a zone by zone basis, have the capacity to heat up a zone far quicker than would normally be deemed necessary. This accelerated heating profile may be useful, as a zone may be heated at a far faster rate than it is ever likely to lose heat. Correspondingly, a

typical hysteresis or on/off controlled heating system would need a proportionally longer ‘off’ time when compared to the ‘on’ time when used with oversized heat emitters and heat source.

Normally, each heat emitter would be operated simultaneously if the boiler is controlled by a central roomstat, or if at the start of heating period all TRVs could be open (on) should all the zones be cold enough. Hence installed central heat source capacity must be at least equal to the sum of the all the heat emitter outputs combined.

A different approach could be employed should it be possible to activate each heat emitter in turn according to a schedule and, of course, this is now possible due to the emergence of CRVs. Considering just a two zone system for example, a simple schedule would be to only activate one emitter at a time, the Zone 1 having priority and Zone 2 being activated during the ‘off’ period Zone 1. If both zones were identical, such a scheme would halve peak heat demand from the central heat source. The success of such a scheduling scheme would depend on the heat loss characteristics of each zone and the rated capacity of both the heat emitter and the power source.

To evaluate the feasibility and any potential benefit from the scheduling heat emitters both the test cell and test dwelling simulations are used. First, the validated test cell model is extrapolated as two separate identical zones that represent a two zone building with relatively low thermal mass. Next, the test zone model is extrapolated in the same manner, so a two zone building of higher thermal mass can be evaluated. Using these extrapolated test cell and test zone simulation models, several scheduled control strategies are examined to determine whether the distributed heat emitters of a typical UK dwelling could be controlled in such a manner to reduce required boiler size. Furthermore, the effects of different heat emitter mechanical constitution on such control schemes may be examined (i.e. steel flat panel or cast iron heat emitters).

As the test cell uses an oil filled heat emitter as a heat source, the electrical power supplied to each heat emitter emulates the heat through pipes supplied by a boiler, the switching on and off of the electrical supply acting like a CRV. For the test cell simulation trials, each heat emitter can only be supplied with its rated demand (as is the reality for an

electrical heater).

For the dwelling test zone simulation trials a central boiler unit is introduced, subdividing its rated power according to which heat emitter has been activated by its CRV. This emulates the possibility that rate of heating of a heat emitter within a central heating system has various rates of temperature change depending on which other heat emitters are on within the whole system. The CRV's are operated by a simple schedule discussed in the next section. At present each CRV is considered ideal, acting like a lossless switch, pipe losses are neglected, allowing the heat supplied to each emitter is of direct influence on the heat emitter with no delay. Both CRVs maintain an ambient set point temperature operating by way of a hysteresis controller, with +2°C bandwidth (as per BS EN 60730).

3.11. Benchmark simulation

Two non-scheduled heating systems are simulated to act as a reference benchmark for the work. The first heating system assumes a flat panel heat emitter is employed. The second heating system uses an emitter of identical heat output but of far greater thermal mass, emulating the behaviour of a cast iron heat emitter. In both of these cases the CRVs are considered to operate independently of each other with no regard for the operational status of the other CRV in the neighbouring zone.

3.12. Proposed scheduled hysteresis control

Only one heat emitter is activated at a time with one zone having priority. That is, the priority zone (Zone 1) is heated first and foremost but when it is deactivated (the off period being determined by its hysteresis controller), the second zone (Zone 2) heat emitter is activated. For both the test cell and dwelling simulations the effects of both scheduling and heat emitter type was investigated as described in table 3.4. If the routine is *Scheduled*, then Zone 1 always has priority.

For the investigation to be as comprehensive as possible each separate trial (1 to 5, table 3.4) is simulated using the initial internal temperature and external temperature profiles depicted in fig. 3.5 Three set points are chosen, 18°C, 20°C and 22°C for each weather profile also. In total 6 (external weather conditions) x 5 (heat emitter combinations) x 3

(set points) = 90 simulations are carried out.

Trial No.	Scheduled	Zone 1 heat emitter	Zone 2 heat emitter
1	No	Steel	Steel
2	No	Steel	Cast Iron
3	Yes	Steel	Steel
4	Yes	Steel	Cast Iron
5	Yes	Cast Iron	Iron

Table 3.4: Schedule of tests

3.13. Scheduling results (test cell)

To enable direct comparison of scheduled and non-scheduled results a specific performance metric is used, namely;

- SF: Satisfaction Factor, (kW): A measurement of user satisfaction based on the duration of time a particular zone is maintained at set point for a given overall energy usage for that heating period.

The lower the value of SF, the less energy is required to maintain a given level of thermal comfort. This performance metric is used because a longer heating period is required for a smaller heat source as during a scheduling routine (but it uses energy at a slower rate). The results of the 90 simulations are illustrated in fig. 3.11, 30 simulations for each set point, 6 simulations for each trial.

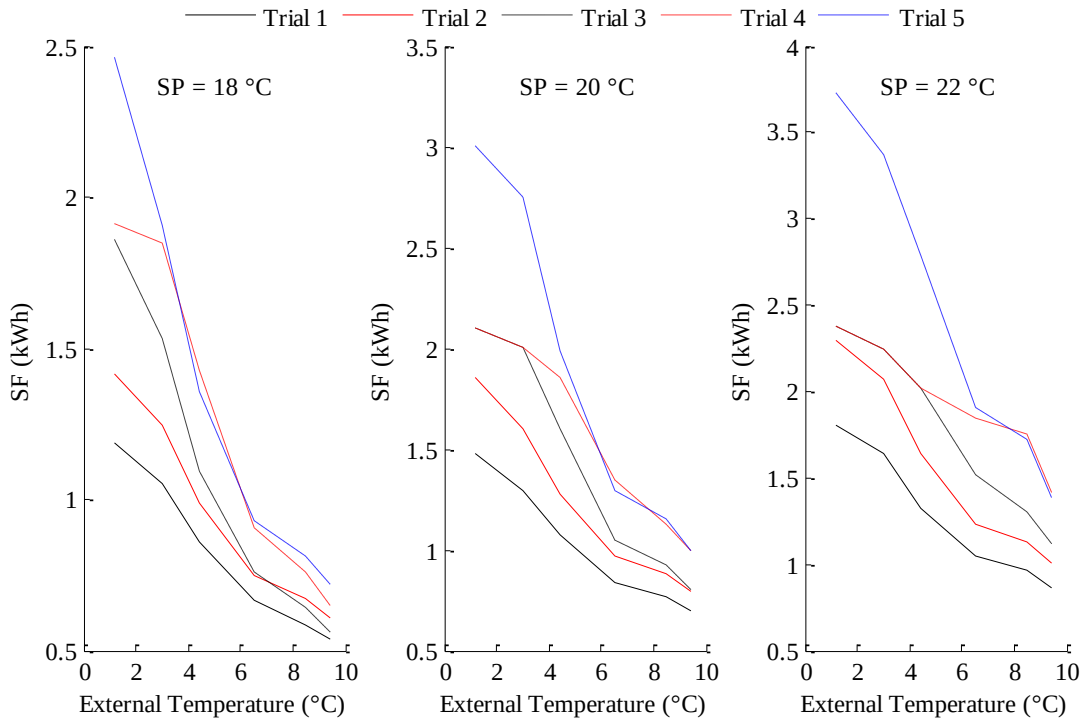

Figure 3.11: Results of scheduling routine using two test cells.

It can be observed that the SF figure for all routines converges as the external temperature increases since the energy requirement as a whole reduces due to mild weather or as the set point is reduced. For all temperature profiles and set points the benchmarking trial (1) performs best, returning the lowest SF figure. However, an interesting point to note is that the scheduling routine using heat emitters with a lower thermal mass performs better than a scheduled routine using one with more dense heat emitters in milder weather. Furthermore, for the lowest set point (18°C) it may be observed that the SF of trial 3 schedule is converging with the benchmarking trial 1. This would suggest that scheduling will perform as well as the traditional TRV control in even milder weather in the test cell.

From these tests, one may conclude for a scheduling system to be beneficial, the zones need to be constructed from materials offering superior insulation properties than the test cell and of greater thermal mass. Moreover, to consume less energy for a given level of thermal comfort, lighter steel heat emitters would be required.

3.14. Scheduling results (test dwelling)

Following on from the idealised simulation investigation, the dwelling zone model is extrapolated into two separate zones. The purpose of these trials is to deduce the merits of a scheduled heating system within a building constructed with materials of increased thermal insulation and greater thermal mass. Using the weather profile and initial temperatures from the test zone modelling data (section 3.8), eight trials were conducted for both a scheduled system routine and a non-scheduled routine. These are detailed in table 3.5 and table 3.6. Two set points were chosen (22°C and 24°C) that were a reasonable margin above initial starting temperature and deemed typical choices for the average occupant and fall within the dead band recommended by the carbon trust [96]. To enable a direct comparison of non-scheduled and scheduled routines, a longer heating period is used for the scheduled routine that enables set point to be maintained for a comparable amount of time. Then, the difference in the energy used by each strategy may be compared. The scheduled tests used a 2kW heat source and the non-scheduled routines used a traditionally sized heat source, rated at the sum of both heat emitters (4kW). The hysteresis band is operated above the set point. A 22°C set point with 2°C hysteresis the controller would aim to operate the ambient temperature between 22°C and 24°C.

Test	Set point	Hysteresis Band (°C)	Time at setpoint (hh.mm)	Energy used (kWh)	SF (kW)	Boiler Cycles
1	22	0.50	4.21	3.50	1.25	2.00
2	22	1.00	4.13	3.62	1.17	2.00
3	22	1.50	4.41	3.70	1.27	1.00
4	22	2.00	5.19	3.71	1.44	1.00
5	24	0.50	6.05	2.66	2.29	2.00
6	24	1.00	6.11	2.74	2.26	2.00
7	24	1.50	6.30	2.97	2.19	2.00
8	24	2.00	7.23	2.98	2.48	2.00

Table 3.5: Non-scheduled simulation results

Test	Set point	Hysteresis Band (°C)	Time at Set point (hh.mm)	Energy used (kWh)	SF (kW)	Boiler Cycles
1	22	0.50	4.40	3.76	1.24	4.00
2	22	1.00	4.47	3.89	1.23	3.00
3	22	1.50	5.05	3.81	1.33	3.00
4	22	2.00	5.18	3.84	1.38	2.00
5	24	0.50	6.00	1.95	3.08	0.00
6	24	1.00	6.00	1.81	3.31	0.00
7	24	1.50	5.53	2.05	2.87	1.00
8	24	2.00	5.53	1.99	2.96	1.00

Table 3.6: Scheduled simulation results

Referring to tables 3.5-3.6, the dwelling results differ markedly from the test cell results. In the majority of cases, a scheduling routine can be seen to use more energy for a given level of thermal comfort. Only for tests 1 and 4 did the scheduling routine achieve a lower figure for SF, (1.38 kW compared to 1.44 kW and 1.24 kW compared to 1.25 kW). Moreover, for lower levels of thermostat hysteresis, the scheduling routine actually induces more boiler cycling. The increased number of cycles is an effect caused by an increase in difference between the size of the heat emitter and the heating demand. In these situations the heating demand has now been reduced by a using a smaller hysteresis band. In essence the heat emitter has become oversized by a greater margin. Greater oversizing can lead to a faster rate of heating of the ambient temperature of the zone, which with a hysteresis controlled system, will lead to greater frequency of switching on/off of the heat source.

As soon as the heat demand is increased (by raising the set point) the central heat source cycles less during a scheduled routine. During tests 5 and 6 the scheduled routine the heat source not cycling at all. The overall energy use increases for a given thermal comfort as shown in higher levels of SF for the scheduled trails 5-8. In particular, during test 5 both scheduled and non-scheduled heating routines both maintain the zones for similar times at above 24 °C (6:00 h and 6:05 h respectively). However, the scheduled routine uses 27% less energy (1.95 kWh compared to 2.66 kWh).

3.15. Summary

The objective of the work as presented in this chapter has been to examine how CRVs

can be employed to reduce energy consumption. By establishing a verified building heating effect model, novel control techniques have been simulated in conjunction with these new physical heating controls (CRVs). Thus, the basic mathematical modelling building blocks for thermal modelling have been presented and subsequently used to derive simulations models for a low thermal mass 'Test Cell' and domestic 'Dwelling' used throughout the thesis. Following the development of these models, a simple scheduled heating system controller was proposed and investigated in an effort to address the oversizing of boilers and utilise the prevalent oversizing of heat emitters.

The main conclusions from the simulations detailed within this chapter are summarised below:

1. Scheduled control may return equivalent thermal comfort levels using reduced capacity central heat units.

2. Scheduled control in conjunction with reduced central heat units may use less energy if properly conditioned.

3. Ill-conditioned scheduling can result in an increase in energy use.

4. Ill-conditioned scheduling can increase the prevalence of heat emitter oversizing.

5. Scheduled control performs best when used with low thermal mass heat emitters.

The foremost conclusion from this chapter is that scheduling of heat emitters may be a viable method of operating heat emitters within a dwelling. The simulations have shown that by implementing a scheduling system in conjunction with CRV's for milder weather conditions, a much smaller boiler may be used than is traditionally thought possible. Substantial manufacturing and installation costs may also be saved by using a smaller boiler unit. Furthermore, if implemented on a larger scale, gas demand may be reduced at peak times reducing the strain on nationwide gas storage facilities.

Such a scheme may also promote an alternative method of controlling heat distribution

around a central heat system. Instead of modulating the heat supply from the heat source, the heat emitters could be operated to modulate demand, in effect a *reverse modulation* process. This would have the benefit of enabling heat sources with a limited turn down ratio to provide a pseudo modulated output by evenly distribute excess heat among distributed zones, dispensing with costly buffer systems often needed with biomass or heat pump systems. In times of more extreme (colder) weather priority zones may be selected which would be guaranteed to at the required level of thermal comfort. Although not strictly a convenient solution for many households, for low income families reverse modulation could be a way of constraining energy use given a set energy budget.

However, simulation results prove a poorly conditioned scheduling routine may actually use more energy, despite using a smaller central heat source. Furthermore, in colder conditions or with zones of lower thermal insulation and mass, scheduling heat emitters will result in poor thermal comfort in lower priority zones. Another point of note is that a poorly optimised scheduling routine may result in an increase in the oversizing of heat emitters, the very condition that it is supposed to alleviate.

For any scheduling or reverse modulation system routine to provide the benefits of reduced central heat source capacity and possibly reduced energy consumption the conditioning of the scheduling routine must be addressed. Here it has been concluded that a predictive algorithm is needed to pre-calculate the scheduling routine including optimal length of heating period and the optimal priority pre-set temperatures of each zone. Also, the physical properties such as type of heat emitter must be chosen carefully; cast iron or high thermal mass emitters performed worse using a scheduling routine.

Finally, hysteresis control is a poor choice for such a scheme. The large oscillatory thermal responses around set point make quantifying occupant satisfaction levels difficult and do impinge on thermal comfort. Using more advanced control towards this aspect of the system is to be investigated in the subsequent chapters. An MPC algorithm as proposed by Liao and Dexter (and others) [53] would seem the ideal solution produce better results, particularly as experience has now been gained in modelling heated zones. Moreover, the ability of MPC to handle multiple performance constraints of a MIMO control systems make it the natural choice. This is demonstrated by the dramatic increase in its use in recent times in the HVAC research community [97] (fig. 3.12).

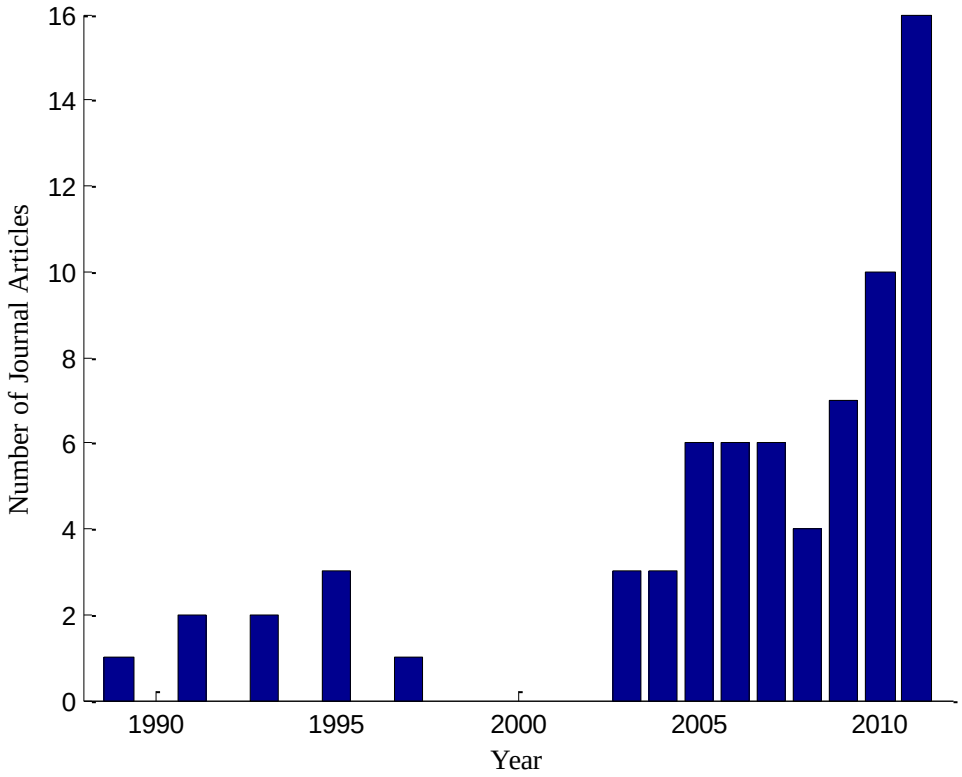

Figure 3.12: Rise in research interest regarding MPC and HVAC

The dominant problem associated with MPC is the construction of the model as outlined by Privara [98]. Usually in an HVAC context this is achieved by physical measurement and assessment of the zones to be controlled. On a small domestic scale this is not really a practical proposition as the costs involved for commissioning would be prohibitive. Moreover, buildings often change in physical construction and layout over their lifetime.

Thus the ideal solution would be to automate the process, utilising a method of adaptive modelling in conjunction with an MPC algorithm. The next chapter investigates the possibility of automating the modelling process with limited user input while implementing an MPC control scheme.

Chapter 4. Online adaptive recursive modelling and control of a hydronic heating system

4.1. Introduction

Although a number of advanced control techniques for HVAC systems have been reported, there has been little focus on domestic dwellings, and in particular 'wet' central heating systems which are of particular importance in the UK and wider EU. In the previous chapter mathematical models were described to predict the thermal responses of the test cell and dwelling and subsequently employed in a simulation investigation of a novel scheduled heating control system. Any heating controller that requires manual intervention to 'program' model parameters is at a disadvantage when it comes to deployment in a domestic environment. Therefore, this chapter develops a recursive modelling framework to allow the thermal model building to be developed on-line with little input from the user.

Recent research has demonstrated the effectiveness of MPC for HVAC systems, with an emphasis on the identification of a building's thermal behaviour. It is widely accepted that system identification is the most difficult and time consuming part of MPC controller design and Prívara et al have provided an excellent review of the current MPC specific preferred techniques [98]. Their research also categorises two different MPC specific paradigms in terms of power-conservative dynamic models or 'traditional' and 'black box' methods.

Although intuitive, the 'traditional' strategy unfortunately yields a model that can contain many hundreds of states, resulting in requirements for high computational effort for subsequent control purposes. Some progress has been made to incorporate model order reduction [99], their structure still needs to be defined prior to commissioning, which is often considered impractical.

Statistical models or black box techniques have been more favoured in the field of building specific MPC. Ferkl et al [100] compared an AutoRegressive Moving Average with eXternal input (ARMAX) and prediction error method (PEM) to subspace model

identification. The subspace method proved easier to implement while the ARMAX model can achieve better results with systems having less identifiable levels of noise. The same research group also examined MPC Relevant Information (MRI) using least squares [62] finding that it outperformed the standard PEM method. Using data collected on-line from a domestic dwelling Ogonowski [101] also used an ARX system in combination with a least squares method to identify fixed model parameters of the dwelling, achieving an error of less than 2% on a daily basis. Finally the method that has been discussed earlier with Fuzzy and ANN techniques is a predefined equivalent circuit model of the thermal characteristics of the building that is updated/corrected using data acquired on-line. Among MPC HVAC research communities the method by which the characteristics of the model are updated can vary. Particularly popular methods are least squared optimisation techniques and Pseudo Random Binary Sequence methods (PRBS). Using the former in conjunction with an MPC controller Široký et al [70] achieved a 15-28% energy saving compared to the previous well-tuned PID controller. Hazyuk et al [65] achieved between 93% and 96% accuracy between the obtained model and recorded results using PRBS and the University of Almeria [69] used a model obtained by exciting an offline model of their test facility using PRBS. Implementing the subsequently obtained model and MPC controller, the HVAC system achieved superior thermal comfort to the existing PI controller.

The chapter details the first stage of the development and implementation of a suitable controller for CRVs within a domestic setting. Here, a novel modelling method introduced, developed and tested. This method drastically reduces the implementation overhead associated with MPC controllers whilst improving performance of the central heating systems compared to conventional control methods. With this far greater ease of application, the use of MPC in conjunction with CRVs and conventional fluid filled central heating systems that are commonplace in the UK may now be realised. The ability to add such devices to an existing central heating system with minimum effort represents an economic opportunity to capitalise on the energy saving advantages offered by more advanced control strategies that have not previously been available, whilst preserving the existing heating system. The proposed MPC is, therefore, centred on an adaptive model of the heating zone using thermal measurements that would be taken from a CRV.

4.2. Thermal comfort and weather effects

ISO 7730 and ASHRAE 55 [5], [102] both define thermal comfort in terms of physiological and psychological satisfaction for occupants. Importantly, these are not directly used in the design of control systems, which use only zone temperature to affect the heat control. Thermal comfort is significantly affected by occupant behaviour, diet and clothing among other factors. For control purposes, therefore, typically a conversion between a subjective (standards/physiological) measure and an objective physical measure (temperature) for space heating, is required. Previously reported work presents many methods for bridging this gap, translating physiological and psychological sensations into hard temperature targets. The MPC strategy proposed in this paper relies on the success of such translations, aiming to achieve an 'ideal' dynamic heating response. Fig. 4.1 illustrates such an 'ideal' response compared to the measured response of a BS EN60730 thermostat controlled system. The BS EN60730 thermostat relies on a hysteresis operation to maintain a minimum desired temperature (in this case, 24°C). As proposed by Gladwin [88], one may make the assumption that the user will be satisfied by the lowest level of the hysteresis characteristic. Thus ideally after the initial start-up transient a perfectly flat temperature response is desired after set point has been reached, eliminating the possible loss in thermal comfort by the deviation in temperature and the energy wasted by heating the system past the set point.

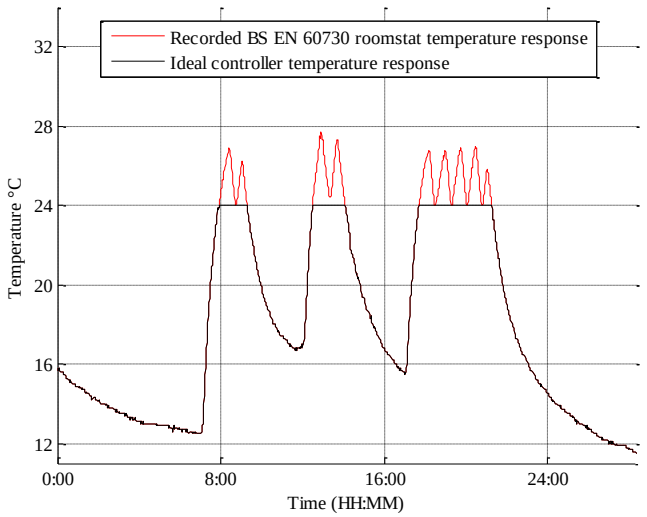

Figure 4.1: Ideal thermal response and traditional control thermal response

Recent studies examining advanced HVAC control [44], provide arguments that ambient temperature measurements with an accuracy of +/-0.5°C provide adequate resolution for most purposes and, therefore, provides the specification for *a maximum temperature ripple of +/-0.5 °C around the desired set-point*.

The previous research using predefined thermal models of buildings [43], [56], [69] use models or model structures that are obtained off-line. These are often Multiple Input Multiple Output (MIMO) models where the inputs include input (boiler) heating power and solar insolation and the outputs include heat emitter and zone temperature. These models have the advantage that they are of low-order, but usually require outside weather conditions to be measured together with zone ambient temperatures. To avoid the need for external sensors, weather data from external sources can be employed [44]. Certain HVAC scheduling products for large commercial premises, such as the aspectFT by AMM [103], have adopted this strategy. However, the additional cost and reliability of such data links makes their suitability for domestic dwellings questionable.

Examining ASHRAE and more recent weather data collected from a local Sheffield (UK) [104] based weather station it can be observed that the local outside temperature varies little day to day. Assessing the months October to March from 2006 to 2011 day to day, in the majority of cases (68%) mean temperature varies only by 2°C and rarely more than 4°C (in less than 6% of cases). From the analysis illustrated in Fig. 4.2 it can be surmised that day to day, the heating performance of a zone may vary little. As a result, it will be shown that it is possible to generate a model over a single heating period (or temperature response,) and use the resulting response as an a-priori model within a MPC framework for the following day.

For domestic applications it is essential that the 'advanced' heating controller be compatible with users' experiences of traditional heating control systems where typically one would set the zone/dwelling heated for periods that coincide with anticipated occupancy. Further investigation of the weather during those heating periods reveal little variation of outside temperature. The histogram depicted in fig 4.3 is for a building featuring three heating periods and shows only during the longer evening heating period, the outside temperature varies more than 1 °C in the majority of cases (54%) and varies less than 4°C in less than 5% of cases.

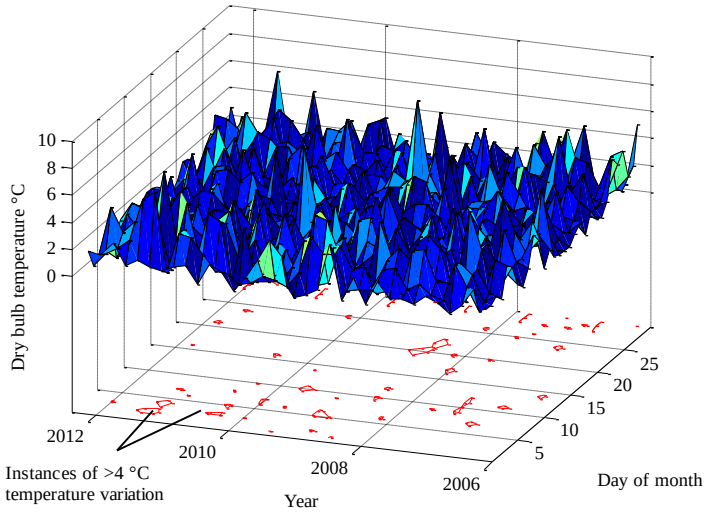

Figure 4.2: Mean day-to-day temperature variations 10/06-04/12

This then suggests that the external factors influencing heating only provide limited effects in the short-term (during a typical occupancy period). Consequently, the MIMO models normally used can be substantially simplified to Single Input Single Output (SISO) counterparts, where both input and output temperatures from each zone are measured—this is now made possible with the emergence of CRVs.

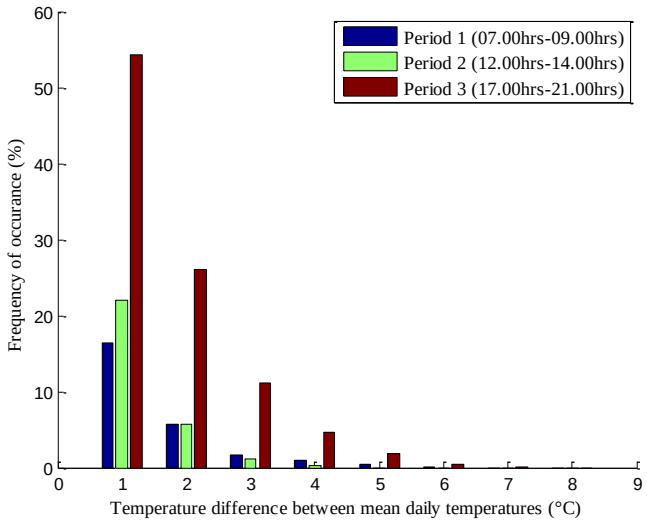

Figure 4.3: Frequency of mean day-to-day outside temperature variations 10/06-04/12

These assumptions have the benefit of mitigating the need for any a priori modelling to implement an MPC system in typical domestic environments. This is essential as any MPC system that relies upon a user/installer/commissioner generated model must be deemed impractical due to the current installation practice found in the UK and the EU. Peeters et al particularly highlight the need for a system that requires minimal commissioning as their surveys revealed very poor implementation of traditional control systems. As stated by Boait [40] any future interface should require minimal commissioning and user training/operation. Thus for any advanced system to achieve widespread adoption it is essential an even lower level of installer commissioning input is required for set up and to maintain successful efficient operation.

4.3. State space modelling and parameter identification

A popular analogy of the operation of an MPC controller is the process of a human being driving a car [105]. A human being controls the car via inputs (steering, throttle, gears etc.), and adjusts those inputs to maintain the desired speed and position on the road. The method and magnitude of adjustment the human applies to those inputs depends on their preconception of the car's performance, or in control terms, an a priori model. When approaching a steep hill the driver will apply throttle to ensure the car climbs the hill and reaches the top (a set point) but not in excess that may cause the car to pass uncontrollably over the other side of the hill (overshoot). The most important part of this analogy is what would happen if the driver changes type of car. The driver will now have an inaccurate model (from the previous car) but as experience tells us it is highly likely the driver will still be able to control the vehicle in a satisfactory manner as the many feedback mechanisms the driver has (eye sight, 'feel' of the controls etc.) will enable the driver to compensate for the difference in this car's a priori model.

The aim of this section is to develop a controllable model of the thermal zone for use with MPC. As highlighted is the previous section, one may assume on a day to day basis the model of the thermal zone changes very slightly. Following the car/driver analogy, this chapter confirms it is possible for a simple linear model obtained by propriety search algorithm the previous day to be suitable for use with an MPC controller operating a heated zone, any inaccuracies of that model compensated by the feedback provided by

continuous temperature measurement.

As previously discussed in chapter 3 the energy or heat loss through each surface area of the zone (wall, floor, ceiling) is represented by (1) where Q is the heat loss through the surface [W], Ψ is the coefficient of heat transfer [°Cm²W^{-1}], A is the area of the surface [m²] and T_1 and T_2 are the temperatures on each side of that surface.

$$Q = \Psi\Lambda(T_1 - T_2) \tag{4.1}$$

The heat loss may be added (or 'lumped') together with any other sources (heating system power output, heat flow from other zones). The net heat gain (or loss) is applied to the zone to give a net temperature gain (or loss). Therefore, assuming a linear approximation, the whole system can be represented by two first order equations (4.2-4.3), one for the emitter and one for the zone assuming outside temperature is constant.

$$\frac{dT_{em}}{dt} = \frac{(P_{input}) - \Psi_{em}\Lambda_{em}(T_{em} - T_{zone})}{(m_{em}c_{em})} \tag{4.2}$$

$$\frac{dT_{zone}}{dt} = \frac{\Psi_{em}\Lambda_{em}(T_{em} - T_{zone})}{\zeta_{zone}} - K_{loss}T_{zone} \tag{4.3}$$

T is temperature (°C), t is time (s), P is heat (W), c is specific heat capacity (Jkg^{-1}°C^{-1}) and m is mass (kg) of the *input* heat source, heat *emitter* (i.e. radiator), the *zone* (room) and *external* environment. As the outside temperature is assumed to be constant (and usually lower than the zone temperature), one may estimate the heat loss from the zone is solely dependent on the zone temperature. The value K_{loss} represents the zone heat loss constant, with units of [W°C^{-1}].

The heat losses from the zone now assumed to be only dependant on the constants specific heat capacity, mass, area and coefficient of heat transfer. These can be combined to form a single state space representation, where (4.2) and (4.3) become (4.4), where A is the state matrix, x the state vector, B the input matrix and u the input or control vector.

$$A_{11} = \frac{-\Psi_{em}\Lambda_{em}}{\zeta_{em}} \tag{4.4}$$

$$A_{12} = \frac{\Psi_{em}\Lambda_{em}}{\zeta_{em}} \tag{4.5}$$

$$A_{21} = \frac{\Psi_{em}\Lambda_{em}}{\zeta_{zone}} \tag{4.6}$$

$$A_{22} = \frac{-\Psi_{em}\Lambda_{em}}{\zeta_{em}} + K_{loss} \tag{4.7}$$

$$B_{11} = \frac{1}{\zeta_{em}} \tag{4.8}$$

$$\overbrace{\begin{bmatrix} \frac{dT_{em}}{dt} \\ \frac{dT_{zone}}{dt} \end{bmatrix}}^{\dot{x}} = \overbrace{\begin{bmatrix} A_{11} & A_{12} \\ A_{21} & A_{22} \end{bmatrix}}^{A} \overbrace{\begin{bmatrix} T_{em} \\ T_{zone} \end{bmatrix}}^{x} + \overbrace{\begin{bmatrix} B_{11} \\ 0 \end{bmatrix}}^{B} \begin{bmatrix} P_{input} \end{bmatrix} \tag{4.9}$$

The second order representation described in (4.9) has five unknowns (A_{11}-B_{11}) that determine the characteristics of the model. A more elegant solution is to rearrange the model in the canonical form. Considering the two differential equations that make up (4.9),

$$\frac{dT_{em}}{dt} = A_{11}T_{em} + A_{12}T_{zone} + B_{11}P_{input} \tag{4.10}$$

$$\frac{dT_{zone}}{dt} = A_{21}T_{em} + A_{22}T_{zone} \tag{4.11}$$

Further differentiating (4.11) to form (4.12) then substituting (4.10) into the result to form (4.13).

$$\frac{d^2T_{zone}}{dt^2} = A_{21}\frac{dT_{em}}{dT} + A_{22}\frac{dT_{zone}}{dT} \tag{4.12}$$

$$\frac{d^2T_{zone}}{dt^2} = A_{21}(A_{11}T_{em} + A_{12}T_{zone} + B_{11}P_{input}) + A_{22}\frac{dT_{zone}}{dT} \tag{4.13}$$

Rearranging (4.12) and substituting into (4.13).

$$\frac{d^2T_{zone}}{dt^2} = A_{21}A_{11}T_{em} + A_{21}A_{12}T_{zone} + A_{21}B_{11}P_{input} + A_{22}\frac{dT_{zone}}{dT} \tag{4.14}$$

$$\frac{d^2T_{zone}}{dt^2} = A_{11}(\frac{dT_{zone}}{dT} - A_{22}T_{zone}) + A_{21}A_{12}T_{zone} + A_{21}B_{11}P_{input} + A_{22}\frac{dT_{zone}}{dT} \tag{4.15}$$

Finally combining the original constants from (4.9) to form 3 new canonical constants, A_{c11}, A_{c12}, B_{c11} to form a new representation of the same system but in terms of only one measurement, zone temperature T_{zone} (4.16). This is presented in state space form by (4.17)

$$\frac{(d^2T_{zone})}{dt^2} = A_{c11}\frac{dT_{zone}}{dt} + A_{c12}T_{zone} + B_{c11}P_{input} \tag{4.16}$$

$$\overbrace{\begin{bmatrix}\frac{(d^2T_{zone})}{dt^2}\\ \frac{dT_{zone}}{dt}\end{bmatrix}}^{\dot{x}_{canonical}} = \overbrace{\begin{bmatrix}A_{c11} & A_{c12}\\ 1 & 0\end{bmatrix}}^{A_{canonical}}\overbrace{\begin{bmatrix}\frac{(dT_{zone})}{dt}\\ T_{zone}\end{bmatrix}}^{x_{canonical}} + \overbrace{\begin{bmatrix}B_{c11}\\ 0\end{bmatrix}}^{B_{canonical}}\begin{bmatrix}P_{input}\end{bmatrix} \tag{4.17}$$

The thermal model is now in controllable canonical form and no further assessments of the model are needed regarding its controllability (as this condition is automatically achieved). Each state represents one order of the heat transfer process, where the

minimum order is 2. For a n^{th} order system, (4.17) can be expanded to become (4.18). It should be noted that the states represent a lumped parameter model and do not correspond to any physical measurements or locations. In effect each state (order) could be considered to be a virtual temperature measurement node.

$$\begin{bmatrix} \frac{(d^{n}T_{zone})}{dt} \\ . \\ . \\ . \\ \frac{dT_{zone}}{dt} \end{bmatrix} = \begin{bmatrix} A_{c11} & . & . & . & A_{c1n} \\ 1 & . & . & . & 0 \\ 0 & 1 & . & . & 0 \\ 0 & . & 1 & . & 0 \\ 0 & . & . & 1 & 0 \end{bmatrix} \begin{bmatrix} \frac{(d^{(n-1)}T_{zone})}{dt} \\ . \\ . \\ . \\ T_{zone} \end{bmatrix} + \begin{bmatrix} B_{c11} \\ 0 \\ 0 \\ 0 \\ 0 \end{bmatrix} \begin{bmatrix} P_{input} \end{bmatrix} \qquad (4.18)$$

The parameters of (4.18) (Ac11 and Bc11) are found using a branching algorithm [106] (which is fully described in appendix II). This technique matches the previous day's response to the set structure of the canonical system model described above on-line while avoiding the need for a dedicated set of tests to characterise the system.

4.4. Branching Algorithm

To acquire the parameters of a system in the form described in the previous section a propriety search algorithm was devised to enable future implementation on inexpensive dedicated hardware.

The requirement of this algorithm is to provide an n^{th} order model of the set form from a training data set. Each heating period requires a dedicated training data set to form a dedicated model for each period. The training data set is the previous day's thermal response over the same heating period.

The training data set is consists normalised temperature (output or y) and normalised heat input (u) measurements for a heating period arranged in a two column vector. For the work presented here the time interval of the training data set was initially set to 1 minute to provide a good compromise between sampling resolution, wireless transmission reliability and training data set size. This interval was subsequently expanded to 5 minute during further trials (see later sections, PWM-MPC).

The curve fitting algorithm operates at predetermined times when there is no heating demand and so the computational overhead is kept to a minimum when the controller is active. An operation is required for each heating period, for the test cell three models are required thus three operations are required. Times chosen for each curve-fitting operation were 23:00hrs, 1:00hrs and 3:00hrs. A detailed description of the curve fitting procedure is included in appendix II.

4.5. Model Predictive Control

In Model Predictive Control a mathematical model of a system is used to predict behaviour of a real system to allow the optimum control signals to be chosen. More specifically, MPC uses plant information to predict the trajectory of the control or input variable u to optimise the plant output variable y while minimising a cost function J. MPC predicts the next N_p control moves (trajectory) using the model and the previous N_c control moves. A weighting factor λ, can be added to control the impact of varying the two horizons N_p and N_c. Since the time frame in which the optimisation takes place is advancing with respect to time, one may consider the horizons to be always moving away or receding. This type of control is often termed a receding horizon strategy.

This section describes a method for using the classical MPC control structure. Using (4.19) and (4.20), the continuous canonical SISO state-space model can be formed (assuming D = 0).

$$\dot{x} = Ax + Bu \tag{4.19}$$

$$y = Cx \tag{4.20}$$

$$A = \begin{bmatrix} A_{c11} & . & . & . & A_{c1n} \\ 1 & . & . & . & 0 \\ 0 & 1 & . & . & 0 \\ 0 & . & 1 & . & 0 \\ 0 & . & . & 1 & 0 \end{bmatrix} \quad B = \begin{bmatrix} B_{c11} \\ 0 \\ 0 \\ 0 \\ 0 \end{bmatrix} \tag{4.21}$$

$$C = \begin{bmatrix} 00001 \end{bmatrix} \tag{4.22}$$

The model can now be discretised using a zero-order hold with a time step of 1 minute and an integrator is embedded to form the new digital augmented model (4.25) and (4.26) [107].

$$x_d[k+1] = A_d x_d[k] + B_d u[k] \tag{4.23}$$

$$y[k] = C_d x_d[k+1] \tag{4.24}$$

$$\overbrace{\begin{bmatrix} \Delta x_d[k+1] \\ y[k+1] \end{bmatrix}}^{x[k+1]} = \overbrace{\begin{bmatrix} A_d & o^T{}_d \\ C_d A_d & 1 \end{bmatrix}}^{A_e} \overbrace{\begin{bmatrix} \Delta x_d[k] \\ y[k] \end{bmatrix}}^{x[k]} + \overbrace{\begin{bmatrix} B_d \\ C_d B_d \end{bmatrix}}^{B_e} \Delta u[k] \tag{4.25}$$

$$y[k] = \overbrace{\begin{bmatrix} o_d & 1 \end{bmatrix}}^{C_e} \begin{bmatrix} \Delta x[k] \\ y[k] \end{bmatrix} \qquad O_d = \overbrace{\begin{bmatrix} 00.....1 \end{bmatrix}}^{n} \tag{4.26}$$

Following the state-space representation of 4.23 and 4.24, *x[k]* and *Δu[k]* can now be calculated in terms of their future control moves. Considering *x[k],*

$$x[k_i+1] = Ax[k_i] + B\Delta u[k_i]$$
$$x[k_i+2] = Ax[k_i+1] + B\Delta u[k_i+1] \Rightarrow x[k_i+2] = A^2 x[k_i] + AB\Delta u[k_i] + B\Delta u[k_i+1]$$
....
$$x[k_i+N_p] = A^{Np} x[k_i] + A^{Np-1} B\Delta u[k] + A^{Np-2} B\Delta u[k+1] + ...A^{Np-Nc} B\Delta u[k_i+N_c-1]$$

and considering *Δu[k]* by substitution,

$$y[k_i+1] = CAx[k_i] + CB\Delta u[k_i]$$
$$y[k_i+2] = CA^2 x[k_i] + CAB\Delta u[k_i] + CB\Delta u[k_i+1]$$
....
$$y[k_i+N_p] = CA^{Np} x[k_i] + CA^{Np-1} B\Delta u[k] + CA^{Np-2} B\Delta u[k+1] + ...C\,A^{Np-Nc} B\Delta u[k_i+N_c-1]$$

The future moves of y where $Y = \overbrace{\left[y[k+1] + y[k+2] + y[k+3] \quad . \quad . \quad . \quad y[k+n]\right]}^{future\ moves}$ and ΔU and is shown by (4.27). The collated constants from the previous substitutions are now grouped in single matrices named F and Φ, shown by (4.28).

$$\Delta U = \overbrace{\left[\Delta u[k] + \Delta u[k+1] + \Delta u[k+2] \quad . \quad . \quad . \quad \Delta u[k+n]\right]}^{future\ moves} \tag{4.27}$$

$$\Phi = \begin{bmatrix} C_e B_e & 0 & . \ . & 0 \\ C_e A_e B_e & C_e B_e & . \ . & 0 \\ C_e A_e^2 B_e & C_e A_e B_e & . \ . & 0 \\ . & . & . \ . & . \\ . & . & . \ . & . \\ . & . & . \ . & . \\ C_e A_e^{(N_p-1)} B_e & C_e A_e^{(N_p-2)} B_e & . \ . & C_e A_e^{(N_p-N_c)} B_e \end{bmatrix} \qquad F = \begin{bmatrix} C_e A_e \\ C_e A_e^2 \\ C_e A_e^3 \\ . \\ . \\ . \\ C_e A_e^{(N_p)} \end{bmatrix} \tag{4.28}$$

The dimensions of Φ and F are governed by the prediction and control horizons, Φ being $N_p \times N_c$ and F being $N_p \times$ number of inputs.

$$R_s^T = \overbrace{[11...1]}^{N_p} r[k] \qquad\qquad \overline{R} = \lambda I_{(N_c \times N_c)} \tag{4.29}$$

Defining R_s and $\overline{R}$ (4.29) where I is an identity matrix, λ is the weighting factor and r[k] is the set point, the complete augmented model is defined as (4.30).

$$Y = Fx(k_i) + \phi \Delta U \tag{4.30}$$

A cost function can now be defined. A cost function J, that reflects the aim of minimising the errors between the predicted output y[k] and set point r[k] while penalising excessive controller effort can be represented by (4.31).

$$J = (R_s - Y)^T (R_s - Y) + \Delta U^T \bar{R} \Delta U \tag{4.31}$$

Substituting (4.30) within (4.31) and expanding the result in (4.32).

$$J = (R_s - Fx(k_i))^T (R_s - Fx(k_i)) - 2\Delta U^T \Phi^T (R_s - Fx(k_i)) + \Delta U^T (\Phi^T \Phi + \bar{R}) \Delta U \tag{4.32}$$

From the first derivative of (4.32) and solving to find the minimum of $dJ/d\Delta U$ arrives at the optimal solution of ΔU (4.33).

$$\Delta U = (\Phi^T \Phi + \bar{R})^{-1} \Phi^T (R_s - Fx[k_i]) \tag{4.33}$$

It may be noted that the cost function is a quadratic, and solving (4.33) subject to constraints would mean solving (4.32) with respect to linear inequalities defined by those constraints. Thus the problem of finding an optimal solution subject to those constraints would involve a quadratic programming algorithm. If we consider ΔU as the decision variable, the standard objective function becomes (4.34).

$$J = \frac{1}{2} \Delta U^T H \Delta U + \Delta U^T V \tag{4.34}$$

From Wang [107] the global optimal solution of objective function (4.35) is represented by (29)

$$\Delta U = -H^{-1} V \tag{4.35}$$

Thus H is represented by (4.36) and V by (4.37) as they are the constituent parts of the optimal solution (27).

$$H = \phi^T \phi + \bar{R} \tag{4.36}$$

$$V = -\phi^T (R_s - Fx(k)) \tag{4.37}$$

The inequality constraints are represented by (4.38) where M is a matrix *reflecting the constraints* and γ translates the magnitude of the constraint limits.

$$M\Delta U \leq \gamma \tag{4.38}$$

For a SISO system, if the normalised control input is constrained between 0 and 1 the M and γ matrices are (4.39).

$$M = \begin{bmatrix} 1 \\ -1 \end{bmatrix} \quad \gamma = \begin{bmatrix} 1-u \\ -0+u \end{bmatrix} \tag{4.39}$$

Thus H, V, M and γ are the compatible matrices and vectors of the quadratic programming problem. With H and V derived from the model and previous feedback variable ($x(k)$) the constraints are set by the limits of the controller used (in this case between 0.2 and 0.9 or 20% and 90% for the PAC, chapter 2)

4.5.1 Requirement for state observer

The methodology described here is sufficient for 2nd-order models. However, for model orders greater than 2, a state observer must be used to predict the virtual unmeasured states since only a single temperature measurement is usually available in each zone. Employing a Luenberger observer, (4.23) becomes (4.40) where G_{ob} is the observer gain matrix and $x_{ob}[k+1]$ is the estimated state matrix. The correction term allows the model inaccuracies to be compensated and control over the dynamic performance using observer gain matrix G_{ob} to suitably place the eigenvalues (poles).

$$x_{ob}[k+1] = \overbrace{A_d x_{ob}[k] + B_d \Delta u[k]}^{augmented} + \overbrace{G_{ob}(y[k] - C_d x_{ob}[k])}^{correction} \tag{4.40}$$

As the dynamics of the observer need to be significantly faster than the system itself the observer gain, G_{ob}, is calculated to place the eigenvalues to impart observer convergence dynamics that are a factor of 5 times the bandwidth of the dominant poles of the system.

4.6. Experimental set up

As described in chapter 2, a dedicated test cell was constructed to assess the efficacy of these proposed techniques. The test cell environment is employed for controller calibration purposes, with the resulting MPC-based scheduled identification and control systems then being transferred to the domestic dwelling to facilitate 'real-world' measurement collection and performance analysis.

4.7. Experimental Results

The experimental results are divided into two sections. The first analysis examines the suitability of using the canonical modelling method. The second section assesses the performance of the controller using the recursive modelling technique.

4.7.1 Model-Order Investigations (Test Cell Trials)

As described earlier, not only are the control moves predicted but the model on which MPC is based is obtained from a curve-fit to the previous day (or heating period) data. This model must be at least 2nd order but it may be possible for higher-order models to provide superior performance. Thus, this section describes an investigation into the effect of model order on the performance of MPC.

Measurements to compare the 2nd order model (section 3) with experimentally measured results have been trialled between 21/1/12 and 27/1/12, and using higher order models, between 22/2/12 and 1/3/12. Trials are separated into daily periods with: Period 1 07:00-09:00h, Period 2 12:00-14:00h and Period 3 17:00-21:00h. The primary purpose of the *model order investigations* is to assess the relative merits of using models of successively higher order (above the standard 2nd order). Studies therefore compare results with those of experimental measurements. Model parameters are generated using the best-fit branching algorithm described in section 3 in each case.

Two scenarios are considered. The first is where the branching algorithm is limited to providing 2nd order models only, and the second is where no bounds on the model order were explicitly defined.

To provide comparative quantitative assessments, performance metrics are used to evaluate the variations in performance when using the different models for system identification. Specifically:

- Set Point Tracking Error (SPTE): the mean error between the desired response (illustrated in figure 4.1) and the actual measured response over a single heating period.

- Modelling Error (ME): the mean error between the measured temperature response of the system and that provided by the canonical model where different orders of model are considered.

- Predicted ME (PME): the mean error between the previous day's model response (or temperature response) and the measured response of the current heating period using the previous day's model.

- Mean Energy Consumed (MEC): the mean energy consumed for each period, 1 2 or 3.

From the 18 heating responses investigated it was found a maximum model order of 5 provided an 'optimal fit' to various experimental measurements. More specifically, only 5% of cases resulted in a 4th order model with the remaining 95% being 5^{th} order. Their underlying performance quantified using the above metrics, in Table 1—note: Mean Total Solar Irradiance (MTSI) and Outside Temperature (OT) are also included as a measure of consistency

From the results in Table 4.1 it can be seen that the higher order models provide improved measurement tracking characteristics (ME), with 5^{th} order being 48% better than the 2nd order counterpart, and the PME typically being around 38% better over the measurement period. Of particular note, the trials using up to 5^{th} order models endured a higher level of external disturbance (solar insolation) during each of the three heating periods and still maintained superior modelling performance. Examining the specific values of ME and PME in more detail, the influence of external factors appear to have minimal influence

on modelling performance. For example the standard deviation between the 3 values of ME between periods 1,2 and 3 for the 2nd order modelling trial is 18% of the mean ME. For the 5th order trial this figure is within a similar range (14%). The trend is mirrored in terms of outside temperature variation. The outside temperature (OT) standard deviation between each heating period is 14% of the mean for the second order trial and also 14% for the 5th order trial. Considering the dramatic variation in actual measurement tracking (ME and PME) despite relatively consistent outside temperature variation (OT) it is clear that the choice of modelling method (2nd order or higher) has far greater influence than on performance external factors. This trend continues if the effects of solar insolation are examined. The standard deviation of the total solar irradiance (represented by MTSI, table 4.1) over the same three periods is 127% of the mean, a demonstration of how solar influence varies significantly during the day. However, such dramatic variation is solar irradiance appears not to effect the modelling ability, as the value of ME for period 2 (when solar irradiance peaks) for both the 2nd order and 5th order cases is the lowest (0.33 and 0.17 respectively).

Period	Performance Parameter	Maximum Model Order	
		2	5
1	MTSI (J/m^2)	82092	433386
2	MTSI (J/m^2)	1209019	2407393
3	MTSI (J/m^2)	184528	254509
1	OT (°C)	5.69	8.74
2	OT (°C)	7.27	11.36
3	OT (°C)	5.90	9.18
1	ME (°C)	0.38	0.18
2	ME (°C)	0.33	0.17
3	ME (°C)	0.46	0.22
1	PME (°C)	2.28	1.41
2	PME (°C)	2.58	1.32
3	PME (°C)	2.32	1.15

MTSI: Mean Total Solar Irradiance
OT: Mean Outside Temperature
ME: Modelling Error
PME: Predicted Modelling Error

Table 4.1: Summary of initial test cell modelling trials

4.7.2 MPC Realisation for Heating Control (Test Cell Trials)

Following the treatment by Gouda [43], a variable electrical supply and oil filled radiator is used as the primary heat source for the closed-loop experimental trials, in effect emulating a water filled heat emitter and CRV. The heat source is directly controlled by a phase-angle power converter that mimics the operation of the CRV, together providing a variable power source input to the heating zone (see chapter 2). For this investigation the control input in this case has fixed limits of 20% and 90% duty, enabling the 'optimal' control input from the MPC scheme to be converted to a realisable power input to the heat emitter—the constraints are imposed due to practical limitations of using the phase angle controller that can only maintain variable control inputs at a accuracy of 1% between these limits. However, the phase angle controller is also able to be operated in an on/off binary mode, thereby facilitating an effective switch-off between heating trials i.e. an effective control input of 0% duty.

Models obtained from parameter matching the heating response during each respective period on the previous day, are used as basis for closed-loop control of the heat source for the same period on the current day. Between measurement acquisition and use of the model on the next day, the MPC controller is tuned. Tuning is completed by simulation, using the acquired data together with the MPC controller and model with a range of parameter sets. After each simulation, the performance of the model is evaluated using the SPTE in order to select the best parameter set. Model parameters that provide the lowest SPTE are used for MPC heating control on the next day. In this manner, the models and resulting MPC realisation are periodically updated every 24 hours. The complete control structure is illustrated in fig. 4.6.

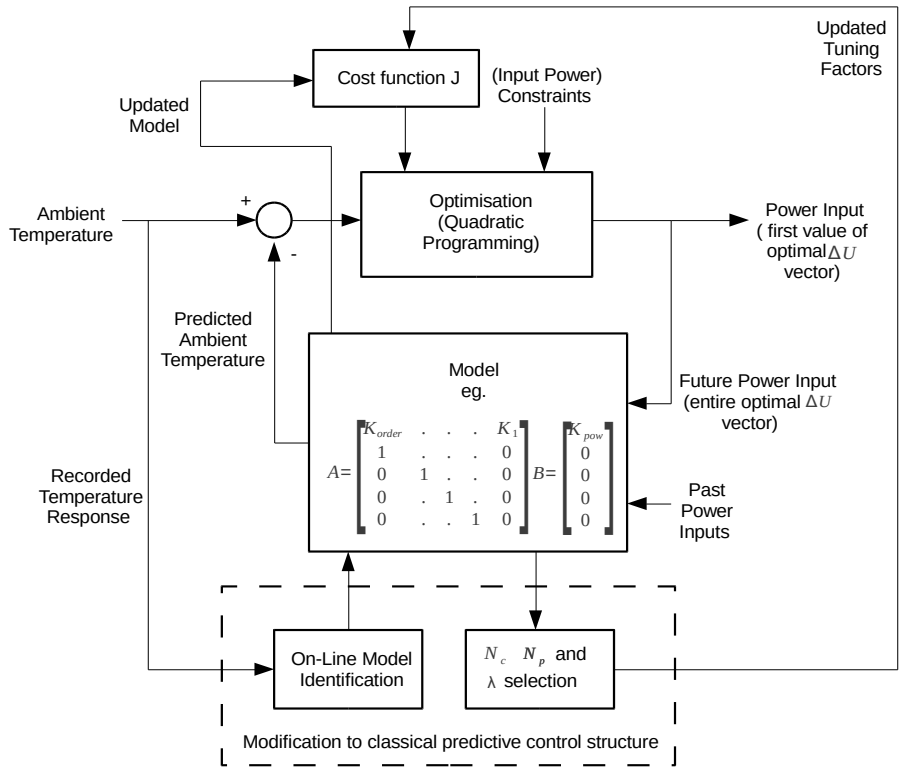

Figure 4.4: Modified classical MPC structure

In practice, the 2nd order model would be the preferred choice for control purposes since it negates the requirement for the implementation of an additional state-observer when using higher order models, and their respective pole-placement requirements, which then necessitates an additional empirical 'tuning' procedure. Nevertheless, it is instructive to consider the merits of using the demonstrably more accurate 5th-order model, with the inclusion of a state-observer, for comparison purposes. Consequently, all initial tests are conducted using both the 2nd (eqn. 10) and 5th (eqn. 11) order. A summary of results from the trials, benchmarked against the performance metrics, are shown in columns 3 & 4 of Table 4.2. For completeness, example real-time responses from both the 2nd and 5th order matched responses, are given in fig 4.4 and fig 4.5.

Comparing trials period for period (table 4.2), the energy use by each trial was relatively consistent. One may conclude that the dominant weather characteristics (MTSI and OT) had more influence on the energy consumption than the change in controller configuration as the performance change (higher energy use) follows the inverse trend in weather (less insolation and lower outside temperatures). The marked change in energy consumption

occurs with the 2nd period, dropping by over 20% following an OT increase by over 3°C and increased TSI of 50%.

Period	Parameter	Model Order		PWM-MPC
		2	5	
1	MTSI (J/m^2)	82092	433386	657555
2	MTSI (J/m^2)	1209019	2407393	n/a
3	MTSI (J/m^2)	184528	254509	5940200
1	OT (°C)	5.7	8.7	7.4
2	OT (°C)	7.3	11.4	n/a
3	OT (°C)	5.9	9.2	8.9
1	MEC (kWh)	0.78	0.75	1.44
2	MEC (kWh)	0.69	0.54	n/a
3	MEC (kWh)	1.40	1.32	1.35
1	SPTE (°C)	0.21	0.14	0.14
2	SPTE (°C)	0.21	0.22	n/a
3	SPTE (°C)	0.21	0.19	0.15

MTSI: Mean Total Solar Irradiance
OT: Mean Outside Temperature
MEC: Mean Energy Consumed
SPTE: Set Point Tracking Error

Table 4.2: Summary of thermal comfort during preliminary test cell trials

Examining the SPTE performance of both trials, the first trial set (column 3, Table 4.2), uses the 2nd order model for parameter matching, and therefore does not incorporate the use of an observer. It can be seen that a mean set point tracking error of < 0.22°C is achieved during all heating periods. Moreover, despite solar irradiance and external temperature increasing during Period 2, SPTE remains unchanged. Unlike the results from the modelling investigations, the combination of model and MPC in a feedback configuration shows that the actual thermal comfort performance improvement using the 5th order model is less apparent—see results in Table 4.2. Negligible change occurs during the 2nd and 3rd heating periods, and SPTE only improves by 33% during the 1st heating period.

With only minor improvements in performance attributable to the 5th order model, and with the added complication of using and tuning a state observer provides a substantial motivation for adopting the 2nd order model identification procedure for practical

purposes.

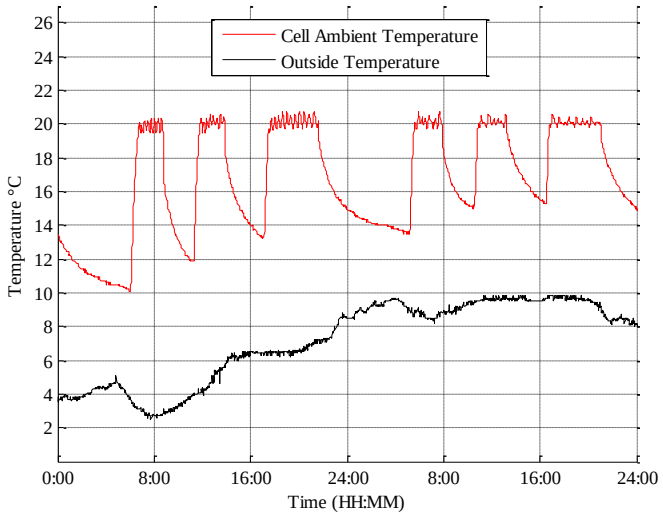

Figure 4.5: Test cell temperature control using 2nd order model

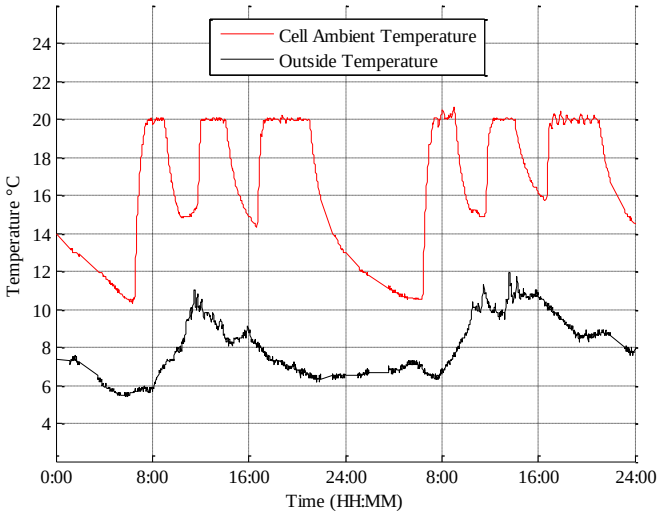

Figure 4.6: Test cell temperature control using 5th order model

4.7.3 The use of PWM controlled heat sources (Test Cell Trials)

For advanced control methodologies to be extensively applied to domestic dwelling environments, in the short term they will have to be used largely as retro-fit solutions

using control schemes that can be readily integrated into current system component technologies. This has also been highlighted by Castilla [69] who showed that an ideal strategy for coupling a fully controlled power input (or heat source) using advanced control schemes, to a HVAC devices, is to use only two modes of 'actuation' viz. on and off ([69] term this Pulse Width Modulation or PWM). Ultimately, the use of this technique has the advantage of greatly simplifying the operation of future CRVs, since they need only operate at discrete (binary) quantised duties, allowing for more cost-effective solutions. Furthermore, it allows HVAC devices that typically operate using on/off thermostats (eg. boilers, fans, or water filled heat emitters) to be readily integrated into a MPC methodology. Consequently schemes are allowed to be tested using an existing central heating system with minimum disturbance to the occupiers. The accommodation of the PWM is therefore an important consideration to enable investigations using test cell trials to be extrapolated to those with other heating zones using existing equipment (i.e. the domestic dwelling discussed in section 5 in this case).

To conclude the test-cell investigations, therefore, the MPC controller is now realised using quantised duties for the heat source, and the impact on the dynamic response of the heating characteristics is investigated—in order that it does not show significant degradation of control performance. In this way, the tests mimic the behaviour of an existing heating system by operating the on/off thermostat input of the boiler using a PWM-output—the most economically beneficial method.

4.7.4 PWM Experimental Results

To investigate the effect of reduced control input resolution, two extended heating periods, respectively of 4 and 5 hours duration, conducted between 22/4/12 and 29/4/12, are used. In line with the treatment described in [69], the maximum period of PWM output period is chosen to be 5 minutes, with discrete quantized duties of 0%, 20%, 40%, 60%, 80% and 100%. The thermal responses from the trials are shown in fig 4.7. By comparison with the results from the 'ideal' response described in Section 1, it can be seen that commensurate performance exists.

More specifically, Table 4.3 shows the resulting SPTE values recorded using the PWM

strategy, where it can be seen that all results meet the required specifications, with less than +/- 0.5°C temperature deviations within the test cell. Notably, some improvement in response is actually exhibited when compared to previous results (Tables 4.1 and 4.2)—however, the trials were undertaken over different heating periods during more a mild weather period as evidenced by the different solar irradiance and temperature levels. Nevertheless, the results provide a significant degree of confidence about the applicability of the PWM heating control scheme within an MPC methodology.

Period	Performance Parameter	Maximum Model Order		PWM Input	Dwelling (Modulated)
		2	5		
1	SPTE (°C)	0.21	0.14	0.14	0.13
2	SPTE (°C)	0.21	0.22	n/a	n/a
3	SPTE (°C)	0.21	0.19	0.15	0.48
SPTE : Set Point Tracking Error					

Table 4.3: Summary to compare continuous control input vs. modulated input

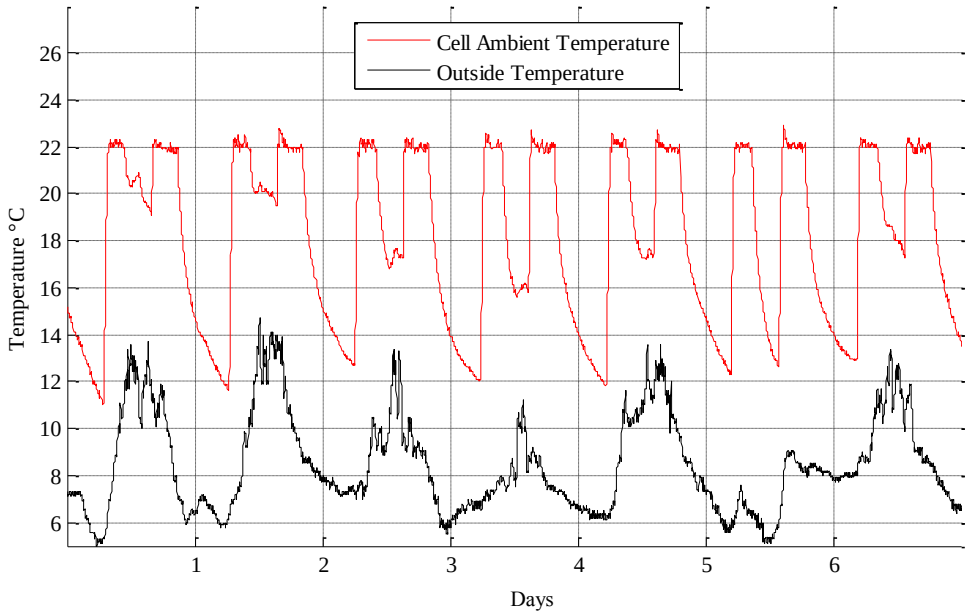

Figure 4.7: Test cell under PWM control

The energy consumption figures for both periods using the PWM-MPC controller were again weather dependant. The most interesting point to note is that despite period 1 being an hour shorter, the MEC figure is 6% greater than the 2nd period. Observing figure 4.7, one can conclude that the solar gain provided during the middle of the day for all but the 28/4/12, substantially aids to reduce the energy consumption. The initial temperatures of all the 2nd periods are indeed greater by as much as 12°C, giving a significant boost to the thermal response.

4.8. Energy savings offered by the control methodology

The PWM-MPC trials using the test cell demonstrate the methodology does achieve the required specifications. One may state thermal comfort is improved due to reduced temperature fluctuation (<+/-0.5°C compared to +2°C offered by the most common heating controllers). To quantify any energy savings achieved is more problematic, as any direct 'real test' comparison is subject to the vagaries of the weather. The probability of two identical weather profiles occurring sequentially to enable direct comparison when testing is minimal.

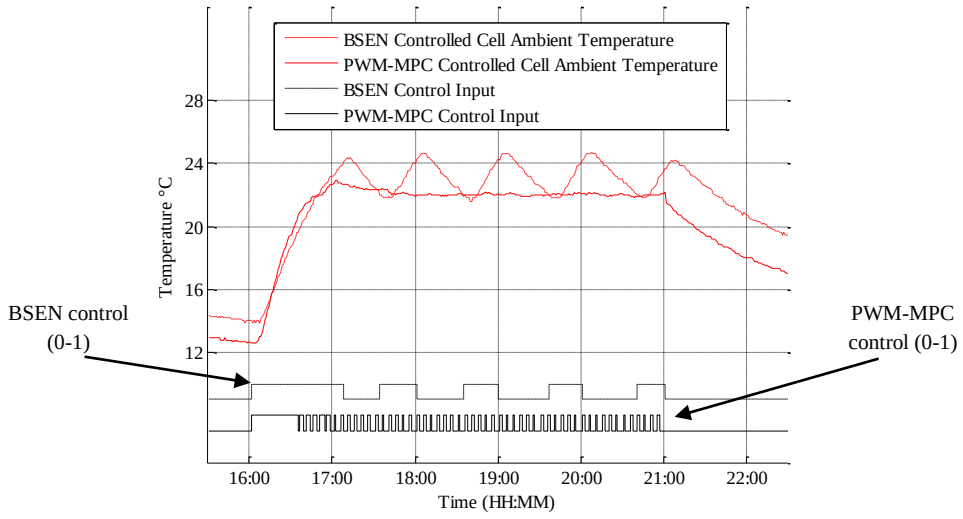

Figure 4.8: Comparison of BSEN and PWM-MPC control

For benchmarking purposes, a BS EN thermostat had been trialled during December 2011. As identical weather profiles are improbable, the preferred commensurate weather profiles to use for comparison offer fewer disturbances to the tests (lower levels of solar

gain). The lowest levels of solar gain during the PWM-MPC tests occurred on the 28/4/12. By choosing the heating period from the bench marking tests with the highest mean outside temperature and negligible solar gain for comparison, a considerable bias favouring the BSEN thermostat has been applied. Such a comparison thus represents the worst possible case scenario for the PWM-MPC controller; using BS-EN thermostat control over that period consumed 1.97 kWh. During the same period (December), with colder outside temperatures, the PWM-MPC test cell only consumed 1.54 kWh, achieving an energy saving of 22%. Both responses are illustrated in fig 4.8. The operation of the PWM of the RM-MPC controller can be clearly be observed, initially remaining 'ON' at start up (16:00hrs~16:30hrs) then reducing to a smaller duty cycle for the remainder of the heating period.

4.9. MPC in a Domestic Dwelling

To demonstrate the practical benefits afforded by the proposed methodologies it is important to consider their implementation in an occupied domestic dwelling. Consequently, a traditional existing central heating system has been modified, by interfacing a PWM signal to the central boiler unit as described in chapter 2. Trials of the PWM-output MPC control scheme conducted between 22/4/12 and 29/4/12.

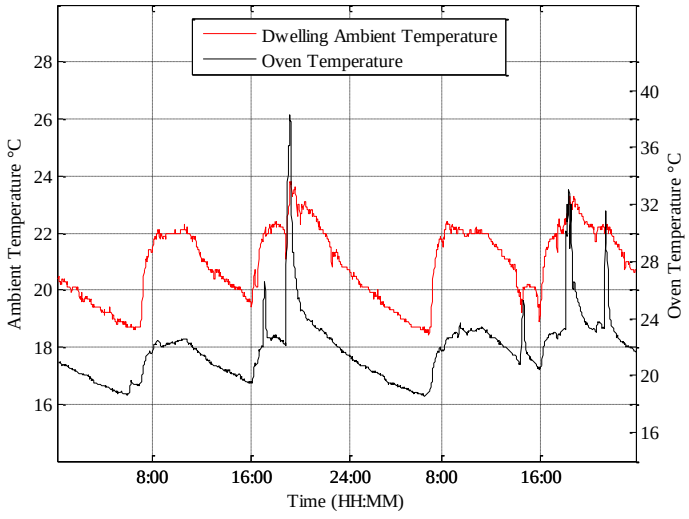

Figure 4.9 Dwelling under PWM-MPC control

The real-time measurements from the trials are shown in Figure 4.9 and presented in Table 4.3. It can be seen that whilst accurate temperature tracking is demonstrated between

08:00 and 11:00, for instance, there also exist periods when significant overshoot is present, >1°C. This is due to heat contributions resulting from the use of cooking appliances in the dwelling during these times, as is demonstrated by the rise in temperature measured 1.5m above the main cooking appliance (oven). Examining fig 4.7, the test cell exhibits no overshoot characteristic occurs as there is no such disturbance source present within the cell. Since the total contribution of the HVAC and other appliances is always summative (there is no cooling mechanism in the test dwelling), this can only be accommodated if prior knowledge of user behaviour is incorporated, or 'learned' a-priori and incorporated into the control scheme. The temperature response of the dwelling during heating period 1 (when no such disturbances are present) closely follows the test cell performance i.e. exhibits a temperature profile characteristic almost identical to the required response described in section 2.

For completeness, the performance metrics are evaluated and given in Table 4.3, which again show the dwelling performing within specification despite significant disturbance from the cooking appliance. With no such disturbance (during the morning heating period) the dwelling endures only a fluctuation in ambient temperature of only +/- 0.13°C around the ideal response, lowest SPTE of all the tests.

4.10. Summary

The chapter detailed the development and implementation of a MPC controller, suitable for use in conjunction with conventional fluid filled central heating systems that are commonplace in the UK. A proposed recursive modelling technique has been shown to offer excellent set point tracking, and at least comparable to the current state-of-the-art systems employed in dwellings. Comparing energy use from the Test Cell using a traditional BS EN 60730 and MPC-PWM controlled system produced an energy saving of 22% during a commensurate weather profile. The short term tests listed in this work prove the efficacy and the viability of this technique and certainly indicate its potential benefits, particular in the case of stabilised thermal comfort levels. However as the previous discussion has detailed, to accurately quantify the definitive energy saving abilities of the controller, long term tests are required to compensate for short term disturbances caused by weather variation.

The presented MPC controller has mitigated the need for any method of weather prediction or real-time external measurements, thereby reducing controller cost. Moreover, no provisional measurements of the zone(s) being heated are necessary, making this system ideal for the domestic householder. Most importantly it has been proven that MPC can be applied in a domestic situation with minimal input from the user or installer. Now the modelling and control method can be expanded to utilise the constraint handling characteristics of MPC which could promise further energy savings, reduced wear of mechanical parts or even optimal heating of zones according to energy prices. The dwelling tests prove that the control method is effective, and that PWM control of heating components is readily accommodated.

The first of the building blocks of an adaptive scheduling system for domestic hydronic heating system has been devised successfully. The next chapter details the development and refinement of the RM-MPC controller into a prototype of a practical system, using inexpensive Commercial-Off-The-Shelf (COTS) hardware including inexpensive CRVs and a microcontroller based controller as opposed to a PC operated one.

Chapter 5. Refinement of the Recursive Model Predictive Control (RM-MPC) system

5.1. Introduction

The previous chapter introduced the concept of Recursive Modelling in the context of its application to the MPC of domestic hyrdronic heat systems. Under the strictly controlled conditions within the test cell the concept had proved successful at providing superior control to the most prevalent systems found in dwellings in the UK. Most importantly, MPC was successful due to the adaptive nature of Recursive Modelling which provided robustness to model parameter approximations. However, the test cell experiments employed an emulator with a response close to the performance of an ideal CRV. Furthermore, using the Recursive Modelling (RM) MPC controller as replacement for a standard roomstat using a PWM technique will lead to an increase in central heat source cycling.

In this chapter, in an effort to realise the proposed control method in a practical manner, the RM-MPC is refined in this chapter for three reasons: 1) The RM principle is valid, but the branching algorithm could prove to be too intensive when implemented on an inexpensive microcontroller when the control system is expanded. 2) The CRV implemented within the test cell was actually an abstraction, using an oil filled heat emitter and phase angle controller. There are no CRVs which have comparable performance that would be an economic proposition to the householder. 3) The ability of the control method to operate an oversized heat emitter was not examined in the previous chapter.

In an attempt to address these points, this chapter presents a new family of Recursive Modelling Model Predictive Controllers (RM-MPCs) for use with low cost thermic CRVs. Furthermore, the Recursive Modelling MPC controller (RM-MPC) is now expanded to enable a Multi Input Multi Output (MIMO) framework to be employed to more accurately represent a multi zone dwelling. The ability of the presented control methodologies to maintain superior temperature regulation despite the use of oversized heat emitters, is a key contribution of the chapter. Moreover, unlike previously the reported modelling techniques used in chapter 4, the underlying recursive modelling method has been

reformulated so that traditional parameter matching calculations do not now require a computationally intensive curve fitting stage. A comparison of control techniques is included using experimental measurements from both an oversized oil filled heat emitter within a test chamber, and also from BS EN 442 water-filled heat emitters within an occupied dwelling. Results show the proposed methodologies can be realised using more cost-effective thermoelectric valves, whilst providing superior set point tracking.

The chapter is organised as follows: Section 5.2 provides an assessment of traditional TRV performance, identifying and clarifying the relative merits of currently employed control methodologies. Section 5.3 describes the principles of MPC and Section 5.4 introduces the proposed recursive modelling concept, the improvements in the modelling procedure and describes the introduction of a smith controller. Section 5.5 details the specification of test equipment used, and Section 5.6 discusses the relative performance of the proposed controller. Finally section 5.7 concludes the chapter by offering insight into the possibilities afforded by the new system.

5.2. Classical Thermal Control of Dwelling using TRVs

In the previous chapter the viability of the RM-MPC controller was first proven by using an emulated CRV within the strictly controlled conditions of the test cell. Subsequently the controller was used to operate a central boiler unit as part of real heating system within an occupied dwelling. To further assess the relative merits of the proposed control methodology compared to the currently employed techniques, in this chapter the test dwelling has been re-commissioned for more test purposes. This chapter details the first use of the RM-MPC controller in combination with real CRVs.

Initially, the dwelling, and its control performance, is monitored without modifying its existing TRV controlled central heating technology. The trial is used to highlight common deficiencies associated with systems deployed in UK homes, and provides a benchmark against which the performance of subsequent solutions/methodologies/tests can be compared. The dwelling trials were conducted the between 24/2/13 and 3/3/13. For all subsequent dwelling trials, Period 1 refers to daily times between 6:00hrs and 10:00hrs, and Period 2 between 16:30hrs and 22:00hrs.

5.2.1 Classical TRV performance monitoring

Within the occupied dwelling, 4 zones are TRV controlled; zone 1 (study), zone 2 (back bedroom), zone 3 (kitchen) and zone 4 (front bedroom). Upstairs and internal doors are opened only for normal entry (exit) to (from) each zone, and zone 7 door is only closed during periods of no human occupancy. The remaining zone doors are always open. The dwelling's habitants are 3 working adults; 2 of which are subject to shift-work, and the 3rd predominantly working from the dwelling (as a working-from-home base).

To provide for quantitative performance comparisons in what follows, two metrics have been adopted, viz.:

- Set Point Tracking Error (SPTE): the mean error between the desired response and the actual measured response over a single heating period once the set point has been achieved. Here the desired response is considered deadbeat.

Thus any discrepancy between the start of the heating period and when the zone first reaches the set point (the start-up transient) is ignored, as this is highly dependent on the initial temperature and can dominate the performance measure and hide any behavioural differences whilst at the set point temperature.

- Maximum Overshoot (MO): mean maximum difference between desired set point and the peak temperature over a single heating period.

- Time Constant (TC): mean time taken to reach $(SP\text{-}T_{initial}) \times (1\text{-}e^{-1})$ where SP is the user defined Set Point and T_{intial} is the initial temperature before heating commences. This figure allows rise time of the thermal responses to be compared.

Results from initial TRV assessment trials are summarised in table 5.1. In each controlled zone the temperature is measured at a height 50mm above the TRV head and at the heat emitter inlet to indicate heat emitter status. The ambient temperatures are also recorded at a height of 1.5m above floor (representative of standard thermostat placement height – indicated as SHT fig. 5.1) level in the zones with distributed furniture arrangements

(zones 1 and 4). Each of these sensors were mounted midway on the north wall of each zone (marked as a red box in figure 5.2).

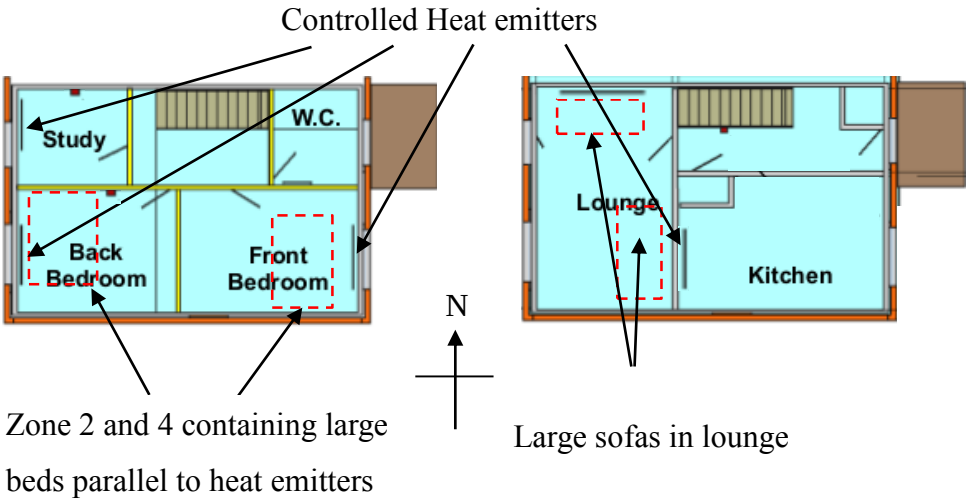

Figure 5.1: Dominant dwelling furniture placement

	Front bedroom		Back bedroom		Kitchen		Study	
Period	1	2	1	2	1	2	1	2
SPTE (°C)	0.75	0.66	1.66	1.29	0.92	0.61	0.55	0.48
MO (°C)	1.91	1.77	4.23	3.3	1.48	1.24	1.64	2.18
TC (mins)	15	12	17	12	17	22	12	13

Table 5.1: TRV assessment test summary

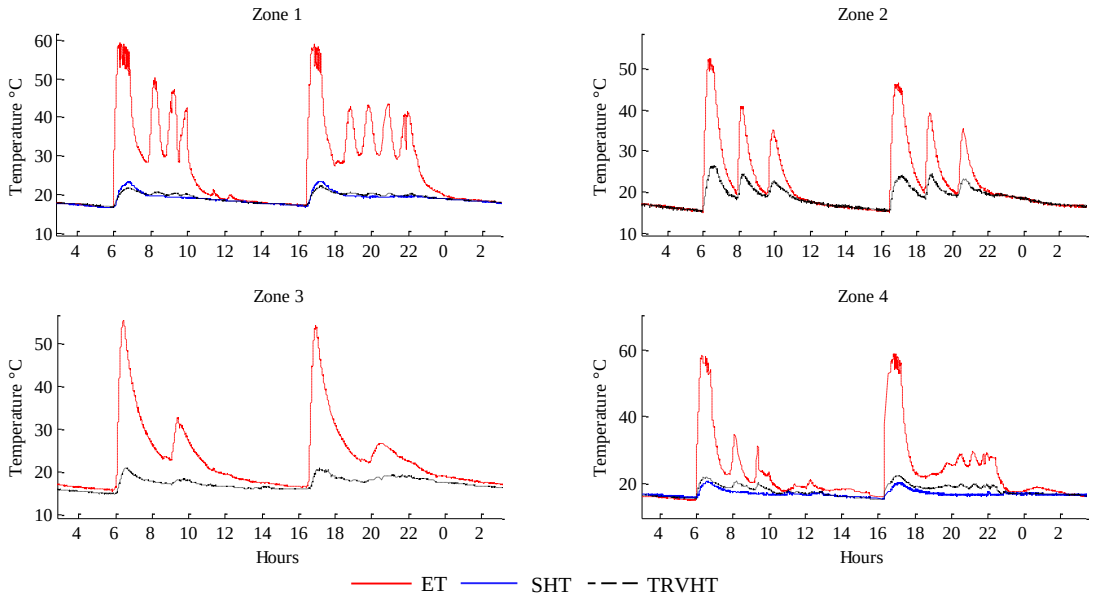

Figure 5.2: Temperature responses of TRV controlled zones (ET – Emitter Temperature, SHT – Standard Height Temperature, TRVHT – TRV Height Temperature. 24/2/13)

From the example measurements in illustrated fig. 5.1 and table 5.1, limitations of traditional TRV systems are evident i.e. each zone is subject to an MO of at least 1.24°C, and in the case of zone 2, a hysteresis temperature profile can also be seen resulting in a MO of > 4°C. The SPTE shows similar trends to the MO performance, where the oscillatory behaviour in zone 2 results in a 71% decrease in performance (0.48°C to 1.66°C) compared to the more sparsely furnished zone 1. It is evident therefore that placement of furniture and furnishings is crucial for the effective operation of the TRV system. All three upstairs zones use identical TRVs but their control performance, and in particular their temperature profile around set points, differ markedly. There are two distinguishing features between all the three zones. The first is the location of furniture and furnishings, with zones 2 and 4 having large beds placed in parallel with the heat emitters. Zone 1 notably has much lower amounts of furniture compared to Zones 2 and 4. The second is that the Kitchen, Zone 3 has a cast iron type heat emitter with significantly larger thermal mass. The effect of this can be seen in the slower thermal response of that zone, particularly in the second period (P2).

The need for a superior control methodology is therefore clear from the performance

assessment using classical TRVs and control structures. Specifically, such systems are limited by furniture and other obstruction placement and can exhibit large overshoot in more mild weather conditions, wasting energy and causing occupant discomfort. The benefits of the proposed RM-MPC controllers stem from their adaptive nature, using a training period of only 48hrs, and their predictive ability to accommodate changing zone topology (for example, addition/change of furniture or a change in the internal structure of the dwelling).

5.3. Model Predictive Control (revisited)

A general formulation of the state space description of the underlying system to be controlled is given by:

$$x[k+1] = A_d x[k] + B_d u[k] \tag{5.1}$$

$$y[k] = x[k] \tag{5.2}$$

Where x is the vector of state variables, u the control variable, y the measured output, and k is the present sample (time interval) under consideration.

Similar to chapter 4, considering SISO systems the model matrices, A_c, B_c and C_c, are required to be determined from a measured thermal response. The updated process for obtaining these model matrices is described in the next section.

5.4. Updated method of obtaining an appropriate thermal model of controlled zones

A key feature of the formulation of an MPC controller is the acquisition of a suitable system model. The RM-MPC controller described in the previous chapter relies on the repeated operation of curve fitting. In a bid to reduce the computational overhead incurred by the process of curve fitting, simplify the hardware requirement and increase the modelling accuracy a new approach was devised.

To enable detailed examination the dynamics of a typical dwelling hydronic heating

system to be controlled, a series of trials are undertaken to assess their thermal characteristics in the test-cell—considered as representative of a single isolated zone. The Dimplex OFC2000 column oil-filled heat emitter is used as a heat source within the test-chamber, controlled by a BS60730 thermostat for two periods per day, (Period 1 = 7:00hrs -11:00hrs and Period 2 = 13:00hrs-17:00hrs). The tests were undertaken between 6/1/13 and 12/1/13.

For completeness, additional sensors were placed centrally within the test cell at heights 1.0m, 1.5m and 1.8m. From the recorded temperature measurements depicted in fig. 5.3, it can be seen that the temperature distribution is highly dependent on the physical height of the measurement sensors. This is known as heated-zone stratification, where the stabilisation of the temperature distribution within a zone separates into a series of temperature 'levels', and has been studied previously by Innard [108] and Howarth [109].

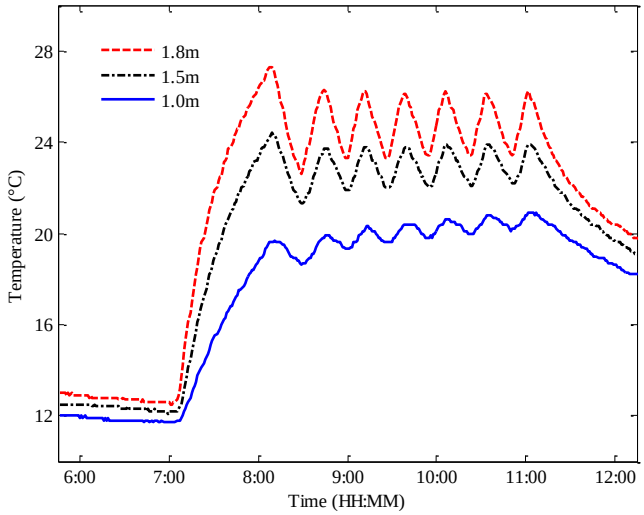

Figure: 5.3 Stratification of ambient temperature

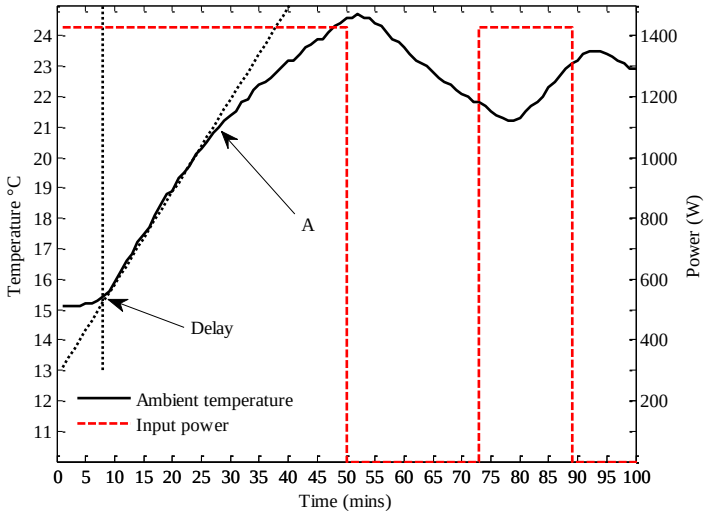

Figure 5.4: Typical test cell thermal response

On closer inspection of the temperature measurements (fig. 5.4) it is evident that two distinct dynamic characteristics are present viz. the transient response, and the steady-state hysteresis response about the set point. Each is represented by a separate dynamic model and a switch between each model occurs at pre-defined conditions. Notably, both the transient response, and the steady-state response about the set-point can be predominantly described by a delayed first-order model prototype to capture both the dynamics and inherent time lag that is inherent in the heating system. When generalising to multi-zone environments, the use of a set of independent first-order models (one for each zone) is preferable since the dynamics of each zone can then be readily combined into a state-space (MIMO) representation, that is readily expanded, and where the system order corresponds to the number of controlled zones.

In contrast to the investigation reported in the previous chapter, use of the proposed 1st order with delay matching scheme facilitates significant reductions in computational load, enabling the use of more cost-effective hardware. The type of control required is readily incorporated on traditional microprocessors used in central heating systems. This is in contrast to other recent reported work that employed dedicated PCs or dedicated controllers requiring substantial processing power [31], [41], [44], [70], [71]. These finding form the basis for a 1st order based model on which the proposed controller is based.

5.5. 1st order model prototype

The net heat gain/loss [W] from a zone can therefore be described by:

$$Q_{net} = Q_{gain} - Q_{loss} \tag{5.3}$$

Where Q_{gain} is equal to the heat input generated by the heat emitter within the zone, and Q_{loss} represents the losses from the zone due to conduction, radiation and convection. As described in section 2, preliminary monitoring of the test dwelling demonstrates neighbouring zones exhibit different thermal characteristics in response to their individual stimuli. This distinct behaviour between zones indicates that the influence of neighbouring zones can be considered negligible for the construction of a suitable RM-MPC model. Defining T_z as the ambient temperature of a zone, with K_{loss} representing an unknown heat loss constant with units of [W/°C], K_{loss} and T_z can be substituted into (5.3) to give:

$$Q_{net} = Q_{emitter} - K_{loss}T_z \tag{5.4}$$

One may note that (5.4) is equating the temperature loss that is due to the temperature difference between zone and external temperature is now solely dependent to temperature within the zone. The additional energy input (E [J]) required to change the temperature (by δT [°C]) of a sample mass (m [kg]) is given by:

$$Q = mc\delta T \tag{5.5}$$

Where c is the specific heat capacity of the material [J/kg°C]. The incremental change in energy required w.r.t. time therefore gives the required heating to affect a change in temperature w.r.t time:

$$Q = \frac{mc\delta T}{dt} \Rightarrow \frac{\delta T}{dt} = \frac{Q}{mc} \tag{5.6}$$

From (5.4), (5.5), (5.6), a 1st order differential equation can be constructed that describes the temperature change within a zone, T_z (assuming lumped parameters):

$$\frac{\delta T_z}{dt} = \frac{(Q_{emitter}) - K_{loss}T_z}{m_z c_z} \Rightarrow \frac{\delta T_z}{dt} = -\frac{K_{loss}T_z}{\zeta_z} + \frac{Q_{emitter}}{\zeta_z} \tag{5.7}$$

Where $m_z c_z = \zeta_z$ for a particular zone z.

From (5.7), at steady state ($dT_z/dt = 0$), heat losses from the zone equal the heat input into the zone, $Q_{emitter} = K_{loss}$, or alternatively $T_z = 1$. Since each zone's environment is relatively constant with only incremental changes seen each day, it can be assumed that the solar gain and contributions from other sources remain similar over a two day rolling window period and so it is possible to use the previous day's thermal characteristics to determine K_{loss}. A 1st-order linear time invariant state space model for the system is therefore described by:

$$\overset{\dot{x}}{\left[\frac{dT_z}{dt}\right]} = \overset{A}{\left[\frac{K_z}{\zeta_z}\right]}\overset{x}{[T_z]} + \overset{B}{\left[\frac{1}{\zeta_z}\right]}\overset{u}{[Q_{em}]} \qquad \overset{y}{[T_z]} = \overset{C}{[1]}\overset{x}{[T_z]} \tag{5.8}$$

Where $K_z = K_{loss}$ when referring to an individual zone, z.

With 1st-order dynamics now formulated for a particular zone, a method for incorporating a delay into the structure is needed. Classically (see [110] for instance) incorporating time delays within the state space model results in high-order approximations to accommodate delays much greater than the sample period. To reduce the computational overhead therefore, an alternative solution used here is to employ a Smith-predictor, which has recently gained popularity for use with MPC controllers [111]–[114]. The predictor (fig. 5.5) consists of a model of the system with a time delay to effectively provide information to the controller during the interim period when the delay is acting.

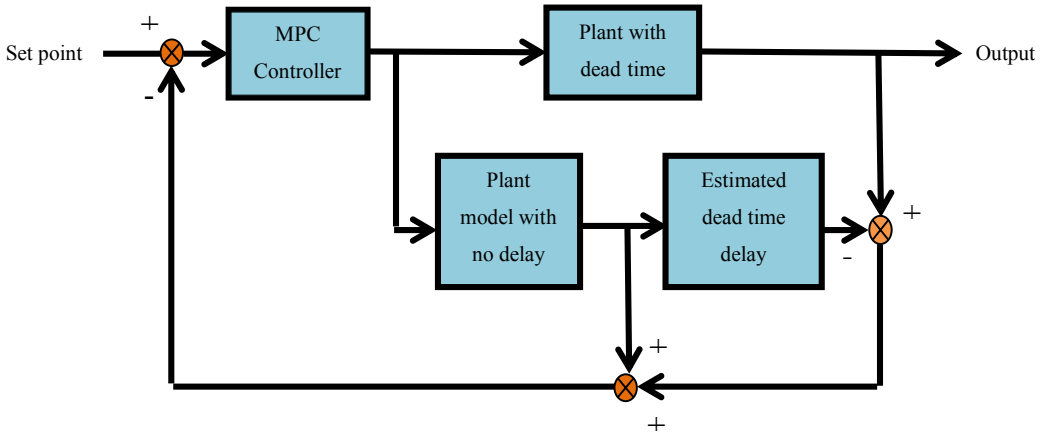

Figure: 5.5: Smith predictor

An estimate of the delay time can be obtained from the thermal response of the zone (eg. fig.5.4). Subsequently, curve fit search methods are then used to estimate the value of ζ_z for i) the start-up transient and ii) for the steady state period. Each estimated value of ζ_z is combined with the measured value of K_{loss} to provide the parameter set.

Each heating period requires a dedicated training dataset so as to calculate the variables of the associated model. Again, following chapter 4, the training data is chosen to be the previous day's thermal response over the same heating period. The training data set is constructed as a two column matrix—one for the normalised temperature (output or y) and one for the normalised heat input (u) of the heating time.

The heat source output is varied by means of a Pulse Width Modulation (PWM) scheme where the duty cycle of heat output is equal to the required normalised heat output of the heat emitter. The sample time of the dataset is dictated by the period of the PWM for modulating the heat emitter output. Following on from chapter 4, a maximum PWM period is chosen to be 5 minutes.

Each zone model consists of three variables ζ_z, K_z and a delay G_z, and each trial is conducted by first simulating the system response using the measured input data and comparing the simulated output data to measured output data. The Normalised Integral Squared Error (NISE) is used to provide an assessment of each model's 'fitness', and the model resulting in the lowest NISE is selected for use within the controller/smith predictor;

$$NISE = \sum_{k=1}^{N} (y_m(k) - y_{rec}(k))^2 \quad (5.9)$$

Where y_m and y_{rec} are the normalised simulated model output and recorded output for each period respectively. Once appropriate values for ζ_z, K_z and delay are chosen, their incorporation into the smith predictor is straightforward.

5.5.1 Modelling and identification of model switching point

Previously in section 5.4 it was illustrated (point A, fig. 5.3) that the thermal response of a zone may be represented by two separate dynamic models. The first model represents the initial start-up transient and the second representing the steady state conditions where the zone temperature is maintained around set point. As these are two separate models are dictating the operation of the controller, this controller that switches between them can be thought of two separate controllers. This mechanism by which multiple controllers are switched between is often referred to in the literature as *supervisory* control [115], [116]. In this context, the supervisor is simply a switch that directs the MPC formulation to use a different model dependant on which stage of the thermal response has been reached. Such supervisory control would enable two 1st order models to approximate the behaviour of a much more complicated system. Indeed, the 4th order system as determined in chapter 3 required extensive empirical calculation and measurement and then further subsequent computational calculation. Even the 2nd order modelling method cited in chapter 4, although successful, required a curve fitting system that proved cumbersome for implementation using inexpensive hardware. On a typical thermal response the location of the transition point between the two start-up and steady-state characteristics can be observed as a point of inflection (point A, fig. 5.4). A common performance criterion for controllers is a maximum 5% overshoot [117]. Thus in this case the steady state region was be assumed to start from 5% below set point. Using this assumption the point of switching (switching point) by the supervisory controller was assumed to be at the point the where the thermal response initially reaches 95% of required set point. By using the responses gained from test cell benchmarking hysteresis controlled trials between 6/1/11 and 11/1/11 for various set points in various external conditions, the validity of such modelling methods could be checked.

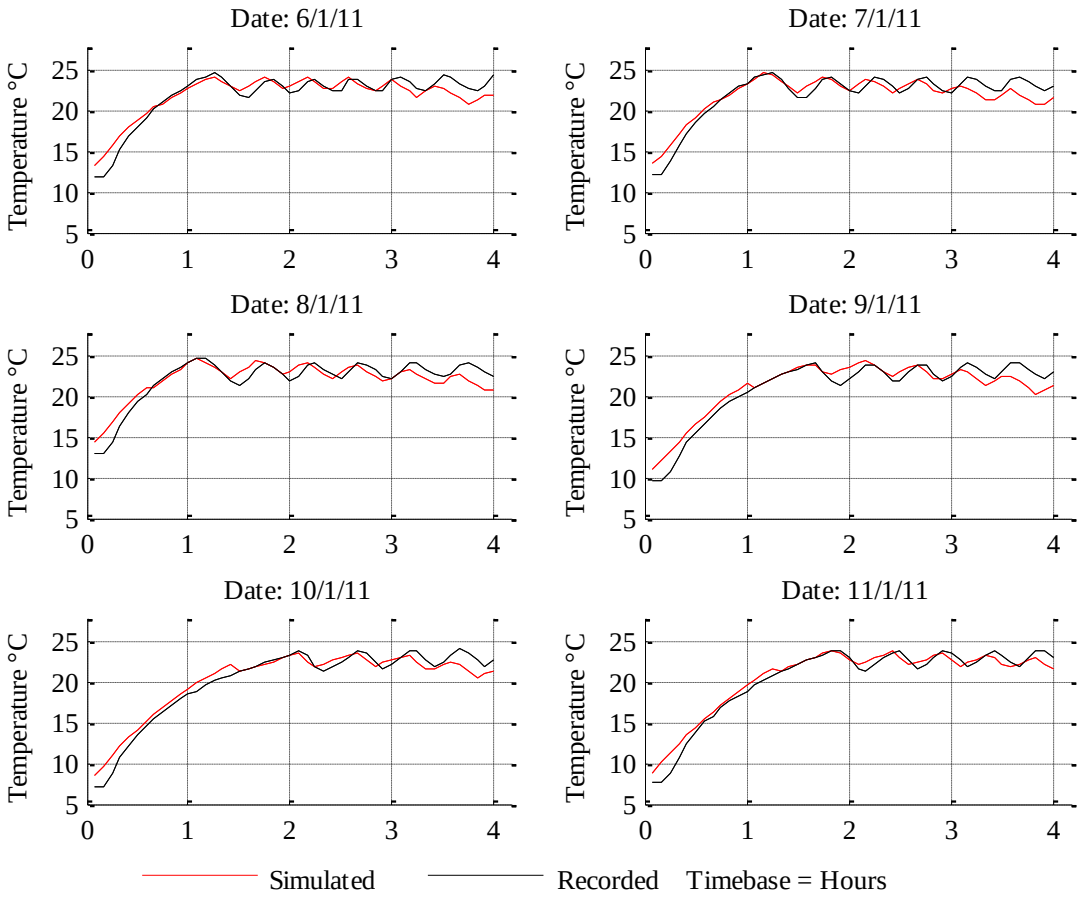

Figure. 5.6 Thermal responses of test cell in comparison with new modelling method

The ME for the start-up transients is 0.44°C and for the steady state transients is at 0.55°C using this modelling method. These simulations endure a greater deviation from their recorded counterparts than the 4th order simulation detailed in chapter 3. Indeed, it can be noted by inspection that the magnitude of model discrepancy is larger than those illustrated in fig. 3.8, chapter 3.

However, the first order sequential models illustrated in figure 5.4 do show commensurate performance with the measured thermal responses. One can observe that the higher ME figure for the steady state simulation, is caused by the 'drift' between simulation and recorded results on each response, particularly at the end. This characteristic is the penalty suffered by using a dramatically lower order representation of a system (1st order with delay) that in reality is of much higher order. Such a notable discrepancy was not present when using the higher order Simulink modelling methods described in chapter 3.

The gain in performance overhead (less computation needed) and an ME that was close to required specification was enough to warrant full investigation under real world conditions and an assessment of the performance of the 1st order model when used in conjunction with an RM-MPC system. If the controller was tuned correctly the feedback within the control system would be able to compensate for model inaccuracies, still providing required performance.

5.6. De-tuning of MPC weight factor (λ) in order to improve robustness

Overall system performance with MPC can be sensitive to the accuracy of the estimated model, since the system is effectively operating in an unmeasured 'open loop' state over the period of the time-delay, relying solely on Smith-predictor 'estimates'. A degree of 'detuning' of the control parameters is therefore advantageous and used here accommodate the effects of discrepancies between model and system outputs over the ensuing heating period. Revisiting the MPC formulation discussed in chapter 4, the optimal solution of ΔU is (5.10).

$$\Delta U = (\Phi^T \Phi + R_b)^{-1} \Phi^T (R_s - Fx[k_i]) \tag{5.10}$$

Whereby;

$$R_b = \lambda I_{(N_c \times N_c)} \tag{5.11}$$

Calculation of the optimal solution (5.10) is dependent on the controller 'tuning' parameters N_p, N_c and the weighting factor λ. The computational complexity of evaluating the cost function increases substantially as the prediction and control horizons increase, placing considerable burden on processor hardware employed to realise the controller. Limited capacity of inexpensive microprocessors, therefore, places practical limits on the chosen horizons. Here, maximum prediction horizons are limited to 6 sample periods.

The remaining weighting factor, λ, governs the 'spread' of the predicted optimal control

moves over the fixed control horizon—a large value of λ allows the error between the set-point and output of the system to reduce relatively slowly. It can therefore be regarded as a 'de-tuning' parameter. Under ideal operating conditions, the model used in MPC is an exact representation of the plant and, therefore, the generated control matrix will provide an optimal response without deviation subject to the constraints imposed. In such situations, the effect of the weighting factor can be neglected (λ=0). However, since discrepancies always exist, a non-zero λ is always recommended in practice, allowing the applied control to take a more cautionary trajectory and reducing the detrimental impact of model mismatches. The choice of weighting factor is dependent on the extent of model mismatch expected to occur in practice. By examining previously recorded data and assessing a worst case scenario of model mismatch, an appropriate λ is determined. Specifically, to choose an appropriate value for λ, a sensitivity analysis is performed using one model to formulate the control move and another to gauge the response of the system. Using the range of model parameters shown table 5.2, two extreme sets of parameters are picked, (and thus the models they formulate) and the effect of model discrepancy assessed. The first extreme formulated model (using ζ_{zc} and K_{zc}, the control model parameters) is used to formulate the augmented model for the prediction equation (5.12). From (5.10), the set point change (ΔSP) is represented by (5.13) whereby the first row represents MPC controller gain, G_{cont}. Thus G_{cont} can be calculated using the parameters used for (5.10) for a given λ as R_b is a diagonal matrix of λ of dimensions equal to N_c x N_c.

$$Y = Fx(k_i) + \phi\Delta U \tag{5.12}$$

$$\Delta SP = (\Phi^T\Phi + R_b)^{-1} \times \Phi^T F \Rightarrow G_{cont} = \overset{N_c}{[1...0]}(\Phi^T\Phi + R_b)^{-1} \times \Phi^T F \tag{5.13}$$

A second set of parameters that form the second extreme model (C_{zs} and K_{zs}) represent the system being controlled and is thus used to formulate the augmented system matrices, A_e and B_e in (5.14). As A_e and B_e have been augmented (and the formulation of K_{gain} has used augmented matrices formed from C_{zc} and K_{zc}), the closed loop system matrix M_{cl} (5.11) is now a 2 x 2 matrix. The eigenvalues of M_{cl} coincide with the poles of the formulated closed loop system of controller and system being controlled, and thus a system response can be assessed.

$$M_{cl} = A_e - B_e G_{cont} \tag{5.14}$$

Parameter	Range
ζ_z	2.00 - 30.00
K_z	0.15 - 0.40

Table 5.2: Parametric sweep value range of models

Considering a system where T_z (temperature of zone) is normalised between 0 and set point, the extreme pairs of values which would result in the greatest discrepancy would be values of ζ_{zc} and K_{zc} 30 and 0.4 (control model) and ζ_{zs} and K_{zs} of 2 and 0.15 (controlled system model). A suitable value of λ would ensure the system is stable by restricting the control action so as to not to be too fast for the system dynamics resulting in instability and not so restrictive as to result in too slow controller response resulting in substantial system performance penalties. In terms of system analysis, preferred eigenvalues of M_{cl} will lie on the real axis of the z-plane circle, ensuring over-damping (no overshoot) and within the unit circle (stable).

Using the extreme parameter values outlined in table 5.2 to formulate (5.14), the system only becomes stable with a weighting factor (λ) above 0.6, with poles at 0.7895+j0 and -0.9927+j0 respectively. However with a pole so close to the outer limit of the unit circle (using this sampling time), the system would be considered to be marginally stable and therefore setting λ = 0.6 would be an ambitious choice. A value of 2.6 results in the poles leaving the real axis of the z-plane (0.6616±j0.0563) and thus a value between 0.6 and 2.5 would ensure that even an extreme case of model mismatch is catered for.

Using a value of λ = 1 and the extreme values highlighted earlier results in poles located at 0.7818 and -0.2695. These would satisfy the stability and overshoot criterion and also reduces computational complexity as the weighting matrix R_b requires less formulation. Furthermore the system remains over damped (as the poles are located on the real axis of the z-plane) nullifying any chance of overshoot in theory and reducing the possibility of this occurring on the actual system.

A further consideration is that at present, the values used for the extreme model analysis are formed from the relatively mild weather recorded in January 2012 at the University of Sheffield New Caledonia car par where the test cell was located. One may extend the value of K_{zc} to go to 1 (i.e. maximum heat power available) representing the most extreme heat demand (coldest possible weather). Such a scenario results in minimal change to the location of the poles of the complete system. Using a value of $\lambda = 1$ and the modified extreme values still results in over damped poles located at 0.7653 and -0.1458, which still meet the desired stability criterion.

5.7. Experimental Results

Having determined appropriate models, the controller is realised and a set of experimental trials undertaken for a week long period—the test cell is employed for initial control performance evaluation, and effectively represents a worst case operating scenario due to the lack of thermal mass and relatively poor insulation qualities (see chapter 2). The control system is then transferred to the occupied domestic dwelling, (chapter 2) to facilitate multi-zone control and performance assessment.

5.8. Model matching performance (test cell trials)

To provide relative performance indicators that allow for direct comparison of control methodologies, the following metrics are used:

- Modelling Error (ME): the mean error between the measured temperature response of the system and that provided by the selected 1st order model with delay.

- Predicted ME (PME): the mean error between the previous day's model response and the measured response of the current heating period.

Moreover, to compare performance with previously reported techniques, the Mean Total Solar Irradiance (MTSI) and Outside Temperature (OT) together with the results from tests conducted during 2012 which employed higher-order models, are used. Table 5.3 summarises the results from the current trials, and those previously reported in 2012.

Period	Parameter	RM-MPC (2012)	SRM-MPC (2013)
24 hours	MTSI (J/m^2)	3769208	7462713
1	OT (°C)	5.69	3.42
2	OT (°C)	7.27	6.16
1	ME (°C)	0.38	0.28
2	ME (°C)	0.33	0.29
1	PME (°C)	2.28	0.51
2	PME (°C)	2.58	1.49

TSI: Mean Total Solar Irradiance
OT: Mean Outside Temperature
ME: Modelling Error
PME: Predicted Modelling Error.

Table 5.3 Summary of modelling performance (test cell trials) using refined RM procedure

By comparing with results from (2012) chapter 4 where higher-order models were used for the classical MPC controller implementation, it can be seen that the method proposed here imparts superior characteristics, with ME reducing by 26% (from 0.38°C to 0.28°C) during Period 1 and by 12% during Period 2 (0.33°C to 0.29°C). This is also commensurate with PME calculations, which are 78% lower in the first period (2.28°C to 0.58°C) and 42% in the second period (2.58°C to 1.49°C). However, it is also apparent that PME varies substantially between periods 1 and 2 using the new modelling procedure (0.58°C to 1.49°C). By consulting prevailing weather conditions, it is noted that trials in period 1 were taken during conditions of relatively low temperature variation on a day to day basis, with the standard deviation of OT being 1.6 °C. By contrast, weather conditions during the period 2 trials were less consistent, with standard deviation for OT being 3.19 °C. It is this greater variation that is impacting on relative performance in this instance. Due to the differing trial periods used here compared to chapter 4, TSI is only considered over the 24 hour period. It is clear from the MTSI values the test cell was exposed to a nearly double the solar irradiance on average during the latest Smith RM-MPC (SRM-MPC) tests over each 24 hour period. The standard deviation of the 24 hour MTSI value for tests in 2012 was 103025 J. The 2013 test (SRM-MPC) endured a standard deviation of 4681367 J. It is clear from these values the later tests were

conducted on brighter colder days with an increased level of variation of external influence, whereas in 2012 the weather followed a more constant overcast behaviour. Despite the greater level of disturbance present, the modelling method achieved lower levels of ME and PME. These results serve to demonstrate an inherent degree of robustness of the adopted control methodology.

5.9. SRM-MPC heating performance (test cell trials)

The realised control scheme is depicted in fig. 5.6, with the key addition of the recursive-modelling component that calculates the steady state heat input power, system delay, and the smith predictor estimates.

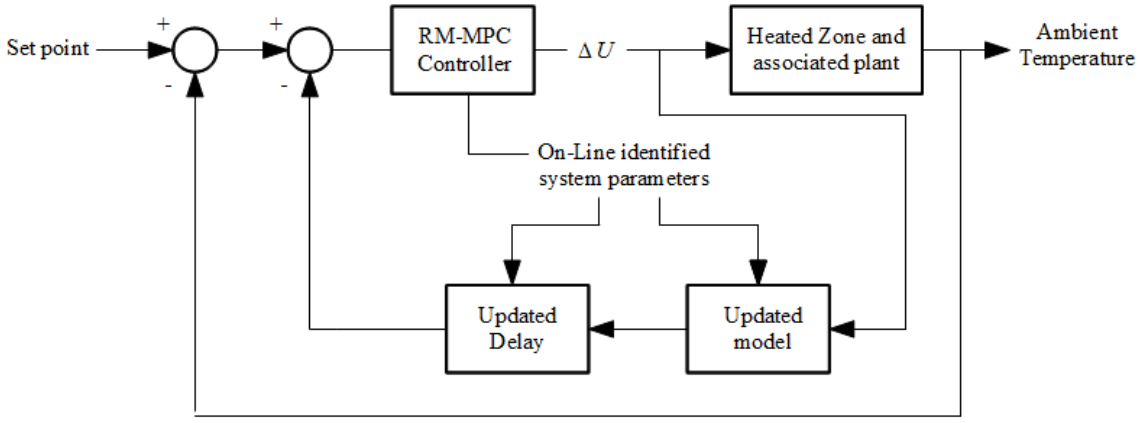

Figure 5.7: Complete SRM-MPC control system

The heat source (oil filled heat emitter) is controlled using Pulse Width Modulation (PWM) with a period of 5 minutes and a duty-cycle resolution of 1% (i.e. a minimum on-period of 3 seconds), with demand communicated using a wireless 2.4GHz link from the dedicated microcontroller board described in chapter 2, section 2.6. To accommodate for worst case scenarios the controlled heat emitter is oversized by a factor of 2; a practice which is common in many UK households [16], [118].

In addition to the SPTE (section 5.2), a further metric is used for performance assessment of the realised closed-loop control structure viz. the Mean Energy Consumed (MEC) during each period. A comparison of thermal comfort performance from the trials

conducted in chapter 4 (2012) and those now considered (in 2013) are summarised in table 5.4.

Period	Parameter	RM-MPC (2012)	SRM-MPC (2013)
24 hours	TSI (J/m^2)	3769208	7462713
1	OT (°C)	5.69	3.42
2	OT (°C)	7.27	6.16
1	SPTE (°C)	0.21	0.26
2	SPTE (°C)	0.21	0.15
1	MEC (kWh)	0.78	1.11
2	MEC (kWh)	0.69	0.56

TSI: Mean Total Solar Irradiance
OT: Mean Outside Temperature
SPTE: Set Point Tracking Error
MEC: Mean Energy Consumed

Table 5.4: Summary of performance of RM-MPC controller using test cell

From the trials, a number of features can be seen:

For both control methods it is evident that a significant difference exists in the energy consumed between periods 1 and 2 (~55%) in the current trials. This is again attributed to prevailing weather characteristics rather than controller performance—specifically the colder OT between 3.42 °C and 6.16 °C during 2013 tests.

During both periods 1 and 2 maintained thermal performance was within the required ±0.5 °C specification despite more severe prevalent weather conditions than those reported in 2012 (chapter 4, table 6). The value of SPTE for period 1 was marginally higher than those reported in these previous trials when a 2nd order parameter matching technique was employed (0.26 °C), but the second period provided results significantly lower (0.15°C).

The MO of the temperature profiles remains below the desired SPTE of 0.5 °C for periods 1 (0.42 °C) and 2 (0.23 °C), as shown by the example measurements in fig. 5.8. The detrimental effects of potential overheating is therefore minimised despite a heat emitter

being used that is considered to be rated 100% higher than necessary according to CIBSE guidelines [15].

The SPTE performance during the first period is lower than the 2012 controller (table 5.4) which used a 2nd order parameter model-matching technique, this is despite a superior match between controller model and controlled system (lower PME). This is a consequence of the method of selecting the 'ideal response' used for performance comparisons. Specifically, by considering the transient portion of the temperature change profile, when a lower 'initial temperature' is used, the 'ideal characteristics' is estimated over a longer period, thereby contributing to a higher SPTE during more inclement conditions. This is exacerbated during the first period whereby there has been negligible total solar irradiance (due to the position of the test cell) before the first period. Thus there is minimal solar influence that may act to increase the thermal storage capacity of the test cells thermal mass before the period. To support this, the OT for the trials in 2012 (table 5.4) indicate milder conditions.

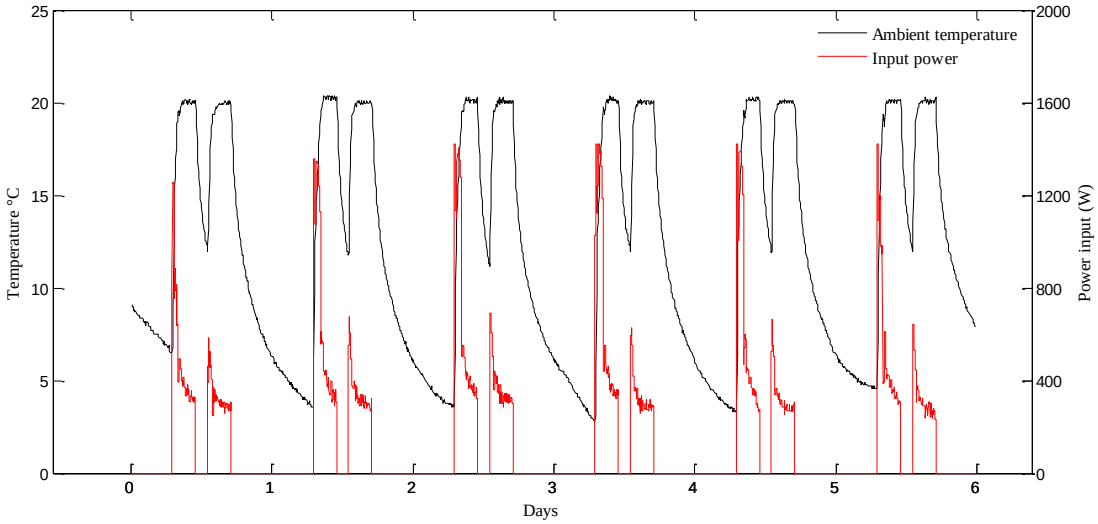

Figure 5.8: Test cell under SRM-MPC control

The test chamber trials have shown that the SRM-MPC scheme can be realised and maintain control performance using a less computationally intensive modelling methodology that previously reported. Specifically, in this case, the computational cycle time using an Atmel ATMEGA2560 based controller was <2 seconds. Execution of the previous parameter matching 'branching algorithm' (chapter 4) on the same platform took

in excess of 30 minutes.

5.10. Experimental trials in an occupied domestic dwelling

To show the benefits afforded by the proposed control scheme, it is also realised in an occupied dwelling using thermic valves. The control structure is identical to that used in the test chamber but extended to control the 4 zones independently using 2.4GHz wireless communication to each zone. Each TRV head is replaced by a normally closed Emmeti Control T™ thermic actuator, with each valve operated by means of PWM control—as in the test chamber trials, with a 100% duty cycle equal to 5 minutes with a minimum duty cycle of 1% or 3 seconds. This, therefore, allows for rapid deployment/retro-fit within an existing central heating system. The trials were undertaken between 7/3/13 – 13/3/13. A summary of results from the trials is given in table 5.5, with measurements from a typical trial period shown in fig. 5.8. From table 5.5 and figure 5.9 it can be seen that thermal comfort is dramatically improved using the new SRM-MPC controller, in all 4 zones. Specifically, improvements in SPTE range from 35% in zone 4, to 86% in zone 2. Although significant benefits are also shown in the kitchen area (zone 3), despite the being dwelling is occupied and the central boiler unit and main cooking appliances being used in a typical household manner. However, in a kitchen area un-modelled temperature disturbances will have a greater effect. This is also supported by the high mean overshoot present in zone 3 during times when cooking is likely to take place (notably with an SPTE > 0.5°C).

Of particular note is that benefits afforded by superior control performance means that furniture placement now has only a minor influence on the temperature dynamics of the respective heated zones—with both zone 1 and zone 4 recording similar measurement profiles (albeit with different actual temperatures, measured at a standard height and 1500mm above floor level). This is also commensurate with results from zone 2, which has a bed in close proximity to the heat emitter. Using TRV control, the thermal response shows substantial oscillatory characteristics (fig. 5.1) whilst fig. 5.9 shows that these have been subdued as a consequence of improved dynamic performance afforded by the use of CRVs.

While offering far superior set point tracking, the cautious control trajectory chosen (to

ensure controller robustness) has resulted in a performance penalty. The more aggressively tuned (mechanical) PI control offered by the TRV, which has been pre-tuned by choosing particular mechanical components (e.g. type of wax, return spring size) offered a far faster thermal rise time as shown by the values of TC table 5.5. The greatest difference was in Zone 4 increasing from 13 minutes to 25 minutes. However, considering this worst increase in TC would only form $\approx$5% of a typical 4 hour heating period, one may conclude the benefits of superior temperature regulation over the entire heating day outweigh the comparatively small increase in time it takes for a particular zone to reach set point.

Finally it can be observed, the benefits of the SRM-MPC controller are more pronounced within the dwelling than the test cell due to the significantly higher thermal mass of the former. The actual controller performance within the test cell was only mildly improved between the RM-MPC controller (previous chapter) and this SRM-MPC controller (although the hardware footprint is now drastically reduced in size and cost). This is due in part to the minimal thermal mass of the test cell. For example, if the test cell were constructed of identical wall materials for each of its four vertical boundaries, its thermal mass would increase from 1008764 $J^{o}C^{-1}$ to 7266024 $J^{o}C^{-1}$. A poorly tuned controller such as the aggressive PI controller of the TRV results in a fast rise time but with significant thermal inertia present (high thermal mass), the temperature profile will overshoot and an oscillatory nature (particularly in Zone 2, figure 5.1) will occur. With minimal thermal mass, the prevalence of system delays are reduced, thus it allows a more aggressive controller or even a poorly tuned one with can implement pronounced control inputs that may be otherwise be unsuitable for a zone with more thermal mass.

The thermal comfort of the dwelling has therefore substantially improved by the introduction of the SRM-MPC control system using thermic valves (with negligible additional installation cost).

Period	Parameter	TRV Controlled Zones				CRV (RM-MPC) Controlled Zones			
		1	2	3	4	1	2	3	4
1	SPTE (°C)	0.75	1.66	0.92	0.55	0.19	0.22	0.45	0.29
2	SPTE (°C)	0.66	1.29	0.61	0.48	0.22	0.31	0.53	0.25
1	MO (°C)	1.91	4.23	1.48	1.64	1.20	0.70	3.00	1.20
2	MO (°C)	1.77	3.30	1.24	2.18	1.20	1.30	1.60	1.10
1	TC (mins)	15	17	17	12	20	20	29	18
2	TC (mins)	12	12	22	13	19	15	33	25

SPTE: Set Point Tracking Error
MO: Maximum Overshoot
TC: Time constant

Table 5.5: Comparison of CRV performance with traditional TRVs

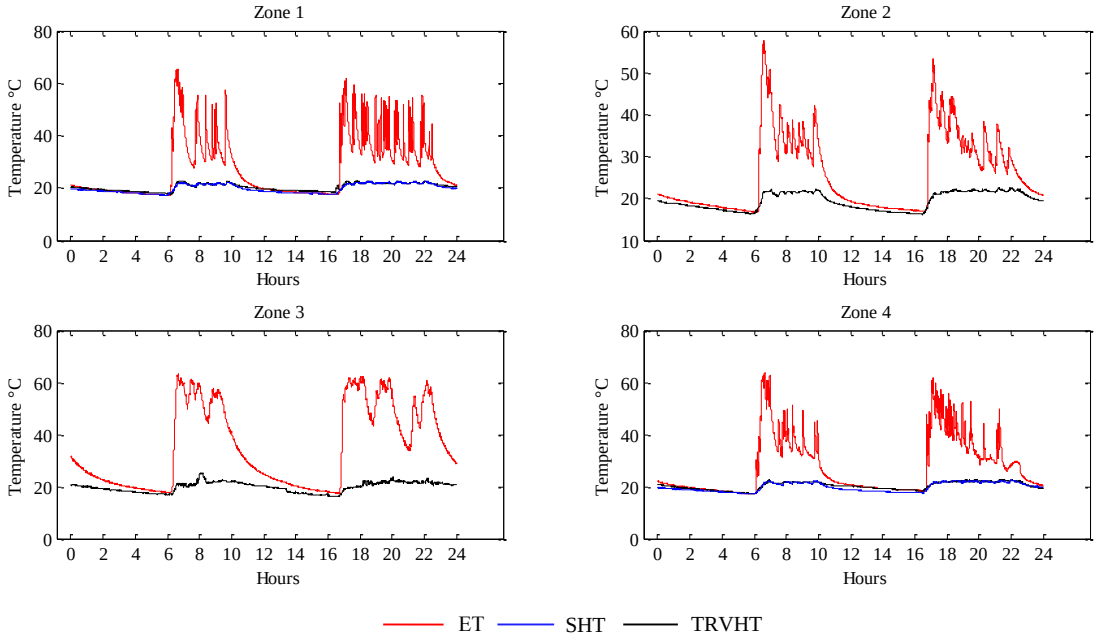

Figure 5.9 Temperature responses of TRV controlled zones (ET – Emitter Temperature, SHT – Standard Height Temperature, TRVHT – TRV Height Temperature. 24/2/13)

5.11. Summary

A new family of controllers have been presented that are suitable for use with low cost thermic valves. The SRM-MPC control scheme proposed can be economically retro-fitted to existing homes with minimal labour and installation overhead. No additional plumbing or use of additional computational hardware above and beyond that now commonly used in conventional boiler systems is required for the proposed system.

By integrating inexpensive thermic valves into a traditional central heating system, and operating through use of the SRM-MPC control scheme, significant improvements in terms of comfort have been demonstrated. Despite some zones being subject to significant disturbances (eg. cooking areas within the test dwelling), ambient temperature regulation is significantly improved.

Now a practicable method of implementing MPC in conjunction with a domestic distributed heating system had been developed. The next stage of the work was to implement the principle benefits of this control method, namely, using the constraint handling mechanisms within the MPC formulation to perform a scheduling method. As mentioned previously, the benefits of such a method could be far ranging, reducing boiler cycling, reducing required boiler capacity and helping low income households more accurately budget their spending on heating. The next chapter details the implementation and analysis of such a system in the spring of 2013 using the test dwelling.

Chapter 6. Experimental investigation into a scheduled RM-MPC heating system

6.1. Introduction

The previous chapter detailed the refinement of the RM-MPC controller that enabled its implementation in combination with COTs controllable thermic valves and a low cost microcontroller. These important stages in development greatly increase the controllability of domestic heating systems by allowing the temperature within each zone to be more independently regulated.

The principal benefit of MPC is its ability to handle constraints. By allowing one to constrain maximum input (heat) level, the resultant determined control moves would be assured not to violate such as zone/emitter temperature and power requirements. Thus, not only does MPC have an inherent constraint handling ability, it has an inherent scheduling ability, dependant on how one chooses those constraints.

Following on from the previous chapters, a further evolution of the RM-MPC controller is described. By utilising the constraint handling mechanism described earlier, a scheduling system that aims ensure minimum levels of thermal comfort within a dwelling despite limited heat resources is implemented. Results show the system allows a non-modulating heat source to be matched to its load hence reducing the possibility of boiler cycling. Furthermore the technique is shown to allow accurate budgeting of energy resources for heating a house and be applicable to a wider range of applications than first thought.

In an effort to clarify how the new test set-up aims to successfully represent a downsized heat source, the test equipment is described first in section 6.2. Subsequently, the use of multiple PWM controllers and a ‘time-slicing’ technique is introduced in section 6.3. In section 6.4 MPC is revisited and applied to an example time-slicing calculation. Section 6.5 includes a summary of tests conducted and a discussion and Section 6.6 concludes the chapter, suggesting other uses for this SRM-MPC scheduled controller.

6.2. Scheduled MPC test equipment

Due to the impracticality and cost of installing a downsized boiler within the test dwelling, an abstracted approach was adopted. Namely, 4 oil filled heat emitters were used to emulate a distributed hydronic heating system, operated by an extension of the multi-output controller as used in chapter 5 (figure 6.1).

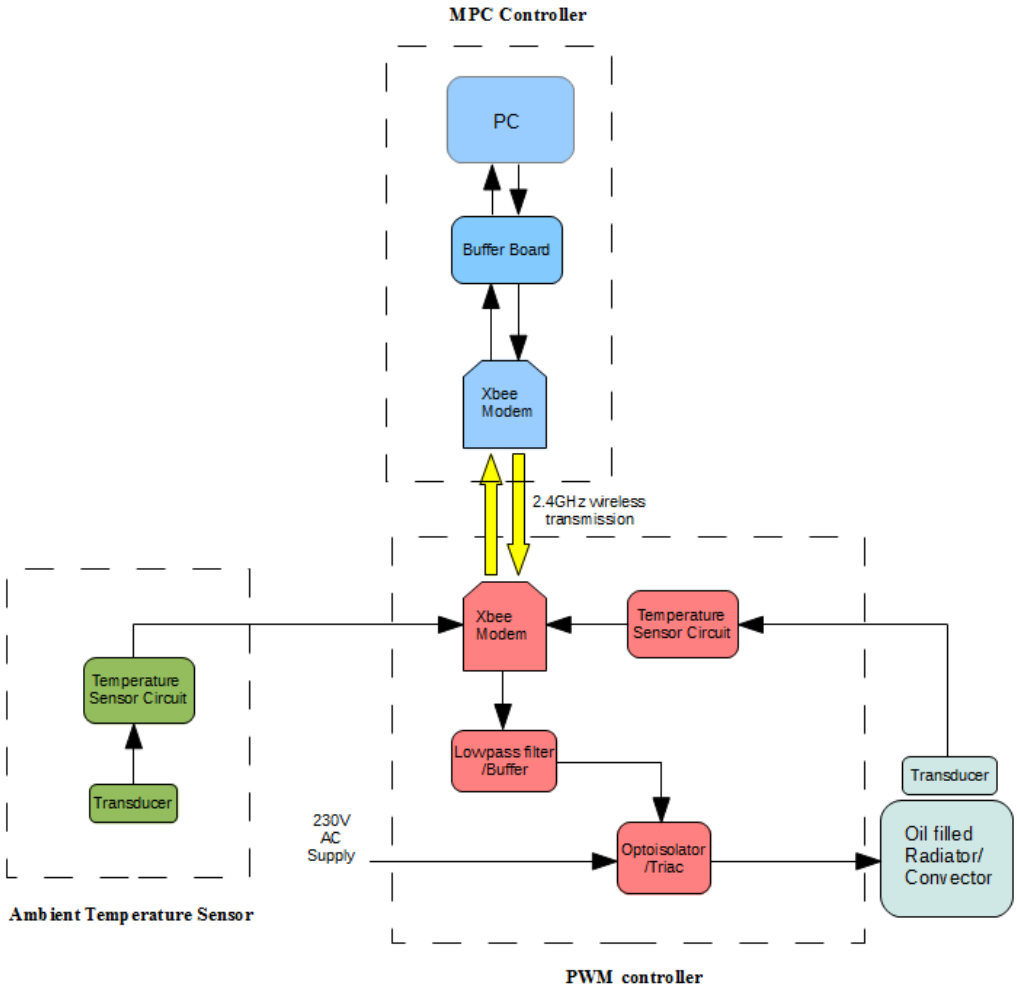

Figure 6.1: Complete distributed emitter controller

The PC remained as the central controller. This system topology enabled remote access and fast updating of code during troubleshooting and initial commissioning.

In essence the test cell PWM controller (previously tested in section 5.9), is duplicated 4 times (one for each zone) within the test dwelling. By choosing how the input

constraints to each of the four controllers is set, one may emulate a downsized of central boiler using a time slicing technique. The next section describes how, using this emulated downsized central heat source, the inputs are 'sliced' according to the heating requirements of the occupiers.

6.3. Time-sliced PWM control

As highlighted by Castilla [69], an ideal strategy for coupling a fully controlled power input (or heat source) using advanced control schemes to HVAC emitters, is to use only two modes of 'actuation' viz. on and off ([69] terms this PWM). This allows HVAC emitters that typically operate using on/off thermostats to be readily integrated within a MPC methodology. This was first demonstrated with considerable success in chapter 4, whereby a central heat source (boiler) was operated by a central heating controller.

The use of a PWM implies that the device will be 'off' for an appreciable time, i.e. for a 40% duty cycle the device will be 'OFF' 60% of the time. Thus this implies that multiple devices can be operated, turning 'ON' another emitter when the first turns 'OFF' as a part of its normal control input. When, say, Emitter 1 turns off, Emitter 2 turns on, and this continues in a sequential manner until all emitters have been activated. More formally, if the PWM period is T then each emitter is active (on) for the interval d_iT where d_i is the duty time for the i^{th} emitter with the restriction $\sum_{i=1}^{N} d_i = 1$ for a building featuring N nodes. This constrained sequential operation of heat emitters is hereafter described as *priority scheduling*.

By operating multiple heat emitters with on-off PWM control, the heat source only needs to be rated for a single emitter. In essence this method becomes a time-slicing system dividing the heat inputs between heat emitters within a limited time period. Fig. 6.2 demonstrates the operating principle where only one emitter is activated at a time, the black line represents zone 1 temperature (solid line) and control input (dashed line) and blue lines represents zone 2.

The constrained MPC is now directly governing the length of time each heat emitter is on due to the power input level being now represented by a PWM duty cycle (d_i). Therefore

the overall schedule of operation of the distributed heat emitters is now constrained by the MPC formulation. Only a simple calculation is now required at every control move to keep power consumption of the distributed heat emitters at a constant level. Due to using this time–slicing technique, MPC can now schedule on extremely short time scale (every 5 minutes) as opposed recently reported methods by Lefort [61] that use a time scale of 7 hours. Moreover, only an extremely simple schedule calculation is now required due the use of MPC as opposed to the HVAC fuzzy logic control scheduling methods that require substantial training [119].

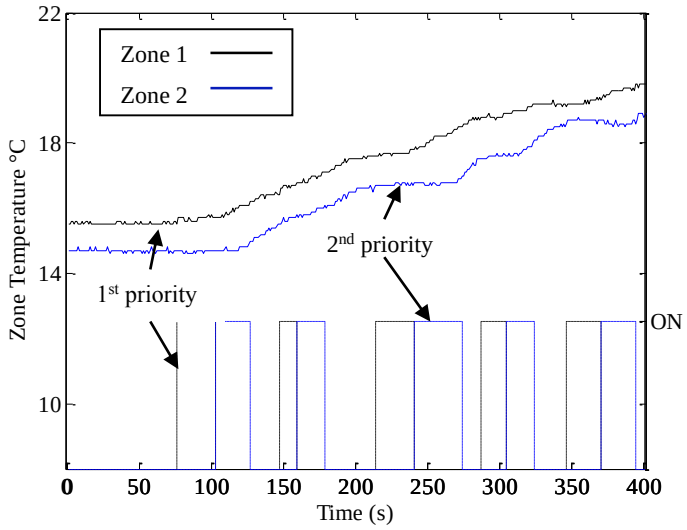

Figure 6.2: Time-sliced prioritised control inputs

Such a priority scheduling system could be of great benefit to people of limited income. It is a cruel irony that the poorest sections of the community are usually paying the most for energy due to practice of fitting key meters which need regular charging to keep the dwelling heated [120]. Unfortunately this often presents a health issue for people on restricted budgets as they balance expenditure between food and heat. Indeed, it was highlighted in a report sponsored by Friends of the Earth and Save the Children in 2011 [121] that many low income families face the choice to "heat or eat". Moreover, a report by the chief medical officer in the UK highlighted that investing £1 in keeping homes warm saved the NHS 42 pence in health costs [122]. The SRM-MPC proposed here could mitigate some of these issues by allowing the occupants to prioritise specific zones (rooms) and to specify maximum energy consumption. By allocating priorities to essential zones, the reduced heat supply budget or downsized heat source would at least keep one or more

zones at the desired comfort level at the expense of other, less frequented zones. Even with a limited set income, in extreme weather at least certain areas within a dwelling could remain at a desired level of thermal comfort.

However, the simplest method to reduce over capacity of a domestic heating system and/or constrain power consumption is to simply restrict the heat budget for the whole system. In such a situation, distributed heat emitters operated by independent controls would be considered to draw heat resources from the boiler in parallel. The limited heat supply would now be spread between zones (as opposed to being prioritised). Each heat emitter demand directly affecting all other heat emitters within the system.

Although such an approach would certainly constrain energy use, a restricted heat budget may not permit the required supply capacity if all heat emitters are activated, as the demand may be too great. Such a situation would result in all zones being detrimentally affected by in terms of thermal comfort. As a benchmarking exercise, this overall downsizing of heat budget with no priority (hereafter described as *non-priority scheduling*) was also to be emulated using the test equipment described in section 6.2. In the next section constrained MPC is revisited and then the application of the formulation to both non-priority and priority schedules is applied.

6.4. Constrained Model Predictive Control (revisited)

A general formulation of the state space description of the underlying system to be controlled is given by:

$$x[k+1] = A_d x[k] + B_d u[k] \tag{6.1}$$

$$y[k] = x[k] \tag{6.2}$$

Where x is the vector of state variables, u the control variable, y the measured output, and k is the present sample (time interval) under consideration. Referring to chapter 3, optimal control moves accommodating the constraints can be calculated by minimising the solution of (6.3) subject to the inequality constraints expressed as (6.4) results in (6.5).

Therefore as in chapter 3, considering SISO systems the model matrices, A_c, B_c and C_c, are required to be determined from a measured thermal response. Once effective model parameters are determined the model is once more formulated in terms of incremental control moves (Δu[k]) by embedding a synthetic integrator into the original system model.

As in previous chapters (3-5), and following Wang [107], the predicted output matrix may be expressed as (6.3). The chosen cost function is defined by (6.4).

$$Y = Fx(k_i) + \phi\Delta U \tag{6.3}$$

$$J = (R_s - Y)^T (R_s - Y) + \Delta U^T \bar{R} \Delta U \tag{6.4}$$

Substituting (6.3) within (6.4) and expanding results in (6.5).

$$J = (R_s - Fx(k_i))^T (R_s - Fx(k_i)) - 2\Delta U^T \Phi^T (R_s - Fx(k_i)) + \Delta U^T (\Phi^T \Phi + \bar{R}) \Delta U \tag{6.5}$$

Finding the derivative of (6.5) and solving to find the minimum arrives at the optimal solution of ΔU (6.6).

$$\Delta U = (\Phi^T \Phi + \bar{R})^{-1} \Phi^T (R_s - Fx[k]) \tag{6.6}$$

It may be noted that the cost function is a quadratic, and solving (6.6) subject to constraints would mean solving (6.3) with respect to linear inequalities defined by those constraints. Thus the problem of finding an optimal solution subject to those constraints would involve a quadratic programming algorithm.

If we consider ΔU as the decision variable, the objective function becomes (6.7).

$$J = \frac{1}{2} \Delta U^T H \Delta U + \Delta U^T V \tag{6.7}$$

Recalling that the objective function is represented by (6.8)

$$\Delta U = -H^{-1}V \tag{6.8}$$

Thus H is represented by (6.9) and V by (6.10) as they are the constituent parts of the optimal solution (6.8).

$$H = \phi^T \phi + \overline{R} \tag{6.9}$$

$$V = -\phi^T (R_s - Fx(k)) \tag{6.10}$$

The inequality constraints are represented by (6.11) where M is a matrix *reflecting the constraints* and γ translates the magnitude of the constraint limits.

$$M\Delta U \leq \gamma \tag{6.11}$$

Thus H, V, M and γ are the compatible matrices and vectors of the quadratic programming problem. With H and V derived from the model and previous feedback variable ($x(k)$) the constraints just remain to be set by the priority system before the MPC formulation can be completed.

6.4.1 Priority scheduling

For example, if the maximum net power chosen by the user was 1000W, and each heat emitter was rated at 1440W, the normalised a priori upper input constraints on input is 0.69. The lower input constraint is zero. For a first order system, the formulation of M and γ is trivial (6.12).

$$M = \begin{bmatrix} 1 \\ -1 \end{bmatrix} \quad \gamma = \begin{bmatrix} 0.69 - u \\ -0 + u \end{bmatrix} \tag{6.12}$$

Minimising (6.6) with respect to (6.12) an updated value of ΔU is formulated. Taking the first value of this vector (Δu_1) and summing with the previous value of u, (u(k-1)), an optimum control input u(k) is calculated. If this proposed value violates the constraints,

(0 and 0.69), a quadratic programming algorithm is implemented. Using either a standard MATLAB function such as 'quadprog' or Hildreth's algorithm as promoted by Wang [107] achieves the same optimum control move subject to those constraints (6.12) using the SRM-MPC controller.

For the two zone example, the control move for zone 1, u, is the optimum control move only considering the input constraint of the control system as in (6.10). The control move for zone 2 is now subjected to a modified set of constraints accounting for the effect of zone 1. Thus, if the desired control move for zone 1 is u = 0.3, the constraints for zone 2 become (6.13), u has been subtracted from the absolute positive power limit.

$$M = \begin{bmatrix} 1 \\ -1 \end{bmatrix} \quad \gamma = \begin{bmatrix} 0.39 - u \\ -0 + u \end{bmatrix} \tag{6.13}$$

For a larger premises, the process continues for the number of zones that require heating.

6.4.2 Non-priority scheduling

To fully mimic a household heating system with a downsized boiler but with no priority scheduling, it is assumed that all the heat emitters are connected in parallel to that heat source. Since all heat sources have a maximum power output the benchmark experiment was performed assuming a maximum power of 1kW and the oil filled heat emitters themselves are individually rated at 1.44kW and have their own MPC controller.

To emulate the 'spread' of heat, first all four MPC controllers formulate their control input move independently and simultaneously (normalised between 0 and 1, for example: 0.6, 0.3, 0.2 and 0.4). Although a constraint of 0.69 is implemented for each controller on an individual basis during the initial MPC formulation, it must be noted that no further constraining is actioned for the actual *non-priority* schedule. To attain an average heat output of 1000W over a five minute PWM period, the duty cycle would have to be 69% (of 1.44kW) or a net control input of 0.69. Considering this value as the maximum net control input level, the control moves for the example would be scaled as the following,

$$Net\ Demand = u_{z1} + u_{z2} + u_{z3} + u_{z4} \Rightarrow 0.6 + 0.3 + 0.2 + 0.4 = 1.5 \quad (6.14)$$

Considering the first zone, its upper constraint (Z_{uc1}) would be modified like so;

$$Z_{uc1} = Net\ Demand\ Limit \times \frac{0.6}{1.5} \Rightarrow 0.69 \times \frac{0.6}{1.5} = 0.28 \quad (6.15)$$

Thus the example control moves must be limited to 0.28, 0.14, 0.09 and 0.18 to emulate physical restriction on the amount of power available. These inputs are then subsequently applied to the distributed heat emitters, resulting in 'ON' time periods of 84 seconds, 42 seconds, 27 seconds and 54 seconds for zones 1-4 respectively.

6.5. Experimental results and discussion

Owing to unseasonably cold temperatures, it was possible to conduct two week long trials during March and April 2013. To enable comparative assessment the three principle performance metrics used were;

- SPTE: Set Point Tracking Error (°C): The mean error between the desired response (illustrated in figure 3.1, chapter 3) and the actual measured response over a single heating period.

- SF: Satisfaction Factor, (kW): A measurement of user satisfaction based on the duration of time a particular zone is maintained at set point for a given overall energy usage for that heating period.

$$SF = \frac{Total\ energy\ used\ during\ a\ heating\ \ period\ (kWh)}{Time\ at\ \ sp\ \ (hrs)}\ .$$

- ST: Start temperature (°C): The initial temperature of a particular zone at the start of the heating period.

Due to the weather improving as the year advanced, the proposed priority controller test was conducted first. This approach provided a worst possible case scenario when

compared to the later results of the constrained no-priority test that emulated a central heat source.

The input constraints were set so the net power consumption was limited to a net mean of 1kW over a 5 minute period consumed by all 4 heat emitters in total. The principle cooking device and other higher load domestic equipment was also using this ring main circuit. Thus 1kW was chosen as a compromise to avoid unnecessary overloading of this circuit of the dwelling. Considering the power input to each heat emitter was measured at 1440W, each duty cycle was constrained to 69% or 207 seconds 'ON' time for each control move.

Period 1 (P1) was defined as between 07:00Hrs and 11:00hrs, period 2 (P2) was defined as between 16:30hrs and 22:00hrs, both in line with occupancy of the test dwelling.

6.5.1 Priority schedule trial results

During the entire heating period the maximum net duty cycle remained at 69%, ensuring the net equivalent loading of the system remained at 1kW. A summary of the results are provided in table 6.1. From table 6.1, it is clear that the scheduled system manages to heat two zones consistently to the required level at the expense of the remaining two zones. The favourable values of SPTE demonstrated that the ability of the system to track the desired set point meets desirable levels (<0.5°C) for zones 1 and 2.

	Zone 1	Zone 2	Zone 3	Zone 4	OT(°C)
SPTE (P1)	0.24	0.21	6.33	6.12	0.05
SPTE (P2)	0.31	0.19	3.53	5.11	0.48
SF (P1)	5.39	10.28	-	-	0.05
SF (P2)	4.16	20.92	-	-	0.48
ST (P1)	15.99	14.82	13.83	14.83	0.05
ST (P2)	16.60	15.44	14.69	15.60	0.48

Table 6.1 Summary of allocated priority controlled trials

Such behaviour is clarified by observing individual response as illustrated in fig. 6.3. Indeed the remaining (lowest priority zone 4) receives no power input whatsoever. Zone

4 ambient temperature does rise, but only due to neighbouring zones heat leakage contributing to its ambient temperature. Zone 1 heats up almost in line with the ideal (deadbeat response), whereas the response for Zone 2 is more hesitant, clearly being penalised before 8:00am. This behaviour is also reflected in the high value of SF, as it has taken proportionally more power to ensure the zone remains at set point for a given time. However, once at set point, the zones heat input requirement drops, allowing to the Zone 3 to be heated. Unfortunately within the time duration of the first period of the day (P1), neither zones 3 or 4 reach set-point, hence no recorded value of SF is possible. Thus the result is void and noted as '-' in subsequent summary tables 6.2-6.4.

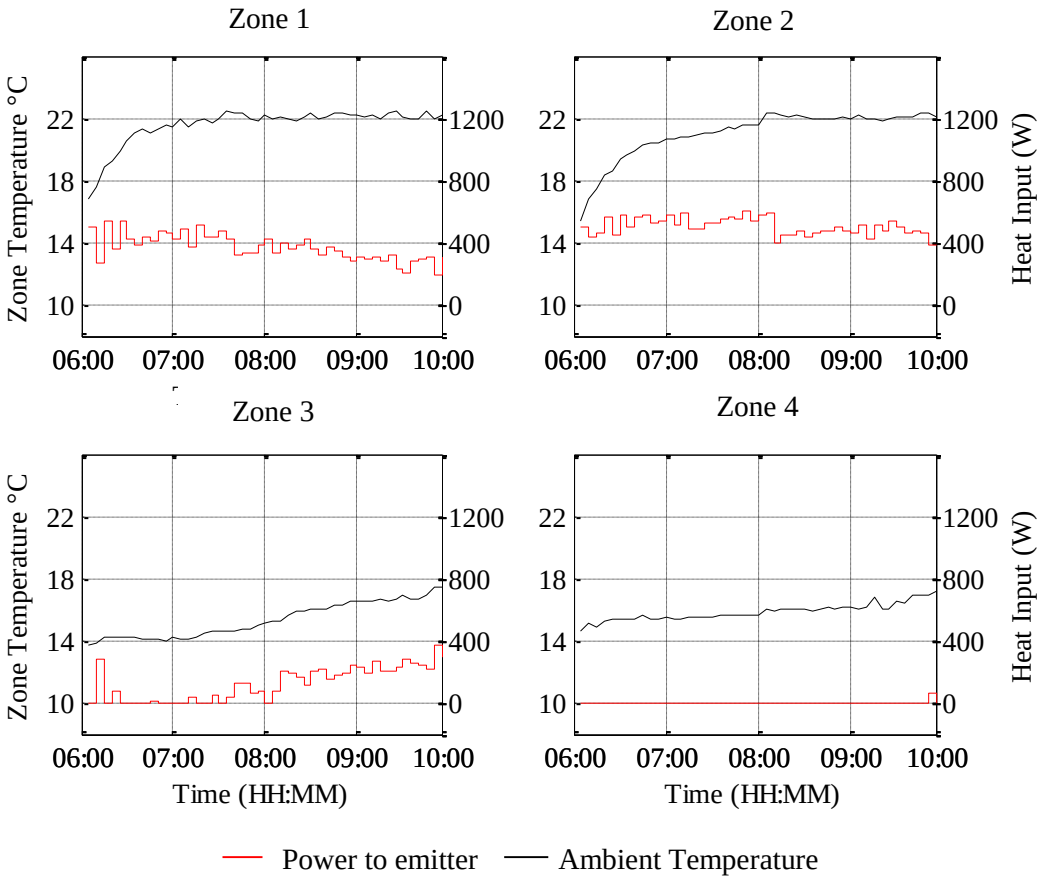

Figure 6.3: Priority scheduled zone thermal responses

6.5.2 Non allocated priority trial results

This control schedule enabled the 4 distributed electrical heaters to mimic the behaviour of a single heat source supplying all four similar to a traditional parallel connected central heating system. As stated earlier, a value of SP = '-' results from the occurrence whereby

the zone has never reached set point. Thus, if averaged, any '-' results will distort the mean and thus mask any response that may have reached set point. During the first, priority allocated system, only the two priority zones reached set point during every heating period. Preliminary examination of the non-priority scheduling scheme revealed occasions where desired thermal comfort levels were reached, though not on a consistent basis. Hence these trials were examined on an individual basis. A summary of these results but on an individual basis are shown in tables 6.2-6.5.

	Zone 1	Zone 2	Zone 3	Zone 4	OT (°C)
03/04/2013	1.34	2.41	2.68	1.57	0.98
04/04/2013	1.91	3.44	3.44	2.48	1.35
05/04/2013	0.63	4.15	3.58	2.53	1.67
06/04/2013	0.89	2.27	2.30	0.20	2.09
07/04/2013	0.19	0.22	1.62	0.20	3.72
08/04/2013	1.33	1.95	2.07	1.37	2.05
09/04/2013	1.39	1.82	2.00	0.20	2.92

Table 6.2: Period 1 individual response Set Point Tracking Error (SPTE)

	Zone 1	Zone 2	Zone 3	Zone 4	OT (°C)
03/04/2013	-	-	-	-	0.98
04/04/2013	-	-	-	-	1.35
05/04/2013	67.81	-	-	-	1.67
06/04/2013	-	-	-	56.84	2.09
07/04/2013	14.54	18.64	-	5.04	3.72
08/04/2013	-	-	-	-	2.05
09/04/2013	-	-	-	25.82	2.92

Table 6.3: Period 1 individual response Satisfaction Factor (SF)

	Zone 1	Zone 2	Zone 3	Zone 4	OT (°C)
03/04/2013	17.6	15.9	15.6	17	0.98
04/04/2013	16.6	15.1	14.7	15.9	1.35
05/04/2013	16.1	14.0	14.8	15.8	1.67
06/04/2013	18.6	15.3	15.3	17.5	2.09
07/04/2013	19.1	17.3	16.2	18.2	3.72
08/04/2013	17.7	16.8	15.8	17.7	2.05
09/04/2013	18.3	16.2	15.7	17.6	2.92

Table 6.4: Period 1 individual response Start Temperature (ST)

	Zone 1	Zone 2	Zone 3	Zone 4	OT (°C)
03/04/2013	1.37	2.08	2.44	1.22	4.54
04/04/2013	0.62	2.37	2.60	1.44	3.85
05/04/2013	0.20	0.25	1.66	0.22	4.81
06/04/2013	0.30	0.19	0.31	0.23	7.68
07/04/2013	0.22	0.23	0.42	0.19	7.71
08/04/2013	0.29	0.23	0.64	0.19	3.76
09/04/2013	0.51	0.22	0.27	0.23	5.08

Table 6.5: Period 2 individual response Set Point Tracking Error (SPTE)

	Zone 1	Zone 2	Zone 3	Zone 4	OT (°C)
03/04/2013	-	-	-	-	4.54
04/04/2013	-	-	-	-	3.85
05/04/2013	3.08	26.20	-	3.95	4.81
06/04/2013	1.12	7.08	14.24	1.49	7.68
07/04/2013	10.14	19.18	45.70	1.86	7.71
08/04/2013	33.41	80.70	227.09	2.77	3.76
09/04/2013	0.45	11.73	7.23	1.15	5.08

Table 6.6: Period 2 individual response Satisfaction Factor (SF)

	Zone 1	Zone 2	Zone 3	Zone 4	OT (°C)
03/04/2013	16.9	16.2	16	16.8	4.54
04/04/2013	17.1	15.4	15.7	16.1	3.85
05/04/2013	18.5	15.4	15.7	16.8	4.81
06/04/2013	19.5	16.7	16.3	18.4	7.68
07/04/2013	18.1	17.4	16.1	18.5	7.71
08/04/2013	17.3	16.9	16.2	17.9	3.76
09/04/2013	19.2	16.8	16.6	18.5	5.08

Table 6.7: Period 2 individual response Start Temperature (ST)

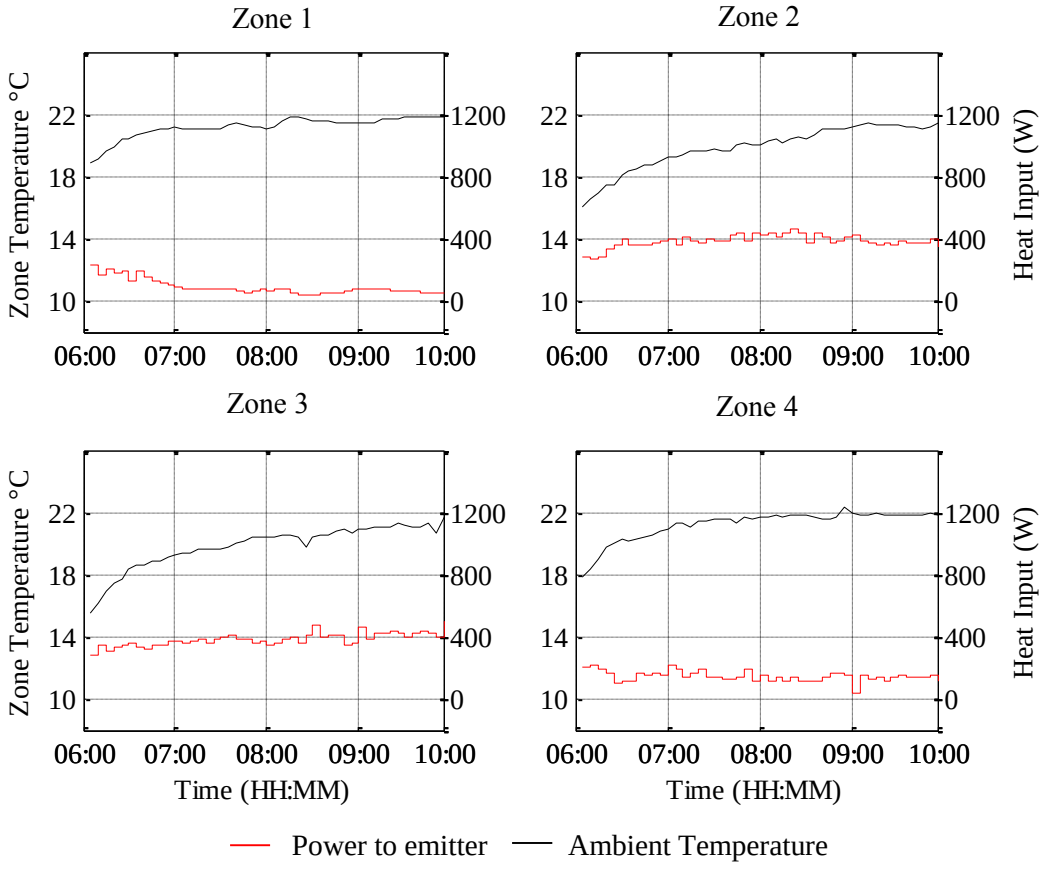

Figure 6.4: Non-priority scheduled zone thermal responses

Examining period 1 (P1), the responses of the 6/04/2013 are illustrated in figure 6.4 and clearly illustrate the inconsistency of the non-priority heating results. Only a single zone reaches the desired set point on that date. During other responses, other zones do reach set point but again not consistently as shown by the table 6.3, with few and scattered valid SP values. Moreover, this is greatly dependant on the prevailing weather conditions.

It may be noted that both days when none of the zones reached set-point were on the two coldest days and the day when three zones reached set point was on the warmest day (07/04/2013). This trend is confirmed examining period 2 (P2) results (tables 6.5-6.7). The more frequent occurrences of non-void SP values indicate a much more consistent satisfaction level is attained in the second period. However, outside temperature (OT) and start point temperatures (ST) for the second period (P2) are far higher on such occasions. Due to less heat losses (as a higher OT would cause) and a higher start point, the probability of reaching set point has been greatly increased.

The most pertinent fact of these trials is that using the priority scheduled system during period 1; two zones were maintained at set-point returning a suitable value of SP even during colder weather (0.05°C and 0.48°C). A traditional centralised non-priority controlled heat source of identical heat output (as emulated by the non-priority test) failed to do so even in occasions of more favourable (warmer) weather during this period. Only during the P2 when external and initial conditions were significantly more favourable, did the non-priority system performance improve.

6.6. Scheduled electric heating summary

The implementation of an SRM-MPC controller in conjunction with a distributed PWM controller for electric heat emitters has proved successful. The constraint handling abilities of MPC have proved ideal for use in this manner, inherently scheduling heat emitters to enable a system rated at 4kW to be powered from a 1kW source. Obviously, there is a trade-off, with thermal comfort noticeably sacrificed in lower priority areas. However, such a system does enable energy use to be accurately budgeted either to enable house holders to have greater control over their energy expenditure. For example, the user would be able to set which zone(s) were prioritised and due to the MPC formulation, the pre-set constraints (i.e. heat input level and thus energy expenditure) would never be violated while simultaneously ensuring set point (desired room temperature) tracking of the higher priority zones. This was demonstrated in figure 6.3 where zones 1 and 2 exhibited excellent set point tracking profiles while the net input power never exceeded 1kW.

An interesting point to note is that such a scheduling technique may have far wider applications. Indeed this work can be considered as a microcosm of various Demand Side Management (DSM) techniques that aim to shift energy demand [123] or the hierarchal control methods proposed for distributing heat and power within a community [124]. Whereas those discussed by Fazeli [123] relate to each specific demand type (heating, cooking, hot water) this work manages the demand within a particular demand type (in this case heating). Thus this method may represent a means of interfacing and optimising the demand of existing electrical systems for use with limited (often renewable) distributed resources, by using the priority time slicing technique.

Two chief stages of development are need to carry this technique forward with regards to hydronic heating systems. The first is a means of switching genuine hydronic heat emitters in a manner that the priority scheduling system can be operated. The second is a method of measuring and predicting occupancy within zones, similar as promoted by Gupta [30] and the Microsoft research centre at Cambridge [31]. Then the choice of priority zones would then be automated in an intelligent manner, thus any penalties suffered by the reduced heating of lower priority zones would be less likely to be of consequence to the user/occupiers.

The next chapter details the development of a novel heat emitter controller that aims address the first stage of development, namely to allow specific temperature levels of heat emitters (and thus the heat they emit) to be controlled using low cost CRVs.

Chapter 7. A novel pre-emptive hysteresis controller for thermoelectric CRVs

7.1. Introduction

The successful implementation of the refined Smith RM-MPC controller in conjunction with thermoelectric valves has demonstrated superior set point tracking to existing prevalent methods. Furthermore, in the previous chapter the use of an MPC algorithm paves the way for its intrinsic optimisation methods to be utilised for scheduling of heat emitters using inexpensive (commercially viable) hardware.

However, results gleaned from the trials using the commercially viable thermoelectric valve heads show that although room set points are maintained at an acceptable level, the existing method has no direct constraining abilities regarding the temperature of the heat emitters. Previous research has demonstrated that excessive heat emitter surface temperature variations can lead to localised hot spots reducing thermal comfort. In more extreme cases, adverse safety conditions causing burns to vulnerable users, may arise from poorly optimised heat emitters [125], [126].

To limit the heat emitted by a fluid filled heat emitter, the energy directed to that individual heat emitter must be controlled. Thus to divide individual heating demands and possibly schedule using thermoelectric valve heads, a method of operating the valve heads in a more refined manner is required.

This chapter details the development of a novel controller suitable for controlling the heat output of heat emitters using thermoelectric CRVs. First the CRV's are characterised using a series of bench-marking tests. Following on, these characterisations enable a simulation method to be devised using Simulink which is then verified using a distributed heating system with the test dwelling. This simulation is subsequently used to determine the favoured course of development for a robust controller suitable for these CRVs under the variable conditions that arise within a central heating system.

7.2. Wax operated actautors

TRVs and Thermoelectric actuated valves could be considered cousins of the same heating control hardware family. Both use a working fluid to operate a pin that opens and closes a valve. In the case of the TRV, the fluid is heated and cooled by the ambient air. Within the thermoelectric valve, the fluid is heated and cooled using a heated element. Benchmarking trials in the previous chapter detailed the drawbacks of TRVs and in particular their performance vulnerabilities due to external factors (placement of furniture, occupancy habits etc.). Fig. 7.1 in particular demonstrates such vulnerabilities, in this case caused by a thermally absorbent mass (a bed) in close proximity to the heat emitter (<0.3m) in Zone 2 (back bedroom, test dwelling). It is clear from fig. 7.1 that these vulnerabilities in some cases can result in poor thermal comfort and wasted energy.

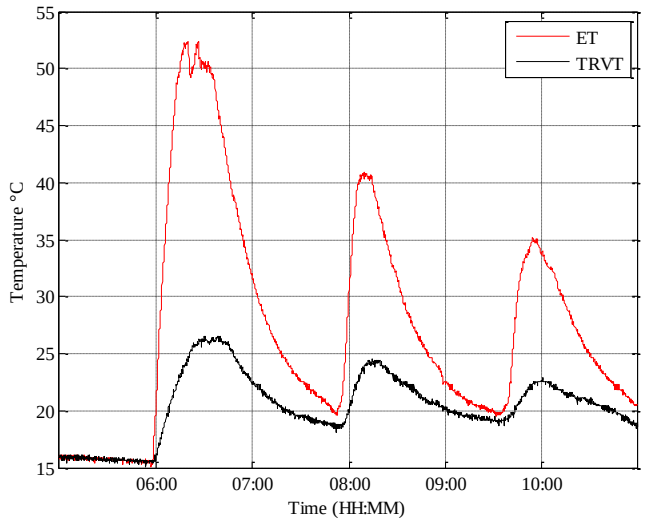

Figure 7.1: Poorly sited furniture causing poor TRV controlled heat emitter response (ET = Emitter temperature, TRVT = TRV height temperature)

7.3. Thermoelectric valve performance

The performance of thermoelectric CRVs is less well documented. Due to cost considerations, ease of UK supply and the availability of TRV adapters (enabling easy swapping between TRV and thermoelectric CRV) Emetti CRVs were chosen as in the last chapter. There are many similar devices on the market and Honeywell in particular are the most descriptive of the performance of their products. A comparable Honeywell device is the MT8 CRV and its performance is detailed in fig.7.2 and table 7.1 [127]. The

datasheets of both the Honeywell and Emetti devices stress that all performance figures may vary according to ambient temperature and no details of such variation are given.

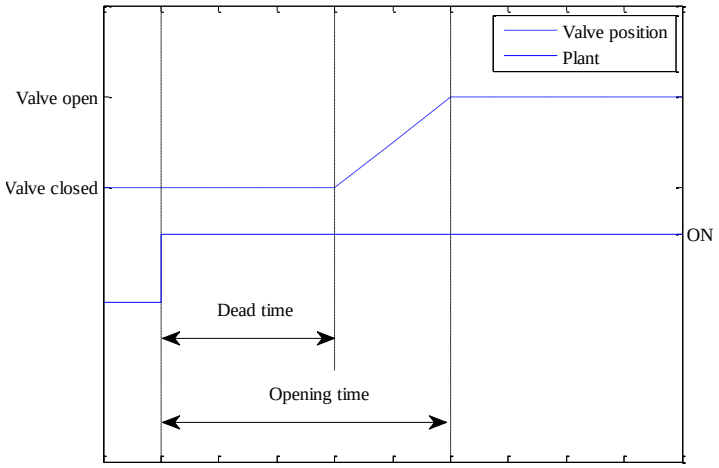

Figure 7.2: Honeywell MT8 valve characteristic

Performance	Honeywell MT8-230-NC	Emetti 230V NC
Stroke (mm)	4	3.6
Power consumption (W)	3	3.45
Run time for full stroke (mins)	2.5	5 to 6

Table 7.1: Emetti and Honeywell CRV performance

Due the vagueness of performance details supplied with such products, a closer examination of the main constituent component of the CRV was conducted, namely the wax piston.

7.4. Wax as a working fluid

The working fluid of the chosen CRV is a wax. Wax has an appropriate co-efficient of expansion for a given temperature change (10-15%) [128]. Coupled with the fact that wax is capable of withstanding significant compressive loads, it is an ideal candidate working fluid for many types of mechanical CRV. Numerous devices have been proposed and manufactured ranging from greenhouse ventilation systems to the familiar TRV.

Incorporating this principle within a CRV head provides an inexpensive alternative to the motorised or solenoid CRV head, which uses a motor or solenoid as an actuator.

Furthermore they require minimal power to impart the large mechanical force required to open and close a valve body (up to 4000N for aerospace applications [129]) ensuring minimised power consumption of the actual control hardware.

Their simple operating principle is also their main disadvantage. Due to the hysteresis properties of the wax, they are slow to respond to input. Great efforts are made by manufacturers to make the opening of the valve linear, using different combinations and grades of wax within a single pellet/piston [130]. The performance of a wax manufactured specifically for use in TRV's is illustrated below, demonstrating the linear expansion (and thus valve opening characteristic) showing the large amount of dead time occurring during heating up. It is remarkably similar to the characteristics found in the Honeywell datasheet.

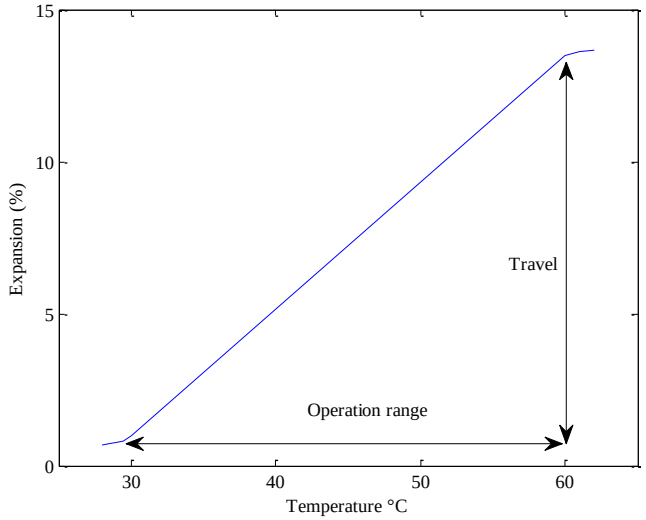

Figure 7.3: DILAVEST 60 operating curve

Ideally one would operate the valve in the operation temperature range (fig. 7.3, 30°C-60°C) allowing careful regulation of the CRV opening and closing. Ideally, this would be achieved by varying the energy supplied to the heating coil within the CRV in a certain manner.

Thus a set of tests using an Emetti CRV and TRV body were conducted to ascertain the behaviour of the typical thermoelectric valve CRV. The performance figures gained from such tests would help to form the basis of any subsequent simulations and thus aid the determination of the most appropriate control strategy.

7.5. CRV performance tests

To test the feasibility of controlling the CRV by means of variable input electrical supply, the CRV head was operated by a variable duty cycle PWM. As opposed to using the dedicated test rig an individual heat emitter within the test dwelling was selected for initial tests (fig. 7.4). This enabled the controller to be tested under a range of conditions in a real occupied dwelling. Subsequent suitable control methods found would then be already validated to work in a 'real-life' situation. A 1400W, 1400mm x 600mm flat panel heat emitter within an upstairs bedroom (zone 1) was chosen due to its standard flat panel design, most common in UK domestic dwellings. Moreover, the bulky test equipment could be secreted within an aesthetically pleasing closed piece of furniture that was resistant to damage caused by occupants.

Figure 7.4: CRV monitoring equipment

As the CRVs require 230VAC, the microcontroller operated burst fire controller described in chapter 3 was used acting as a PWM supply input. A PC connected to the burst fire controller via an RS232 serial interface acted as a data-logger. The PC also acted as a video recording device, monitoring the Vernier calliper movement which could then be subsequently correlated with time and energy input to the CRV. The central heating

system was off with no heat was being supplied from the central heat source during initial tests as this could inhibit each characteristic being obtained under similar conditions.

7.5.1 CRV performance test results (1)

Observing the opening characteristics of the CRV illustrated in fig. 7.5, it is clear that energy input supplied to the CRV can attenuate the performance characteristics of heat emitter. Both dead time and the rate of CRV displacement is dependent on PWM duty and the trend follows that less input extends dead time and decreases rate of CRV displacement. However, the relationship is non-linear, performance markedly changing between 10% and 40% duty cycles. The most interesting point of note is the rate of CRV displacement exhibits a near linear characteristic for each duty cycle input. This is in line with the illustration given within the Honeywell MT8 documentation (fig. 6.3).

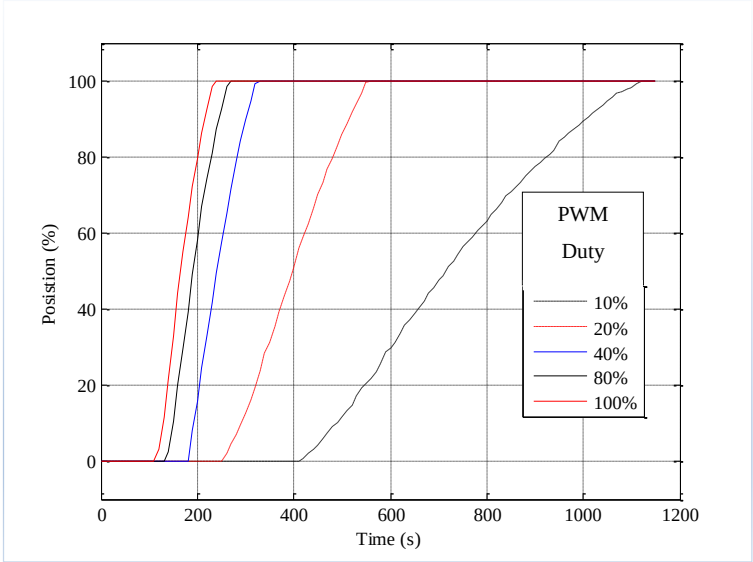

Figure 7.5: CRV operating characteristics (1)

To examine the effect of valve CRV movement and heat emitter performance a further test was carried out using the 10% duty cycle with the central heat source activated. This duty cycle was chosen as this gave slowest rate of opening allowing easier determination of actual valve travel at each point in time. The results of this test are illustrated in fig 7.6.

Examining fig. 7.6 the emitter starts to rise in temperature and reaches a relatively

constant heat input over a particular CRV position range. Indeed, the CRV actuator has moved over 25% of its range of travel before any heat is introduced to the heat emitter (as the heat emitter temperature has not risen). After this, the temperature of the heat input rises in a non-linear fashion until approximately 370 seconds. The heat emitter leaves this period of changing heat input after less than 60% of actuator movement. Thus in this situation the actuator would need to be maintained within this region (25%-60% of total available travel) to be able to moderate heat supply.

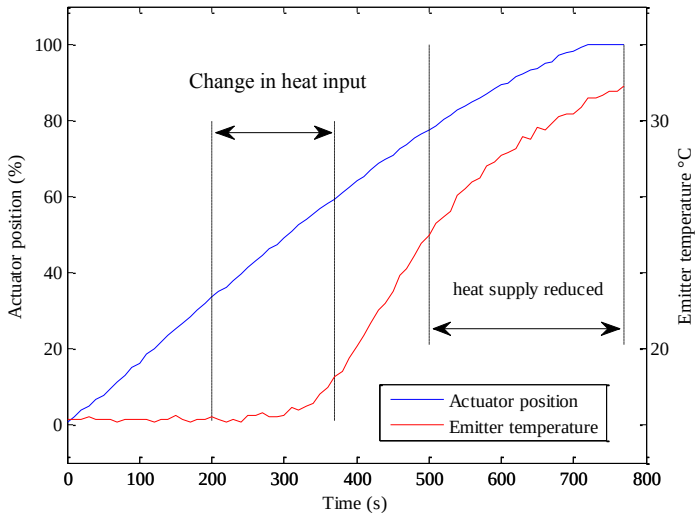

Figure 7.6 CRV operating characteristics (2)

After approximately 500 seconds the rate of change of temperature of the heat emitter begins to reduce despite the actuator now increasing the valve orifice opening further. Thus this indicates the actual heat supply from source is reducing, demonstrating the vulnerability of any proposed control system relying on actuator position to the demands from other parts of the system and/or the status of the central heat source.

In an effort to further understand the effectiveness of moderating the heat input to this CRV, tests were conducted but monitoring two distributed heat emitters within a central system over a single heating period. The purpose of these tests was to examine the dependency of the valve opening/closing times with regard to emitter size and location.

7.5.2 Test apparatus and test trials

Extended the test equipment within the dwelling, a multi-output burst-fire controller was constructed. As opposed to previous work, a wired control system was installed within the test dwelling. Due to the previous installation of a more powerful DrayTek wireless LAN router, the XBee based monitoring and control system had become too unreliable for second by second measurement and control. A central control unit was constructed using an ATMEL2560 based prototyping board, which provided the 10% PWM output that corresponded to an 'On' command. The main function of such a device was to provide an interface that would enable a PC to receive temperature endings and dispense control commands accordingly. Furthermore, this system topology enabled remote access and fast updating of code during troubleshooting and initial commissioning. The full monitoring/control system is illustrated in fig. 7.7.

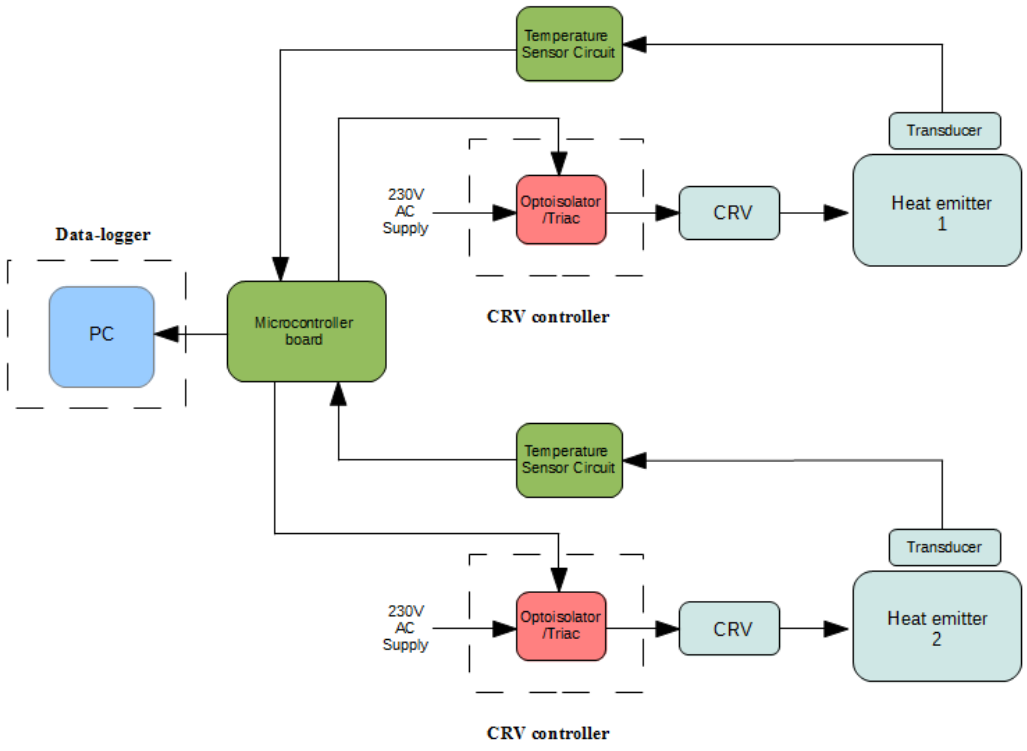

Figure 7.7: Complete distributed burst fire controller

Each CRV was operated by an isolated triac circuit contained within an earthed aluminium enclosure (fig. 7.8). The input to the CRV switch consisted of a 3 standard BS1363 13A plug, fused at 1A. The output was a BS1363 13A socket. Each CRV was

fitted with a BS1363 plug to enable easy disconnection and testing.

Figure 7.8: Triac operated CRV

Temperature was measured via Vishay 4K7 NTC thermistors attached to 3 of the four pairs of core cables within the CAT 5 cable. The fourth core pair delivered the control signal. As these cables and the voltages present within them come under SELV regulations according to BS7671, these could be run underneath carpets.

Following from the previous results gained from the valve characterisations (fig. 7.6), three duty cycles that exhibited distinct phase change characteristics, namely 10%, 20% and 100% where tested. Two heat emitters were chosen, the first was the one used for initial characterisations and the second was a heat emitter located the furthest from the central heat source. The specifications of each heat emitter are included in table 6.2. The length of pipework to each heat emitter was determined by tracing each route using the TI25 FLUKE thermal camera.

Emitter	Distance from boiler (m)	Rated size (W)
1	2.4	1400
2	10.6	1400

Table 7.2 Heat emitter characteristics

Each trial operated each heat emitter using a simple hysteresis controller; turning on each CRV once the measured zone ambient temperature at had dropped below 20°C and only turning off the CRV when the zone ambient temperature had reached 22°C. The ambient temperature was measured in the same manner as the chapter 5, 50mm above the CRV head. The ambient temperature was measured at 50mm above the CRV in accordance with a standard TRV. Using such a controller enabled different duty cycle PWM inputs to be examined while maintaining an acceptable level of thermal comfort the occupants.
To enable practicable assessment measurement of opening and closing time (no physical measurement of valve position), these performance metrics have been abstracted namely;

- Mean Abstract Opening Time (MAOT) is defined as the mean time (s) duration between when CRV is first turned on and when the heat emitter first starts to warm.

- Mean Abstract Closing Time (MACT) is the mean time (s) duration between the CRV being turned off and when the heat emitter first stats to cool.

7.5.3 CRV performance test results (2)

A summary of results of regarding varying PWM duty is illustrated in fig. 6.9 and described by table 6.3.

Zone	Duty (%)	MAOT (s)	MACT (s)
1	10	508	177
2	10	808	109
1	20	283	234
2	20	405	173
1	100	174	282
2	100	303	285

Table 7.3: Summary of CRV performance under variable PWM control

Examining table 7.3 it is clear that the opening and closing times do follow the trends illustrated in fig. 7.5-7.6. For Emitter 1, the MAOT value diminishes by 44% in line with an increase in duty cycle from 10% to 20%. It diminished a further 39% when the duty cycle is raised to 100% indicating that the dead time of the CRV is indeed decreasing. Moreover, the MACT values increases with duty cycle. For emitter 1 the MACT increases by 24% then 17% with increases of cycle 10% and 80% respectively. Emitter 2 follows the trend, increasing by first 37% and then 31% for identical duty cycle variations.

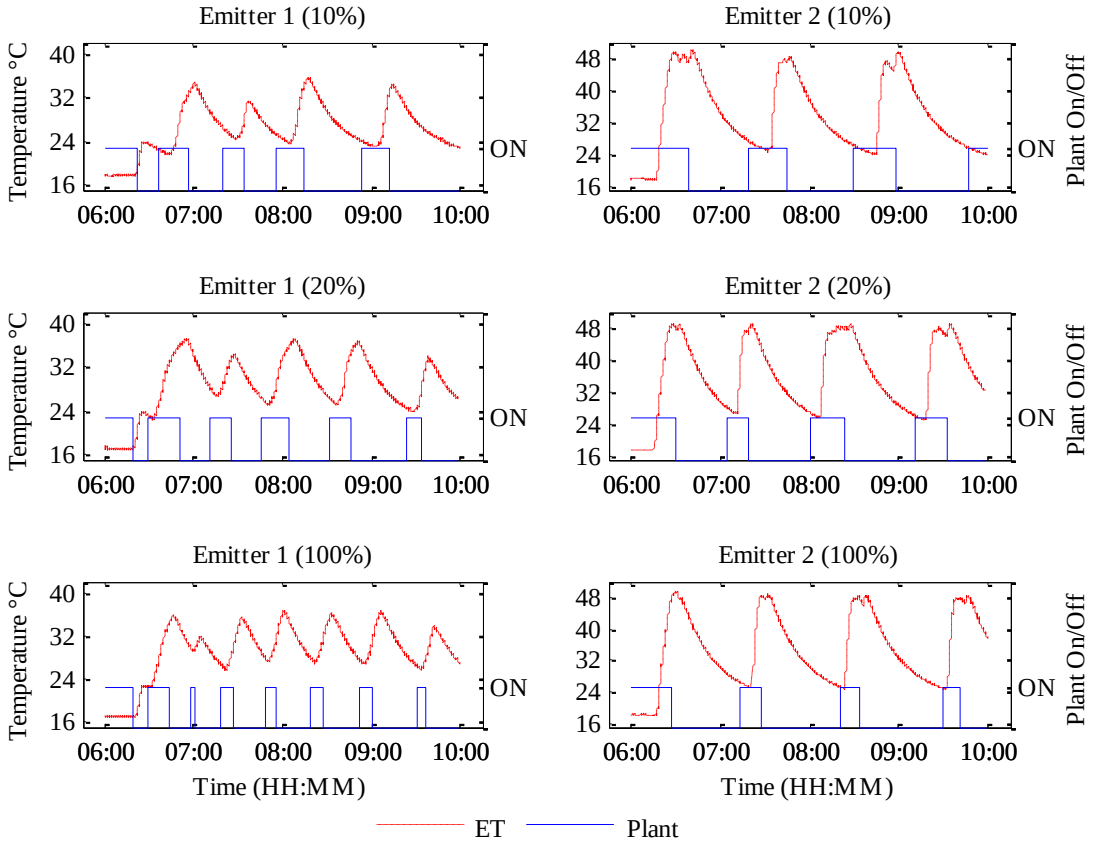

Figure 7.9 Dual heat emitter variable PWM duty trials

Although the trends of such figures are in line with expectations the variation between opening and closing times for each heat emitter is pronounced. For example, the difference between the MOAT value for emitter 1 and emitter 2 differs by 57% (100% duty) and 70% (20% duty). The difference in MACT for differing PWM duty cycles is inconstant too. The difference between abstract closing times is near negligible for a 100% duty but varies by 74% between emitter 1 and 2 using a 20% duty.

Examining the test heating system as whole, one must remember that the test dwelling uses a combination boiler unit (of which there are over 15 million in the UK[131]). Due to this boiler configuration, the use of hot water can dramatically affect heating profile too. One may observe that during the 100% duty cycle trial, the emitter 1 temperature suffers an aberration at around 07:00 hrs. For completeness, the flow pipe of the heating system and the hot water supply pipe from the boiler had also been monitored together with the habits of the occupants. When hot water is called from this particular combination unit, the pressure drop that results from a hot water tap being opened causes the boiler to redirect the flow of water. This is accomplished by a manifold within the boiler unit that contains a three way valve, ensuring the demanded domestic hot water and not the heating circulating fluid is passing through the heat exchanger. This use of domestic hot-water supply by an occupant temporarily caused the circulating fluid to cool, causing the heating system circulating fluid to drop in temperature (see figs 7.10-7.11).

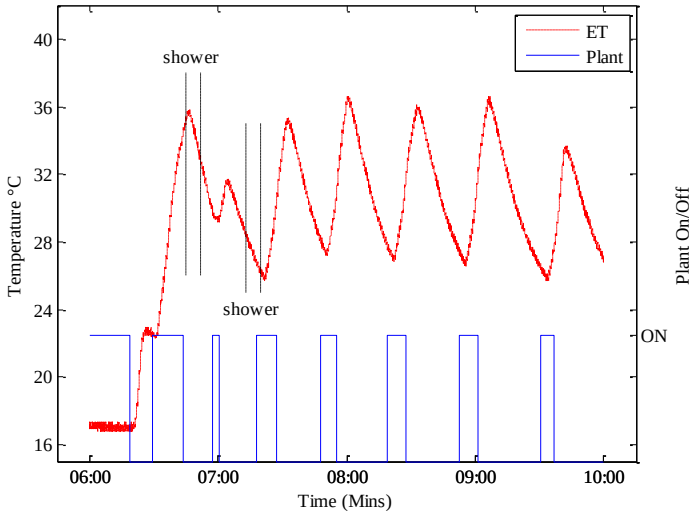

Figure 7.10: Zone 1 heat emitter operation

From these preliminary trials one may conclude that the opening and closing characteristics of these inexpensive CRVs may be varied by altering PWM duty cycle. However, a myriad of factors including domestic hot-water use and physical constitution of heat emitters can affect their performance.

Ideally, monitoring the precise position of the CRV would represent a means of progression, though this would represent a significant hardware addiction to the CRV and the associated cost. A more tractable solution would be a narrow band hysteresis controller.

A particularly narrow hysteresis band would be needed as the high rate of temperature change of the heat emitter once the CRV starts to operate can cause significant overshoot.

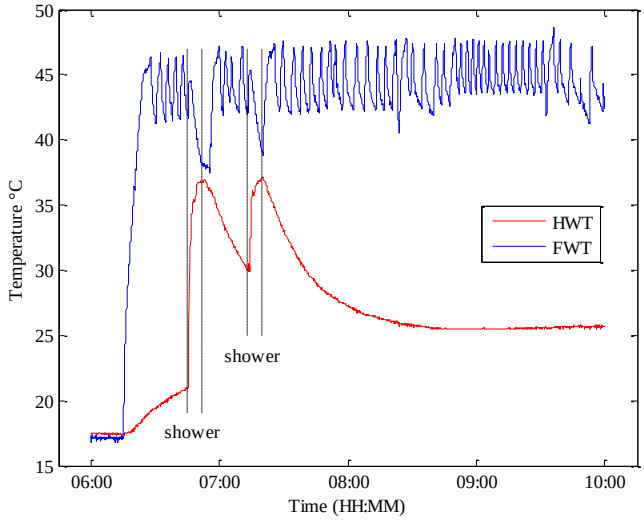

Figure 7.11 Boiler operation (HWT = Hot water temperature, FWT = Flow water temperature)

To recap previous work (chapter 3) one may consider the heat output variation that may arise from such an emitter surface temperature variation as (1).

$$P_{em} = P_{rated} \times Operating\ Factor \quad (1)$$

Operating factor (1) is determined by the heat emitter manufacturer's data and is dependent on the temperature difference between emitter surface temperature and zone ambient temperature (table 7.4 [91]).

Using standard tables from a leading heat emitter manufacturer (table 7.4), it is clear that for a flat panel heat emitter the power output variation will be less than 10% between high operating levels (over 50°C above ambient, [T_{em}-T_{zone}] = 60°C-65°C). This figure increases to 18% at lower output levels ([T_{em}-T_{zone}] = 30°C-35°C). Considering successful implementation of an RM-MPC controller in chapter 3 only needed a PWM resolution of 20%, a narrow band hysteresis controller that can maintain a heat emitter temperature that does not oscillate more than +/-5 °C will be suitable. Such a controller could then be utilised within RM-MPC framework to control, schedule and limit temperature of distributed heat emitters. Such a system using inexpensive COTS hardware would

provide an increased level user comfort and safety within a dwelling.

$[T_{em}-T_{zone}]$ (°C)	Operating Factor
5	0.05
10	0.123
15	0.209
20	0.304
25	0.406
30	0.515
35	0.629
40	0.748
45	0.872
50	1
55	1.132
60	1.267
65	1.406
70	1.549
75	1.694

Table 7.4: Stelrad Elite® flat panel heat emitter operating factor values

To enable the formulation of tighter band hysteresis controller using these CRV, two problems need to be addressed; 1) The sharp rise in emitter temperature once the CRV opens 2) The long hysteresis time associated with opening the CRV.

To counter the sharp rise in temperature of the heat emitter once the heat emitter temperature has started to rise, and given the hysteresis time within the CRV profile, one would require the CRV to change direction of travel (start to close) as soon as this has been observed. A rise in heat emitter temperature is detected by the temperature rising by 0.5°C due to the prescribed accuracy of the temperature sensor (chapter 4).

The PWM duty cycle input that has the shortest closing time is 10% (MACT, table 7.3). Thus this would be the required PWM level for the control of the CRV. Unfortunately, if using the 10% value, the opening hysteresis time is now significant (>500s, table 7.3), which would lead to an excessive fall in heat emitter temperature before the CRV starts to open. The solution would be to turn the plant ‘ON’ (turn on the CRV) at a predetermined time compensating for the hysteresis time. As has been already established, predicting the hysteresis time is impracticable, due its variability due to ambient temperature [127] and

heat emitter temperature (table 7.3).

The remainder of this chapter concerns the formulation, implementation and testing of a novel hysteresis controller that utilises thermoelectric CRVs. The first stage in the formulation of a suitable controller is the derivation of a simulation method to enable rapid evaluation and analysis.

7.6. Simulation of CRV and heat emitter

To preliminary assess the efficacy of any subsequently derived control methods a simulation model using Simulink was constructed. The CRV is modelled in two parts (figs. 7.12-7.13). The first considers the opening and closing dead time and the second considers the actual actuation of the valve.

7.6.1 CRV model (dead time)

The two dead time variations are switched between whether the CRV is on or off. Each dead time is represented by an integer delay block.

7.6.2 CRV model (CRV displacement)

Within the CRV model (fig. 7.13), the valve opening curve is represented by a variable summing loop that adds or subtracts a rate of displacement depending on the CRV being in the opening or closing phase. The rate of displacement when opening is dependent on the PWM control level and has been determined from the empirical trials summarised in table 7.3 The closing rate of change is always the same as this is not determined by the PWM input but a return spring.

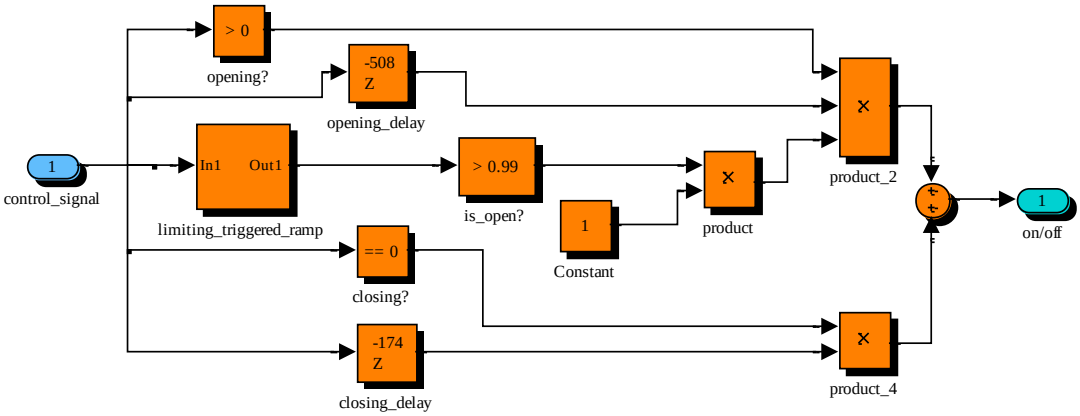

Figure 7.12 Simulink model of CRV dead time

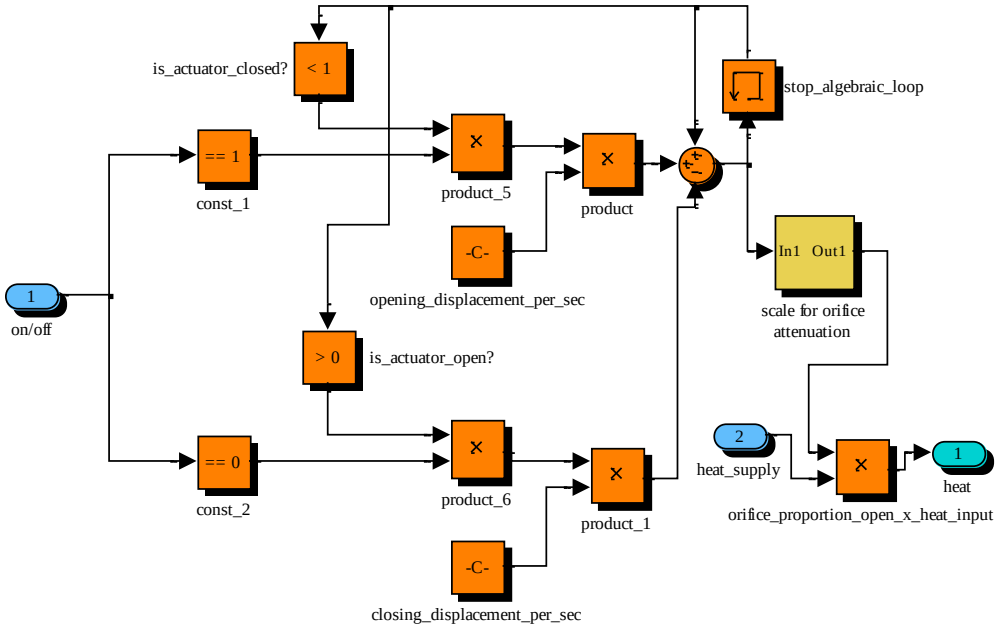

Figure 7.13 Simulink model of actuator displacement

To provide data to validate the simulation a benchmarking trial was undertaken. Monitoring zones 1 and 2 heat emitters used in the previous trial (section 7.5), a heat emitter set point of 30°C and a dead band of 2°C were chosen as control parameters. The actuators was operated using a PWM duty 10% PWM between 06.15 Hrs and 10:00 Hrs on 09/01/14.

As can be noted from the zone 1 heat emitter characteristic illustrated in Figure 7.14, there are limitations of using the mean recorded values of opening and closing time. During

the initial start-up phase (06.15 Hrs – 6:45 Hrs) of the valve operation it has a slower closing time initially. This non uniform characteristic causes the valve to close slower only at the start of the bench marking trial leading to an increased rise in heat emitter temperature when compared to the simulation. The shorter plant (heat source) 'On' period that causes this aberration is due to the CRV being stationary when the trial commences as opposed to moving in the opposite to the desired direction of travel during all subsequent switching between 'OFF' and 'ON' commands. However, once this phase is over, the simulation demonstrates commensurate performance between 07:00hrs and 10:00hrs. The most interesting point to note that in this guise, even at a low heat emitter temperature, the benchmarking trial demonstrates that a traditional 2°C hysteresis band can result in a measured temperature deviation of +/- 7 °C.

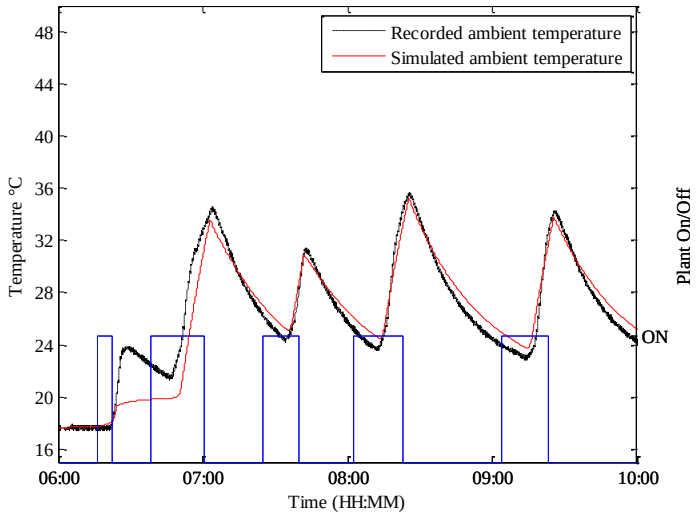

Figure 7.14 Comparison of simulation with recorded data (zone 1)

The same limitation of inconsistent opening times is present using the same simulation method in conjunction with recorded data from zone 2. Observing fig. 7.14, after an initial inaccuracy period (before 07:00 Hrs) the simulation once again demonstrates commensurate performance with recorded data. Moreover, the smaller heat emitter used within zone 2, has significantly less thermal mass which contributes to a faster response to CRV opening (and the subsequent heat introduced). This faster response results in greater oscillation around the 30°C set-point of the zone 2 heat emitter, contributing to a maximum recorded overshoot of >12°C. Extrapolating the operating values summarised in table 7.4, such occurrences would lead to a power deviation of 36% for a flat panel

heat emitter of identical design. Such output deviation is beyond the scope of required performance (>20% set point deviation, section 7.3). The remaining sections of this chapter describe the formulation, implementation and testing of a novel hysteresis controller that aims to address excessive dead band oscillation using thermoelectric CRVs.

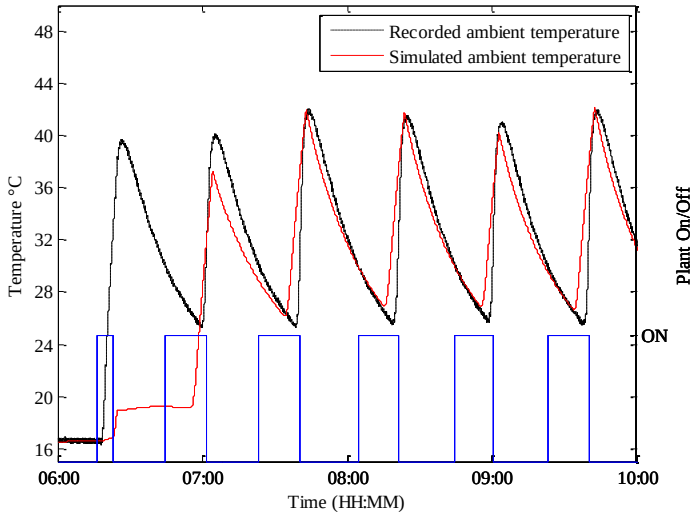

Figure 7.15 Comparison of simulation with recorded data (zone 2)

7.7. Novel thermic CRV controller

Due to the proportionally significant dead times of the wax based CRV, a traditional hysteresis controller with upper and lower band limits (or upper and lower set points) is impractical. An alternative method is to dispense with a dead band as such and change the nature of the controller set point. Once the heat emitter has closed and the temperature has been determined to be falling, turn the plant on when it drops below a pre-determined level. Once the heat temperature starts to rise again, turn the plant 'OFF'. In essence, the controller is *pre-emptive*, turning the plant 'ON' and 'OFF' before the effect of those control actions on the system (heat emitter) are detectable (temperature trend change). Instead of having two set points, an upper and a lower that prescribe the hysteresis band, only one set point is now required. This *temperature drop set point* actually utilises the hysteresis time of the CRV and heat emitter responses to set the hysteresis band. Such a controller is easily realised on an inexpensive microcontroller and a flow chart representation of the controller is detailed in fig. 7.16.

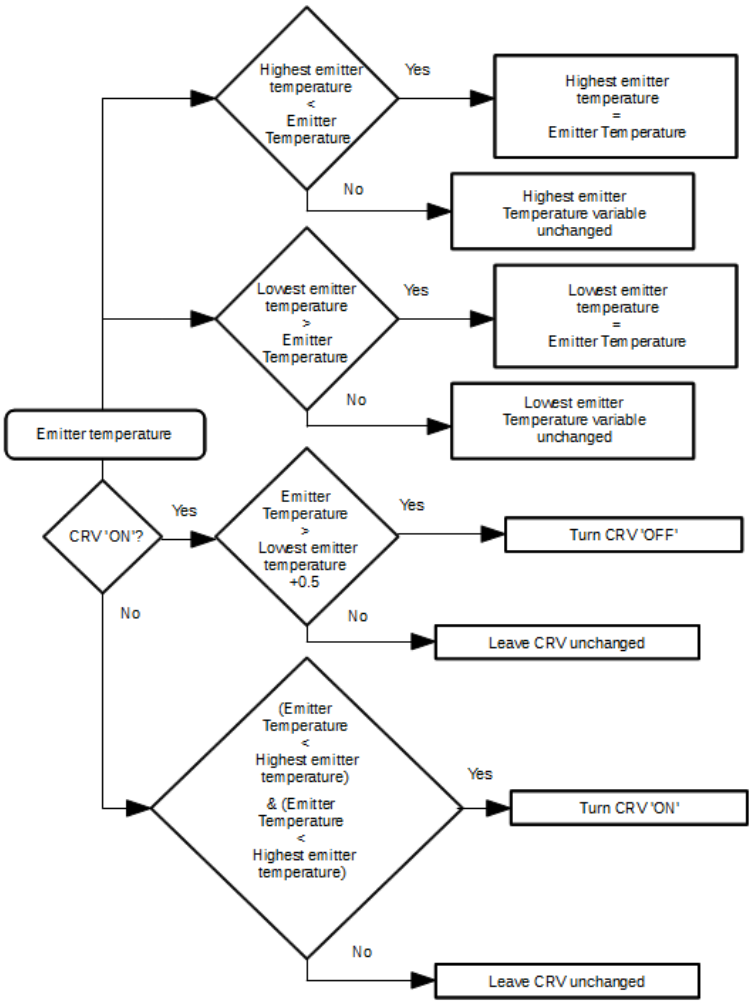

Figure 7.16: Flowchart of pre-emptive (PE) hysteresis controller

7.8. Simulation of traditional hysteresis band controller

By simulating the proposed Pre-Emptive (PE) controller a better understanding may be attained. Using the simulation method described in section 7.6, the heat emitter is simulated using both a 2°C hysteresis band and 0.5°C hysteresis band (the minimum given the resolution of the temperature measurement devices). Figs 7.17-7.18 demonstrate the pronounced effect of the hysteresis band and time taken for the CRV to open and close.

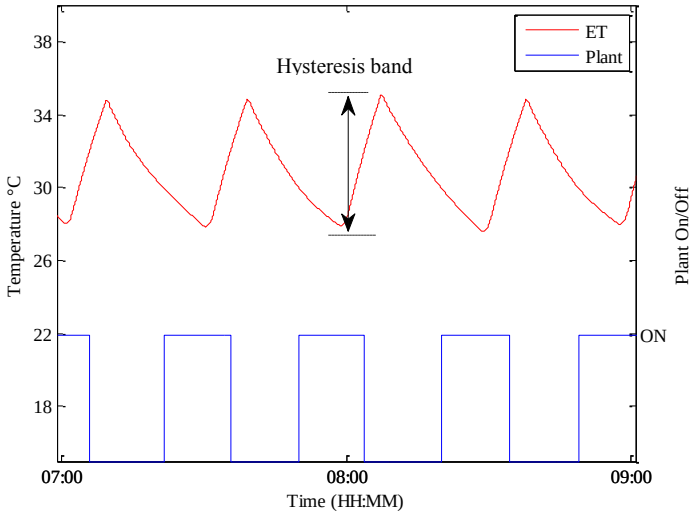

Figure 7.17: Traditional 2°C hysteresis thermal response

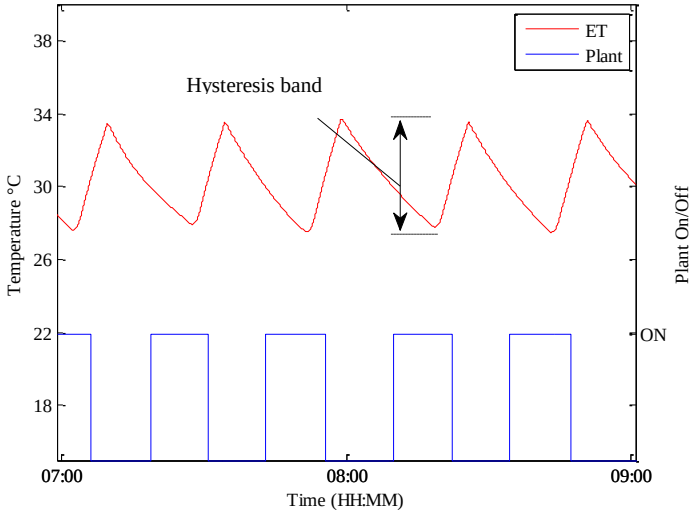

Figure 7.18: Traditional 0.5°C hysteresis thermal response

The hysteresis band is extending considerably the beyond the controller defined limits. The 2°C controller resulting with a peak temperature of 34.2°C and standard deviation from set point of 2.1°C. Even with a substantially reduced prescribed hysteresis level, the 0.5°C resulted in a peak temperature of 33.7°C and a standard deviation from set point of 7.16°C. Fig 7.19 demonstrates the operation of the novel controller, where the temperature profile of the heat emitter can be seen to exhibit less hysteresis band. In simulation, the novel controller resulted in a standard deviation of 1.1°C, a reduction of 39% of compared to the traditional (0.5°C) hysteresis band hysteresis control. By utilising the turn on delay (hysteresis time of CRV) of the system a turn off temperature (point D)

that is less than the turn 'ON' temperature (point C) may be selected, as opposed to traditionally the turn 'OFF' point (point B) being higher than turn 'ON' (point A) . Thus the overshoot between set point and peak temperature above set point will always be less using the new PE controller.

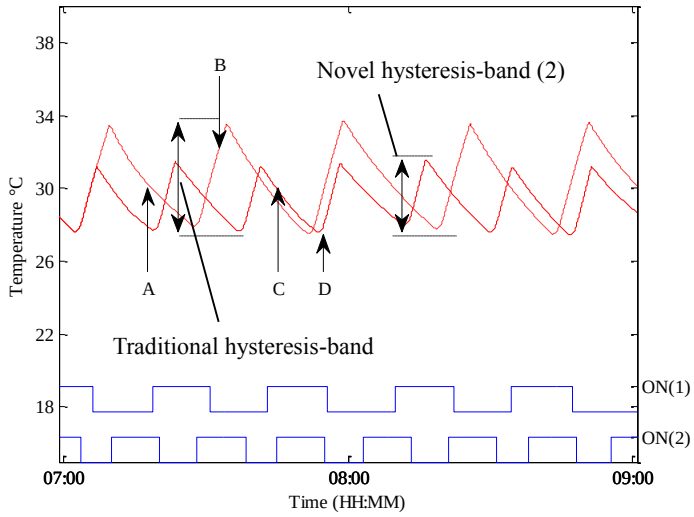

Figure 7.19: Traditional 0.5°C hysteresis vs PE control

7.9. Results

Due to two other heat emitters within the central heating system being uncontrolled for safety reasons (by pass radiators) the set point of the central boiler circulating fluid does determine ambient temperature in large parts of the test dwelling. The oversizing of the heat emitters limited the range of temperatures that could be tested, as what would normally be considered low heat emitter temperatures [118] would still correspond to large heat output levels. For this reason only relatively low heat emitter set points (30°C, 40°C and 50°C) could be examined without affecting the occupant's thermal comfort. For each test the boiler set point was set 20°C higher than the required set point of the heat emitters to give ample headroom.

The PE controller was implemented using the existing distributed burst fire controller described in fig. 7.7. For completeness a set of trials using conventional hysteresis control were completed using the same set points. For consistency the performance parameters used for comparison of the two techniques used the period between 09:00Hrs and 10:00Hrs for the first two trials where no aberrations of heating profile occurred due to

domestic hot water use (showers). A summary of both set of results is included in table 7.5. The latter (50°C set point) uses the period between 7:00Hrs and 08:00Hrs.

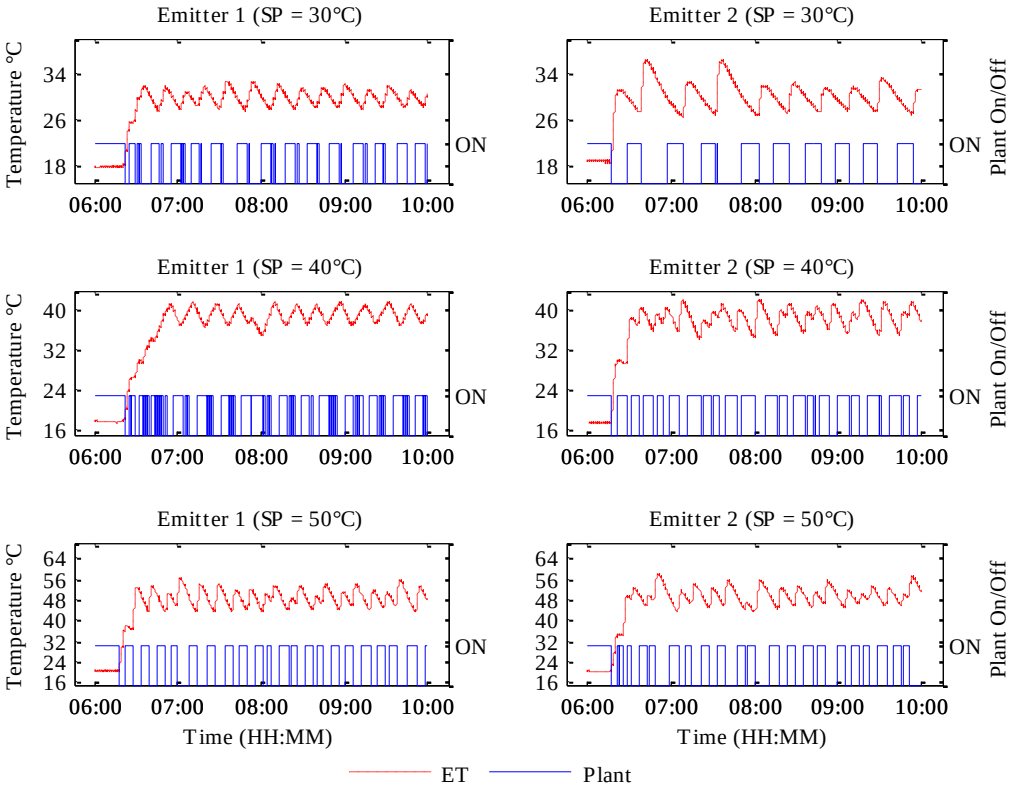

Figure 7.20 PE controller results

Set point (°C)	Conventional		PE	
	Emitter 1 Standard deviation (°C)	Emitter 2 Standard deviation (°C)	Emitter 1 Standard deviation (°C)	Emitter 2 Standard deviation (°C)
30	1.7	4.9	1.1	1.7
40	5.2	4.7	1.3	1.9
50	5.5	4.4	3.0	2.9

Set point (°C)	Conventional		PE	
	Emitter 1 Peak (°C)	Emitter 2 Peak (°C)	Emitter 1 Peak (°C)	Emitter 2 Peak (°C)
30	33.5	40.8	32.1	36.4
40	52.6	48.1	41.9	42.3
50	59.8	58.0	55.8	57.2

Table 7.5: PE vs traditional 0.5°C hysteresis controller results

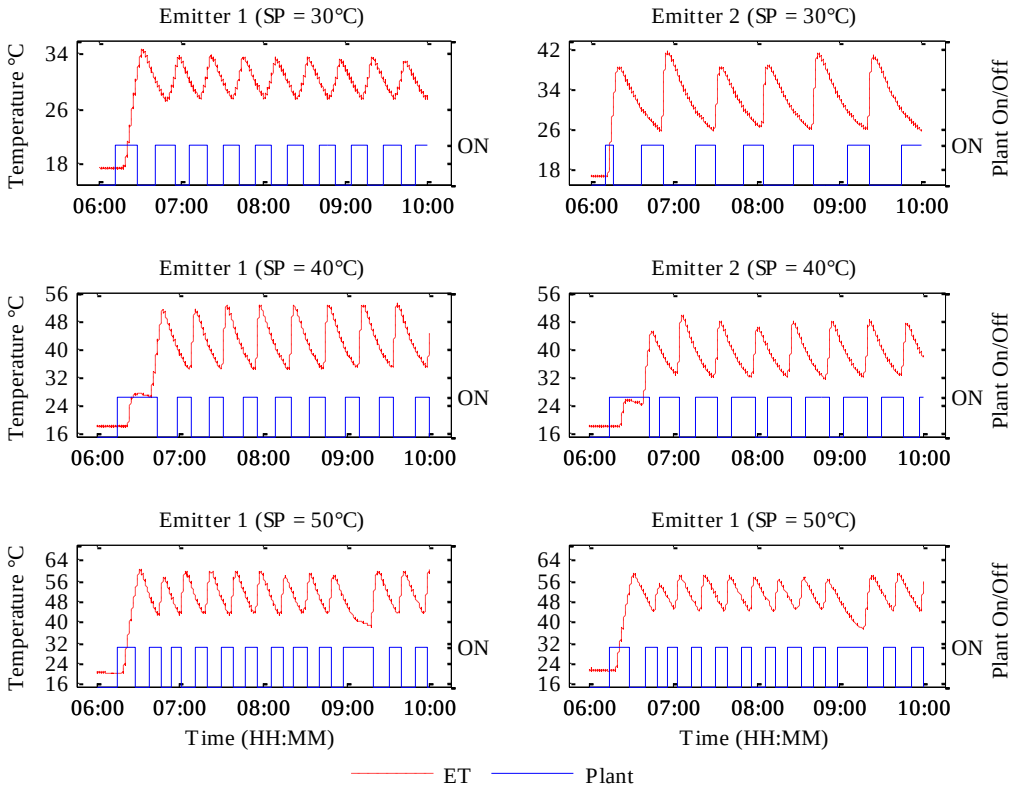

Figure 7.21: Traditional 0.5°C hysteresis controller results

Using the lower set point of 30°C, the new PE controller performs significanty better than the conventional type using both heat emitters. The results of the heat emitter 1 almost mirror the simulation results described in section 7.6, the new controller returning a 37% reduction in standard deviation (1.7°C to 1.1°C). For emitter 2, the improvement is more pronounced, returning a 65% in standard deviation (4.9°C to 1.7°C). Emitter 2 has a more inconsistant heating profile using the new controller particaularly between 6:30hrs and 8:00hrs, which can be attributed to more heat being directed towards the heat emitter due to other parts of the system being off. Even considering such extremes, the maximum peak recorded using the new controller was 36.4°C for a 30°C set point. This is 15% below the recorded peak temperature endured by the heat emitter using the conventional controller (40.8°C) for the same set point.

The effect of hot water usage using both controllers can be clearly seen, particularly during the test using the conventional controller between 9:00hrs and 10:00hrs for the 50°C test (fig.7.21).

Examining standard deviation of heating profiles, the new controller exhibits far superior perfomance too. At 40˚C heat emitter 1 experiances a reduction by 75% and heat emitter 2 is reduced by 40%. The improvements remain pronounced for the higher 50˚C setpoint, both heat emitters experiancing reductions of 45% and 34% for emitter 1 and emitter 2 respectivily at a 50˚C set point.

7.10. Summary

A set of COTS CRVs have been evaluated in terms of performance parameters, namely, hysteresis time and opening time. Furthermore, their effect on heat emitter heating characteristics within a central heating system has been evaluated. Following on from these results, a new premeptive hysterisis controller has been proposed that is suitable for controlling heat emitters with these low cost CRVs. Using the proposed contoller togther with these CRVs allows previously unobtainable heat emitter output control using COTS equipment.

By closely controlling heat emitter temperature, the safely of heat emitters can be assured in terms of limiting heat emitter temperature within safe levels reducing the risk of burns to occupants. Furthermore, the prevalance of hot spots near heat emitters can now be reduced due to this new method.

Most importantly, as the heat output of heat emitters can now be constrained within pre-defined limits, heat can now be allocated more accurately from a central heat source, regardless of heat source output. This may have far reaching effects, enabling the scheduling of heat among distributed hyronic heat emitters within a building using low cost COTS equipment.

Chapter 8. Conclusion

8.1. Summary

The use of a central heat source supplying distributed heat emitters dates back millennia [132]. In recent times, it has been recognised by commercial interests, research establishments and legislative bodies that domestic central heating is a key area where energy use levels and carbon dioxide emissions can be cut in the UK.

In response to this, during the last five years the choice of 'energy saving' commercial heating control devices that aim to reduce heating energy consumption has dramatically increased. However, at present their principle method of 'energy saving' is by optimising heating schedules according to occupancy level (NEST®, HIVE® for example). At present the task of tackling energy wastage caused by poor thermal comfort regulation or poor temperature set point tracking has mostly been the preserve of academic research establishments. Following on from these current research trends then, this thesis presents a number of controllers that aim to address the three other key research areas which would greatly increase the efficiency of the central heating system. These are central heat source oversizing, improved domestic zone set point tracking using inexpensive hardware and the control of heat emitter temperature.

By constructing a dedicated test cell and a number of flexible temperature monitoring/control systems a simulation method together with a new family of MPC controllers has been developed and tested.

First a MATLAB/Simulink heating simulation method has been devised which has shown commensurate performance with recorded results. This validated simulation model allowed the merits of operating distributed heat emitters in a manner not possible before the introduction of CRVs. In simulation the distributed heat emitters were operated in a sequential scheduled manner in comparison to a conventional operating (parallel) procedure. These simulation results demonstrated that the scheduling of heat emitters sequentially may offer distinct advantages such as reduced boiler cycling, reduced capacity central heat source and associated material cost. However, the simulations also

proved that a poorly conditioned scheduling routine may actually consume more energy for a given level of thermal comfort and that an advanced control technique was needed for any such sequential operation method to work.

Following on from these simulation results Model Predictive Control (MPC) was chosen as the preferred control method due its rapid rise in popularity among the academic HVAC research community. Its main benefit of inherent constraint handling was thought paramount to achieving superior set point tracking while conserving energy use. At the time of writing, no reasonably practicable method existed for the implementation of MPC with a traditional domestic setting, thus an adaptive *recursive* modelling technique was developed. Relying on the relative constancy of outside temperatures in the heating season of the UK, the Recursive Modelling MPC (RM-MPC) controller demonstrated superior set point tracking compared to traditional heating control methods. Under commensurate weather conditions the RM-MPC controller returned an energy saving greater than 20% when compared to conventional methods in the test cell. Moreover by use of a PWM interface, the technique was proven feasible using existing heating system hardware within an occupied dwelling.

In an effort to reduce computational complexity, increase speed and reduce price and power consumption of hardware, the RM-MPC controller was refined by the addition of a smith controller. The Smith RM-MPC (SRM-MPC) controller was demonstrated to exhibit excellent set point tracking capabilities using an oil filled heat emitter within the test cell. Continuing, the controller proved suitable for operating distributed heat emitters with low cost thermic CRVs. The complete control system was now at a demonstrator level, requiring only minimal hardware modification to be developed as commercially viable product.

The test dwelling was now subsequently re-commissioned to test the viability and performance of the SRM-MPC acting a sequential/time-slicing controller. By using its inherent constraint handling properties as a means of operating multiple heat emitters with a heat source rated at a fraction of what otherwise would usually be required. Although thermal comfort was penalised in lower priority heated zones, the technique proved an ideal method for limiting energy consumption while providing the maximum thermal possible thermal comfort in designated zones. However, the sequential/time-

slicing technique was only tested using electrical heaters, of which their power consumption is far easier to control than hydronic heaters that are part of a central heating system. To use this MPC time slicing technique the hydronic heater's temperature (and thus the power they consume) would have to be controlled.

In response to this, a novel hysteresis controller has been developed, to further aid the application of a scheduling method to existing central heating systems using low cost hardware. The developed controller was demonstrated to exhibit performance characteristics ideal for interfacing with advanced control systems regardless of the temperature of fluid with complete heating system. Such a controller would not only aid accurate control of heating within a dwelling but also greatly reduce the risk of injury directly caused by central heating system heat emitters. Heating systems, together with oven doors caused 43% of contact burns to persons under the age of 16 admitted to emergency department in the UK between 2008 and 2010 [125].

8.2. Further Work

As discussed earlier in this work, the commercial inertia required to switch the prevailing heating topology discussed in this work to newer designs is infeasible in the short to medium term nationwide. The work presented in this thesis represents a complete method for interfacing superior control methods on existing central heating systems. Such methods not only represent an opportunity to bridge this gap, the preservation of existing systems may offer distinct advantages. For example, the method proposed for budgeting energy use would be less feasible with heat emitters of higher thermal mass (underfloor heating). Moreover, considering a recent report by the UK government climate change committee stating "heat pumps are likely to be an important part of meeting 2050 carbon targets" [133], a method of operating heat emitters in a manner that matches demand may be ideal for the future of domestic HVAC technologies. However, there are two crucial areas of research require investigation to carry this work forward and ensure impact within the wider community.

The first is the long term testing of the SRM-MPC controller operating the pre-emptive controller (with low cost CRVs) within a dual loop configuration (fig 8.1). Such a method

would enable genuine hydronic heat emitters as part of central heating system to be scheduled and also kept within predetermined surface temperature limits.

The next stage would be to interface the complete system with an occupancy prediction system as proposed by Gupta [30] or even using motion sensors like NEST® and the system tested by the Microsoft research centre in 2011[31].

The work in this thesis delivers a strong contribution to the field of domestic HVAC research and also provides an advanced novel prototype system, proven to work in the real environment for which it is destined.

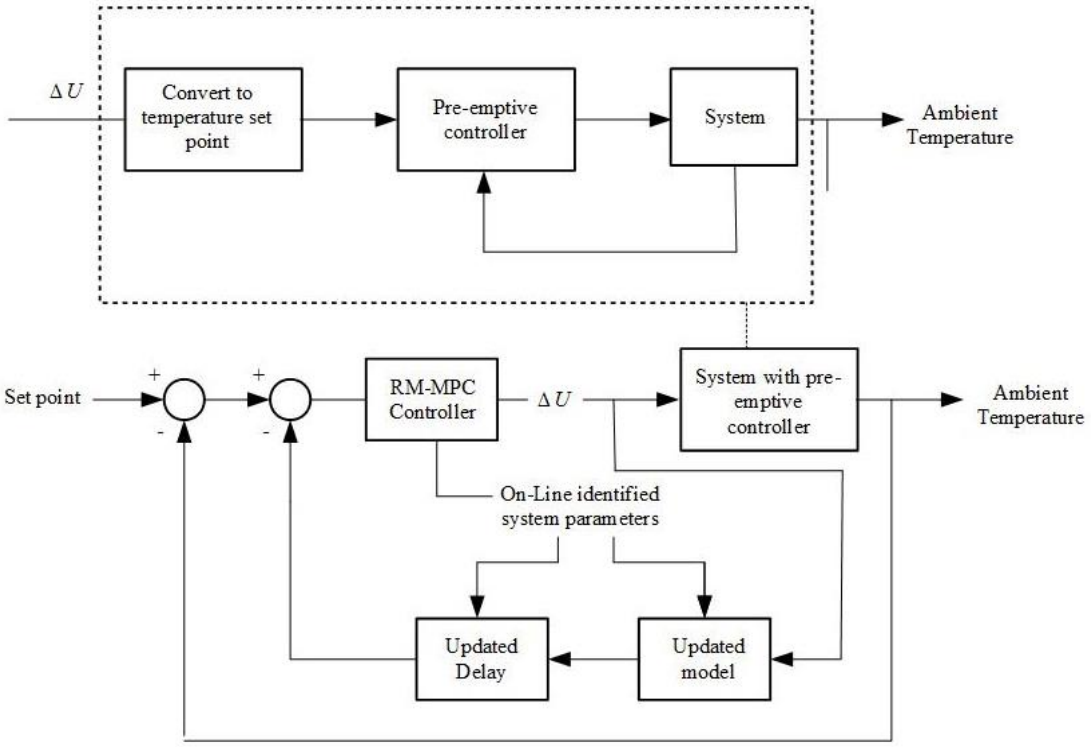

Figure 8.1: Proposed complete dual loop SRM-MPC/Pre-emptive controller

References

[1] J. I. Utley and L. D. Shorrock, “Domestic energy fact file 2008,”, BRE, 2008.

[2] J. Palmer and I. Cooper, “Great Britain ’ s housing energy fact file,” , DECC, 2011.

[3] UK Government," Climate Change Act 2008 ”, HMSO, 2008.

[4] P. J. Munton, A.G., Wright, A.J., Mallaburn, P.S, & Boait, “How heating controls affect domestic energy demand : A Rapid Evidence Assessment,”, DECC, 2014.

[5] ASHRAE, "*ASHRAE 55-2004: Thermal Environmental Conditions for Human Occupancy*. Techstreet", ASHRAE, 2004.

[6] P. Fanger, “Assessment of thermal comfort practice,” *Bitish. Journal of Industrial. Medicine.*, vol. 30, pp. 313–324, 1973.

[7] J. van Hoof and J. L. M. Hensen, “Quantifying the relevance of adaptive thermal comfort models in moderate thermal climate zones,” *Building and the. Environment.*, vol. 42, no. 1, pp. 156–170, Jan. 2007.

[8] DAIKIN, “Remote Controller BRC1C61 instruction manual”, *DAIKIN Controller*s, 2014.

[9] P. Broad, “Consumers and domestic heating controls : a literature review,” *Consumer Focus*,. July, 2012.

[10] HMGoverment, “Conservation of fuel and power in existing dwellings, L1b.” 2010.

[11] R. Rayment and K. Morgan, “Comparing conventional and electronic roomstats,” *Building Research and Practice,* vol 12, no. 2, pp. 114–121, 1984.

[12] Honeywell, “Frequently Asked Questions Thermostatic Radiator Valves (TRV ’ s).” , *Honeywell UK*, 2014.

[13] BEAMA, “Results of Research Carried Out on the Effectiveness of Domestic Heating Controls,”, BEAMA, 2013.

[14] Z. Liao, M. Swainson, and a. L. Dexter, “On the control of heating systems in the UK,” *Buildin and the Environment*, vol. 40, no. 3, pp. 343–351, Mar. 2005.

[15] CIBSE, "*Cibse Guide B1: Heating*", CIBSE 2005.

[16] L. Peeters, J. Van der Veken, H. Hens, L. Helsen, and W. D’haeseleer, “Control of heating systems in residential buildings: Current practice,” *Energy and Buildings.*, vol. 40, no. 8, pp. 1446–1455, Jan. 2008.

[17] DOE, “Energy Tips, Minimize Boiler Short Cycling Losses.”, DOE, 2014.

[18] Reuters, “Options dwindle for UK facing winter tied to tight Norway gas,” *http://www.reuters.com/article/2013/09/30/energy-europe-gas-outlook-idUSL5N0HN31B20130930*, 2013.

[19] Potterton, “Potterton commercial boiler guide”, *www.potterton.co.uk*, 2014.

[20] H. Kershaw, G. Orr, M. Crowther, and I. Summerfield, “Final Report for – In-situ monitoring of efficiencies of condensing boilers", *TPI control project extension Prepared by the energy saving trust*:, 2010.

[21] Johnson Boiler Company, “Johnston Boiler Company Technical Brief, Efficiency Comparison: 4:1 turndown and 10:1 turndown.” , *Johnson boilers*, 2003.

[22] Potterton, “Potterton commercial boiler guide”, *www.potterton.co.uk*, 2014.

[23] DECC, DOT and DEFRA “UK Bioenergy Strategy,” , DECC, 2012.

[24] Windhager, *“http://www.windhager.co.uk/products/wood-pellet-boilers”* 2014. .

[25] E. Johnson, “Goodbye to carbon neutral: Getting biomass footprints right,” *Environment. Impact Assessment. Revue.*, vol. 29, no. 3, pp. 165–168, 2009.

[26] BGS, “Ground source heat pumps: development of GeoReports for potential site characterisation, issue 1.2,” , *British Geological Survey*, 2004.

[27] EST, "http://www.energysavingtrust.org.uk/Generating-energy/Choosing-a-renewable-technology/", *Energy saving trust*, 2012.

[28] T. Malinick, N. Wilairat, J. Holmes, and L. Perry, “Destined to Disappoint : Programmable Thermostat Savings are Only as Good as the Assumptions about Their Operating Characteristics", *Procedings of 2012 ACEEE Summer Study on Energy Efficiency in Buildings*, pp. 162–173, 2012.

[29] F. O’Connell, “Inside the Nest Learning Thermostat,” *New York Times*, 2012.

[30] M. Gupta, S. S. Intille, and K. Larson, “Adding GPS-Control to Traditional Thermostats : An Exploration of Potential Energy Savings and Design Challenges,” *MIT*, 2009

[31] J. Scott, A. J. B. Brush, J. Krumm, B. Meyers, M. Hazas, S. Hodges, and N. Villar, “PreHeat : Controlling Home Heating Using Occupancy Prediction”, Proceedings of 13th International Conference on Ubiquitous Computing, Sep. 2011.

[32] WARMWORLD, “Dataterm the intelligent heating controller” *http://www.warmworld.co.uk*. 2011.

[33] T. Peffer, M. Pritoni, A. Meier, C. Aragon, and D. Perry, “How people use thermostats in homes: A review,” *Building and the Environment.* vol. 46, no. 12, pp. 2529–2541, Dec. 2011.

[34] TEC, The Energy Master “*http://www.totalenergycontrols.co.uk/p/energy_master.php*” 2014.

[35] Honeywell, *“www.honeywelluk.com/products/Systems/Wirelss/CM-Zone”* Honeywell, 2013

[36] HouseTech, *“http://www.housetechsolutions.co.uk/.”* Honeywell, 2014.

[37] A. I. Dounis and C. Caraiscos, “Advanced control systems engineering for energy and comfort management in a building environment—A review,” *Renewable. Sustainable Energy Revue.*, vol. 13, no. 6–7, pp. 1246–1261, Aug. 2009.

[38] B. D. Snoonian, “Can building automation systems overcome interoperability problems to assert control over our offices, hotels, and airports? By Deborah Snoonian,” *IEEE Spectrum*, 2003.

[39] V. Boonsawat, J. Ekchamanonta, K. Bumrungkhet, and S. Kittipiyakul, “XBee Wireless Sensor Networks for Temperature Monitoring,” *proceedings of the 2nd ECTI conference on Antennas and Propogation*, May. 2010.

[40] P. J. Boait and R. M. Rylatt, “A method for fully automatic operation of domestic heating,” *Energy and Buildings.*, vol. 42, no. 1, pp. 11–16, Jan. 2010.

[41] J. Miriel and F. Fermanel, “Classic wall gas boiler regulation and a new thermostat using fuzzy logic Ð Improvements achieved with a fuzzy thermostat,” *Applied Energy*, vol. 68, pp. 229–247, 2001.

[42] J. Sedano, “A fuzzy logic based efficient energy saving approach for domestic heating systems,” *Integrated Computer Aided Engineering*, vol. 15, pp. 1–9, 2008.

[43] M. M. Gouda, S. Danaher, and C. P. Underwood, “Quasi-adaptive fuzzy heating control of solar buildings,” *Building and the Environment*, vol. 41, no. 12, pp. 1881–1891, Dec. 2006.

[44] D. Kolokotsa, K. Niachou, V. Geros, K. Kalaitzakis, G. S. Stavrakakis, and M. Santamouris, “Implementation of an integrated indoor environment and energy management system,” *Energy and Buildings*, vol. 37, no. 1, pp. 93–99, Jan. 2005.

[45] R. Z. Homod, K. S. M. Sahari, H. a. F. Almurib, and F. H. Nagi, “Gradient auto-tuned Takagi–Sugeno Fuzzy Forward control of a HVAC system using predicted mean vote index,” *Energy and Buildings*, vol. 49, pp. 254–267, Jun. 2012.

[46] R. Z. Homod, K. S. Mohamed Sahari, H. a. F. Almurib, and F. H. Nagi, “RLF and TS fuzzy model identification of indoor thermal comfort based on PMV/PPD,” *Building and the Environment*, vol. 49, pp. 141–153, Mar. 2012.

[47] R. L. Navale and R. M. Nelson, “Use of genetic algorithms to develop an adaptive fuzzy logic controller for a cooling coil,” *Energy and Buildings*, vol. 42, no. 5, pp. 708–716, May 2010.

[48] S. Soyguder, M. Karakose, and H. Alli, “Design and simulation of self-tuning PID-type fuzzy adaptive control for an expert HVAC system,” *Expert System Applications*, vol. 36, no. 3, pp. 4566–4573, Apr. 2009.

[49] A. Argiriou, I. Bellas-Velidis, and C. Balaras, “Development of a neural network heating controller for solar buildings.,” *Neural Netorks*, vol. 13, no. 7, pp. 811–20, Sep. 2000.

[50] S. Jassar, Z. Liao, and L. Zhao, “Adaptive neuro-fuzzy based inferential sensor model for estimating the average air temperature in space heating systems,” *Building and the Environment*, vol. 44, no. 8, pp. 1609–1616, Aug. 2009.

[51] D. Kolokotsa, a. Pouliezos, G. Stavrakakis, and C. Lazos, “Predictive control techniques for energy and indoor environmental quality management in buildings,” *Building and the Environment*, vol. 44, no. 9, pp. 1850–1863, Sep. 2009.

[52] L. Liu, L. Fu, C. Wang, and Y. Jiang, “A novel on-off TRV adjustment model and simulation of its thermal dynamic performance,” *Building Simulation.*, vol. 2, no. 2, pp. 109–118, Apr. 2009.

[53] Z. Liao and A. L. Dexter, “An Inferential Model-Based Predictive Control Scheme for Optimizing the Operation of Boilers in Building Space-Heating Systems,” *IEEE Transactions on Control Systems Technology*, vol. 18, no. 5, pp. 1092–1102, Sep. 2010.

[54] M. M. Gouda, S. Danaher, and C. P. Underwood, “Building thermal model reduction using nonlinear constrained optimization,” *Building and Environment* , vol. 37, pp. 1255–1265, 2002.

[55] M. M. Gouda, S. Danaher, and C. P. Underwood, “Low-order model for the simulation of a building and its heating system,” *Building Services Engineering Research and Technology*, vol. 21, no. 3, pp. 199–208, Jan. 2000.

[56] S. Prívara, J. Široký, L. Ferkl, and J. Cigler, “Model predictive control of a building heating system: The first experience,” *Energy and Buildings*, vol. 43, no. 2–3, pp. 564–572, Feb. 2011.

[57] E. Zacekova and L. Ferkl, “Building modeling and control using multi-step ahead error minimization,” *2012 20th Mediterranian Conference on Control and Automation*, pp. 421–426, Jul. 2012.

[58] R. Bălan, J. Cooper, K.-M. Chao, S. Stan, and R. Donca, “Parameter identification and model based predictive control of temperature inside a house,” *Energy and Buildings*, vol. 43, no. 2–3, pp. 748–758, Feb. 2011.

[59] D. Molina, S. Member, C. Lu, V. Sherman, and R. Harley, “Model Predictive and Genetic Algorithm Based Optimization of Residential Temperature Control in the Presence of Time-Varying Electricity Prices ” *Proceedings of the IEEE Industry Applications Society Annual Meeting (IAS),* pp. 7–13, 2011.

[60] M. Short, “Real-time infinite horizon adaptive/predictive control for Smart home HVAC applications,” *Proceedings of the 17th Int. Conference on Emerging Technolologies Factory. Automation (ETFA 2012)*, pp. 1–8, Sep. 2012.

[61] A. Lefort, R. Bourdais, G. Ansanay-Alex, and H. Guéguen, “Hierarchical control method applied to energy management of a residential house,” *Energy and Buildings.*, vol. 64, pp. 53–61, Sep. 2013.

[62] S. Prívara, J. Cigler, Z. Váňa, F. Oldewurtel, and E. Žáčeková, “Use of partial least squares within the control relevant identification for buildings,” *Control Engineering Practice*, vol. 21, pp. 113–121, Oct. 2012.

[63] S. Prívara, J. Cigler, Z. Váňa, F. Oldewurtel, and E. Žáčeková, “Use of partial least squares within the control relevant identification for buildings,” *Control Engineering Practice.*, vol. 21, pp. 113–121, Oct. 2012.

[64] S. Prívara, Z. Váňa, E. Žáčeková, and J. Cigler, “Building modeling: Selection of the most appropriate model for predictive control,” *Energy and Buildings.*, vol. 55, pp. 341–350, Sep. 2012.

[65] I. Hazyuk, C. Ghiaus, and D. Penhouet, “Optimal temperature control of intermittently heated buildings using Model Predictive Control: Part I – Building modeling,” *Building and the Environment.*, vol. 51, pp. 379–387, May 2012.

[66] I. Hazyuk, C. Ghiaus, and D. Penhouet, “Optimal temperature control of intermittently heated buildings using Model Predictive Control: Part II – Control algorithm,” *Building and. Environment*, vol. 51, pp. 388–394, May 2012.

[67] M. Maasoumy and A. Sangiovanni-vincentelli, “Total and Peak Energy Consumption Minimization of Building HVAC Systems Using Model Predictive Control,” *Green electronics and computing*, pp. 26–35, Oct 2012.

[68] S. Goyal, H. A. Ingley, and P. Barooah, “Effect of Various Uncertainties on the Performance of Occupancy-Based Optimal Control of HVAC Zones,” pp. 7565–7570, 2012.

[69] M. Castilla, J. D. Álvarez, M. Berenguel, F. Rodríguez, J. L. Guzmán, and M. Pérez, “A comparison of thermal comfort predictive control strategies,” *Energy and Buildings.*, vol. 43, no. 10, pp. 2737–2746, Oct. 2011.

[70] J. Široký, F. Oldewurtel, J. Cigler, and S. Prívara, “Experimental analysis of model predictive control for an energy efficient building heating system,” *Applied Energy*, vol. 88, no. 9, pp. 3079–3087, Sep. 2011.

[71] Z. Yu and A. Dexter, “Simulation based predictive control of low energy building systems using two stage optimisation”, *Proceedings of the Eleventh IBPSA Conference*, pp. 1562–1568, Jul, 2009.

[72] M. Varchola and M. Drutarovský, “ZIGBEE BASED HOME AUTOMATION WIRELESS SENSOR NETWORK,” *Proceedings of Acta Electrotechnica et Informatica 2007*, vol. 7, no. 4, pp. 1–8, 2007

[73] A. Wheeler, “Commercial Applications of Wireless Sensor Networks Using ZigBee,” *IEEE Communications Magazine*, Vol 45, no 4, pp. 70–77, April 2007.

[74] D. Egan, “Emergence of ZigBee in Building Automation and Industrial Controls,” *IEE Computing and Control Engineering*, pp 14-19, May, 2005.

[75] R. Belliardi, "ZigBee Building Automation Standard", *The ZigBee Alliance*, 2011.

[76] P.Malmsten, G. Rapp, B. Lalor, “https://pypi.python.org/pypi/XBee/2.1.0,”, 2014

[77] J. Eaton, “https://www.gnu.org/software/octave/,” 2014.

[78] D. Kushner, “http://spectrum.ieee.org/geek-life/hands-on/the-making-of-arduino,” *IEEE Spectrum*, 2011.

[79] D. J. Norris and E. S. Trickett, “A simple low cost pyranometer,” *Solar Energy*, vol. 12, pp. 251–253, 1968.

[80] M. a Martínez, J. M. Andújar, and J. M. Enrique, “A new and inexpensive pyranometer for the visible spectral range.,” *Sensors (Basel)*, vol. 9, no. 6, pp. 4615–34, Jan. 2009.

[81] M. Sengupta, P. Gotseff, and T. Stoffel, “Evaluation of Photodiode and Thermopile Pyranometers for Photovoltaic Applications,” *National Renewable Research Laboritory*, Sep. 2012.

[82] “http://www.sheffieldsolarfarm.group.shef.ac.uk” *Project Sunshine*, 2014.

[83] D. B. Crawley, L. K. Lawrie, F. C. Winkelmann, W. F. Buhl, Y. J. Huang, C. O. Pedersen, R. K. Strand, R. J. Liesen, D. E. Fisher, M. J. Witte, and J. Glazer, “EnergyPlus: creating a new-generation building energy simulation program,” *Energy and Buildings.*, vol. 33, no. 4, pp. 319–331, Apr. 2001.

[84] D. B. Crawley, J. W. Hand, M. Kummert, and B. T. Griffith, “Contrasting the capabilities of building energy performance simulation programs,” *Building and Environment*, vol. 43, no. 4, pp. 661–673, Apr. 2008.

[85] DOE, “apps1.eere.energy.gov/buildings/energyplus,” *US Department of Energy*, 2014.

[86] “apps1.eere.energy.gov/buildings/energyplus/ep_interfaces.cfm,” 2013.

[87] DOE, “http://apps1.eere.energy.gov/buildings/energyplus/openstudio.cfm,” *US Department of Energy*, 2014.

[88] D. Gladwin, D. Rogers, M. Street, S. Sheffield, C. Bingham, and P. Stewart, “Building heating simulation design for control analysis,” Proceedings of *Modelling and Simulation (AfricaMS 2010) Gaborone, Botswana*, 2010, pp. 685–040.

[89] M. Wetter and P. Hayes, “A Modular Building Controls Virtual Test Bed for the Integrations of Heterogeneous Systems.” Proceedings of SimBuild, Berkely, Jul. 2008.

[90] V. K. Goel, "*Fundamentals Of Physics Xi*." Tata McGraw-Hill Education, 2007.

[91] Stelrad, “Stelrad Temperature Table.” *Stelrad*, 2014.

[92] Z. Liao and a. L. Dexter, “A simplified physical model for estimating the average air temperature in multi-zone heating systems,” *Building and Environment*, vol. 39, no. 9, pp. 1013–1022, Sep. 2004.

[93] G. H. & C. P. Underwood, “A simple building modelling procedure for MATLAB/Simulink”, Proceedings of the 6th International Conference on Building Performance Simulation (IBPSA´99), September, Kyoto-Japan, pp.777-783. 1999.

[94] X. Xu and S. Wang, “A simplified dynamic model for existing buildings using CTF and thermal network models,” *Interational Journal of Thermal Science*, vol. 47, no. 9, pp. 1249–1262, Sep. 2008.

[95] W. Feist, J. Schnieders, V. Dorer, and A. Haas, “Re-inventing air heating: Convenient and comfortable within the frame of the Passive House concept,” *Energy and Buildings.*, vol. 37, no. 11, pp. 1186–1203, Nov. 2005.

[96] B. Hyndman, “Heating, Ventilation, and Air Conditioning,” *Carbon Trust*, 2004.

[97] “www.sciencedirect.com,” 2011.

[98] S. Prívara, J. Cigler, Z. Váňa, F. Oldewurtel, C. Sagerschnig, and E. Žáčeková, “Building modeling as a crucial part for building predictive control,” *Energy and Buildings*, vol. 56, pp. 8–22, Oct. 2012.

[99] S. Goyal and P. Barooah, “A method for model-reduction of non-linear thermal dynamics of multi-zone buildings,” *Energy and Buildings*, vol. 47, pp. 332–340, Apr. 2012.

[100] L. Ferkl, “Ceiling radiant cooling: Comparison of ARMAX and subspace identification modelling methods,” *Building and Environment*, vol. 45, no. 1, pp. 205–212, Jan. 2010.

[101] S. Ogonowski, “Modeling of the heating system in small building for control,” *Energy and Builings*, vol. 42, no. 9, pp. 1510–1516, Sep. 2010.

[102] ISO, "ISO 7730: Moderate Thermal Environments - Determination of the PMV and PPD Indices and Specification of the Conditions for Thermal Comfort". *International Standards Organisation*, 1994.

[103] AAMatrix, “http://www.aamatrix.com/solutions/aspectft0old.asp,”, AAMatrix 2012.

[104] “http://www.sheffieldweather.co.uk,” 2012.

[105] E. F. Camacho and C. Bordons, *Model Predictive Control*. Springer-Verlag GmbH, 2004.

[106] Z. Michalewicz and D. B. Fogel, *How to Solve It: Modern Heuristics*. Springer, 2004.

[107] L. Wang, "*Model Predictive Control System Design and Implementation Using MATLAB"* Springer, 2009.

[108] C. Inard, H. Bouia, and P. Dalicieux, "Prediction of air temperature distribution in buildings with a zonal model," *Energy Buildings*, vol. 24, no. 2, pp. 125–132, Jul. 1996.

[109] A. T. Howarth, "The prediction of air temperature variations in naturally ventilated rooms with convective heating," *Building Services. Engineering. Research and Technolgy*, vol. 29, pp. 275–281, 1985.

[110] F. Franklin, Gene, J. D. Powell, and L. Workman, Michael, *Digital Control of Dynamic Systems (3rd Edition)*. Addison Wesley Longman, 1998.

[111] V. Feliu-Batlle, R. Rivas Pérez, F. J. Castillo García, and L. Sanchez Rodriguez, "Smith predictor based robust fractional order control: Application to water distribution in a main irrigation canal pool," *Journal of Process Control*, vol. 19, no. 3, pp. 506–519, Mar. 2009.

[112] A. Núñez-Reyes, J. E. Normey-Rico, C. Bordons, and E. F. Camacho, "A Smith predictive based MPC in a solar air conditioning plant," *Journal of Process Control*, vol. 15, no. 1, pp. 1–10, Feb. 2005.

[113] V. Feliu-Batlle, R. Rivas Pérez, F. J. Castillo García, and L. Sanchez Rodriguez, "Smith predictor based robust fractional order control: Application to water distribution in a main irrigation canal pool," *Journal of Process Control*, vol. 19, no. 3, pp. 506–519, Mar. 2009.

[114] A. Núñez-Reyes, J. E. Normey-Rico, C. Bordons, and E. F. Camacho, “A Smith predictive based MPC in a solar air conditioning plant,” *Journal of Process Control*, vol. 15, no. 1, pp. 1–10, Feb. 2005.

[115] J. P. Hespanha, D. Liberzon, and A. S. Morse, “Overcoming the limitations of adaptive control by means of logic-based switching,” *System Control Letters*, vol. 49, no. 1, pp. 49–65, May 2003.

[116] L. Vu, D. Liberzon, and S. Member, “Supervisory Control of Uncertain Linear Time-Varying Systems” *IEEE transactions on Automaitic control*, vol. 56, no. 1, pp. 27–42, 2011.

[117] K. Astrom and T. Hagglund, *PID Controllers: Theory, Design, and Tuning*. 1994.

[118] P. J. Boait, D. Fan, and a. Stafford, “Performance and control of domestic ground-source heat pumps in retrofit installations,” *Energy and Buildings*, vol. 43, no. 8, pp. 1968–1976, Aug. 2011.

[119] R. Alcalá, J. Alcalá-Fdez, M. J. Gacto, and F. Herrera, “Improving fuzzy logic controllers obtained by experts: a case study in HVAC systems,” *Applied Intelligence*, vol. 31, no. 1, pp. 15–30, Dec. 2007.

[120] E. Lunn, “Energy bills prepay meters cost poorer households,” *The Guardian*, 2013.

[121] I. Geddes, E. Bloomer, J. Allen, and P. Goldblatt, “The Health Impacts of Cold Homes and Fuel Poverty,” *Save The Children*, 2011.

[122] L. Donaldson, “2009 Annual Report of the Chief Medical Officer,” *UK Department of Health*, 2009.

[123] A. Fazeli, E. Christopher, C. M. Johnson, M. Gillott, and M. Sumner, “Investigating the effects of dynamic demand side management within intelligent Smart Energy communities of future decentralized power system,” in *2011 2nd IEEE PES International Conference and Exhibition on Innovative Smart Grid Technologies*, 2011, pp. 1–8.

[124] A. Fazeli, M. Sumner, C. M. Johnson, and E. Christopher, “Coordinated Optimal Dispatch of Distributed Energy Resources within a Smart Energy Community Cell,” in *2012 3nd IEEE PES International Conference and Exhibition on Innovative Smart Grid Technologies*, 2012, pp. 1–10.

[125] M. Kemp, S. Jones, Z. Lawson, and S. a Maguire, “Patterns of burns and scalds in children.,” *Archives of Disease in Childhood*, vol. 99, no. 4, pp. 316–21, Apr. 2014.

[126] R. D. Harper and W. A. Dickson, “Domestic central heating radiators: a cause for 7concern in all age groups” *Burns*, vol. 22, no. 3, pp. 217–220, 1996.

[127] Honeywell "http://ecc.emea.honeywell.com/europe/ecatdata/pdf_mt_mt8-230-nc.html” Honeywell, 2014..

[128] J. S. Lee and S. Lucyszyn, “Thermal analysis for bulk-micromachined electrothermal hydraulic microactuators using a phase change material,” *Sensors and Actuators*, vol. 135, no. 2, pp. 731–739, Apr. 2007.

[129] S. Tibbitts, "High-output paraffin linear motors: utilization in adaptive systems", *Active and Adaptive Optical Components*, pp. 388, Jan.1992.

[130] Dilavest, “dilavest TM as an expansion wax in mechanical pressure and temperature controllers.” 2014.

[131] DECC, “Housing energy fact file”, DECC, 2013.

[132] Vitruvius, *De architectura*. 15BC.

[133] Frontier Economics Ltd, “Pathways to high penetration of heat pumps", *a report for the UK commitee on climate change,* 2013.

Appendix I. Hardware circuits

Distributed temperature monitoring system.

The distributed temperature sensing system circuit is illustrated in figure II.1. As with all hardware associated with this research the design revolved around the supply of components from the University of Sheffield EEE stores. For example two resistors in series were used to form the required value for adjusting the LM317 voltage regulator. Only the 2mm spaced connectors for the XBee modem (J1 and J2) and the voltage regulator were sourced from outside the department.

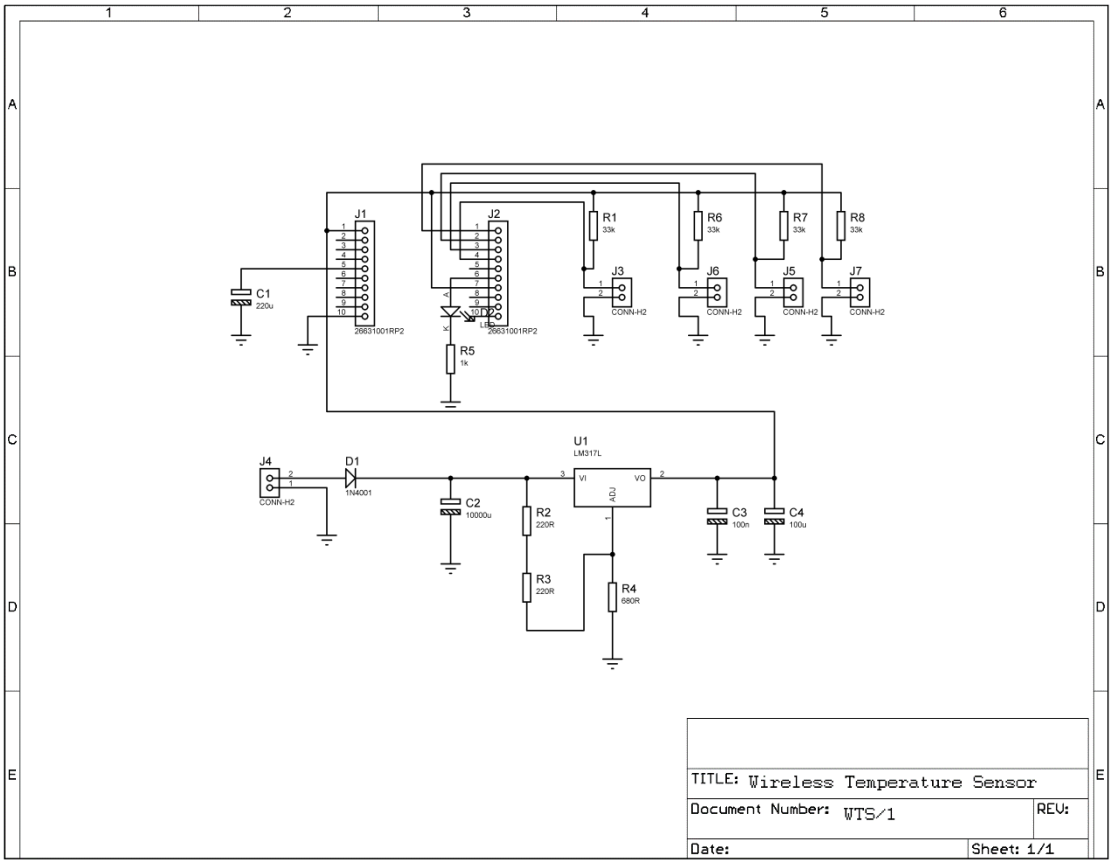

Figure II.1: XBee temperature sensing transmitter circuit

Constant current PAC

The phase controller circuit is illustrated in fig. II.2. Again, the design revolved around the supply of components from the University of Sheffield EEE stores. Thus the ubiquitous 555 timer was used as the central IC, controlling the point at which the supply was activated after a zero crossing point was detected. The XBee was mounted on a separate PCB although manufactured as part of the same board and cut off later. This allowed the XBee to be mounted under a plastic cover even though the controller as a whole was mounted within a durable metal case. Single insulated wires with molex connectors could form the interconnection between central control board and the XBee Transmitter/Receiver modem.

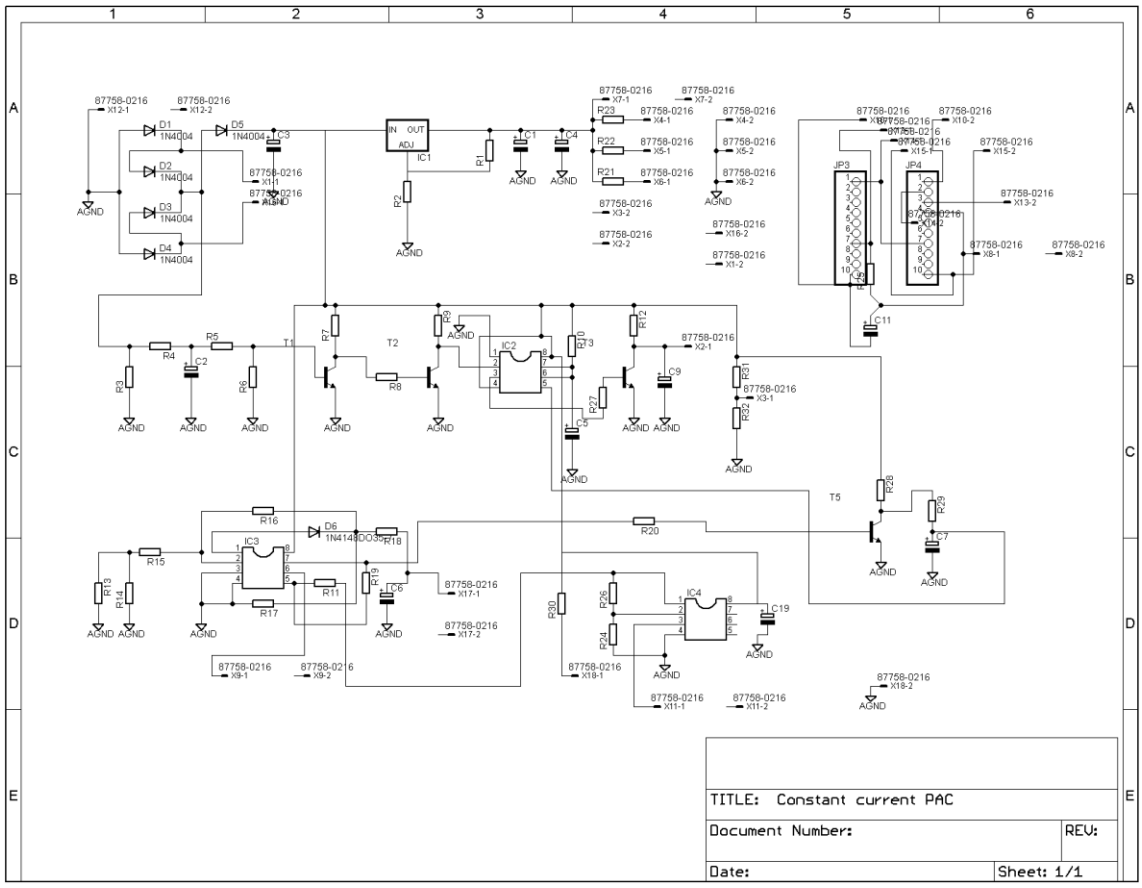

Figure II.2: Constant current PAC circuit

Appendix II. Search software

Branching Algorithm

This algorithm was developed specifically to allow an inexpensive microcontroller to curve fit, matching a canonical model to thermal response.

$$\overbrace{\begin{bmatrix} \frac{(d^2T_{zone})}{dt} \\ \frac{dT_{zone}}{dt} \end{bmatrix}}^{\dot{x}_{canonical}} = \overbrace{\begin{bmatrix} A_{c11} & A_{c12} \\ 1 & 0 \end{bmatrix}}^{A_{canonical}} \overbrace{\begin{bmatrix} \frac{(dT_{zone})}{dt} \\ T_{zone} \end{bmatrix}}^{x_{canonical}} + \overbrace{\begin{bmatrix} B_{c11} \\ 0 \end{bmatrix}}^{B_{canonical}} \begin{bmatrix} P_{input} \end{bmatrix} \quad (1)$$

Considering (1) the constants A_{c11} and A_{c12} are set to -0.01 and B_{c11} is set to 0.01 and the model is converted to discrete time using a zero order hold operation. The thermal zone is now simulated using A (state matrix), B (input matrix) and the recorded normalised heat input setting the value of values of the input vector (u). The error^2 between simulated output and recorded normalised ambient temperature at each point is recorded and cumulatively summed. At the end of the simulation, the A matrix constants are decremented so every combination between -0.01 and -1 are trialled. The constant B_{c11} is simultaneously incremented so every combination between 0.01 and 1 is trialled. The simulation is now recommenced. This process is repeated until all combinations are exhausted and the constants offering the lowest cumulative error^2 are selected. At this point a decision is made (or where the algorithm *branches*). If one of the constants offering the lowest cumulative error^2 is at an upper or lower bound (-0.01 or -1 for matrix A and 0.01 or 1 for B matrix), the bounds of search for that particular constant are incremented by a factor of a 100 and the search is recommenced. This process is repeated until both A and B matrices have constants between their bounds of search.

This method can quickly be expanded to become an n^{th} order search method by gradually expanding the model order as shown in (2). Fig. II.1 provides a pictorial explanation of the operation of the branching algorithm and how the model is expanded to incorporate parameter matching up to 5th order.

$$\begin{bmatrix} \frac{(d^{n}T_{zone})}{dt} \\ . \\ . \\ . \\ \frac{dT_{zone}}{dt} \end{bmatrix} = \begin{bmatrix} A_{c11} & . & . & . & A_{c1n} \\ 1 & . & . & . & 0 \\ 0 & 1 & . & . & 0 \\ 0 & . & 1 & . & 0 \\ 0 & . & . & 1 & 0 \end{bmatrix} \begin{bmatrix} \frac{(d^{(n-1)}T_{zone})}{dt} \\ . \\ . \\ . \\ T_{zone} \end{bmatrix} + \begin{bmatrix} B_{c11} \\ 0 \\ 0 \\ 0 \\ 0 \end{bmatrix} \begin{bmatrix} P_{input} \end{bmatrix} \qquad (2)$$

Due to the daily updating of each heating period model, the system only requires a maximum of 48 hours from once the controller is activated to have models suitable for the MPC formulation. The flow chart representation is shown in figure II.1.

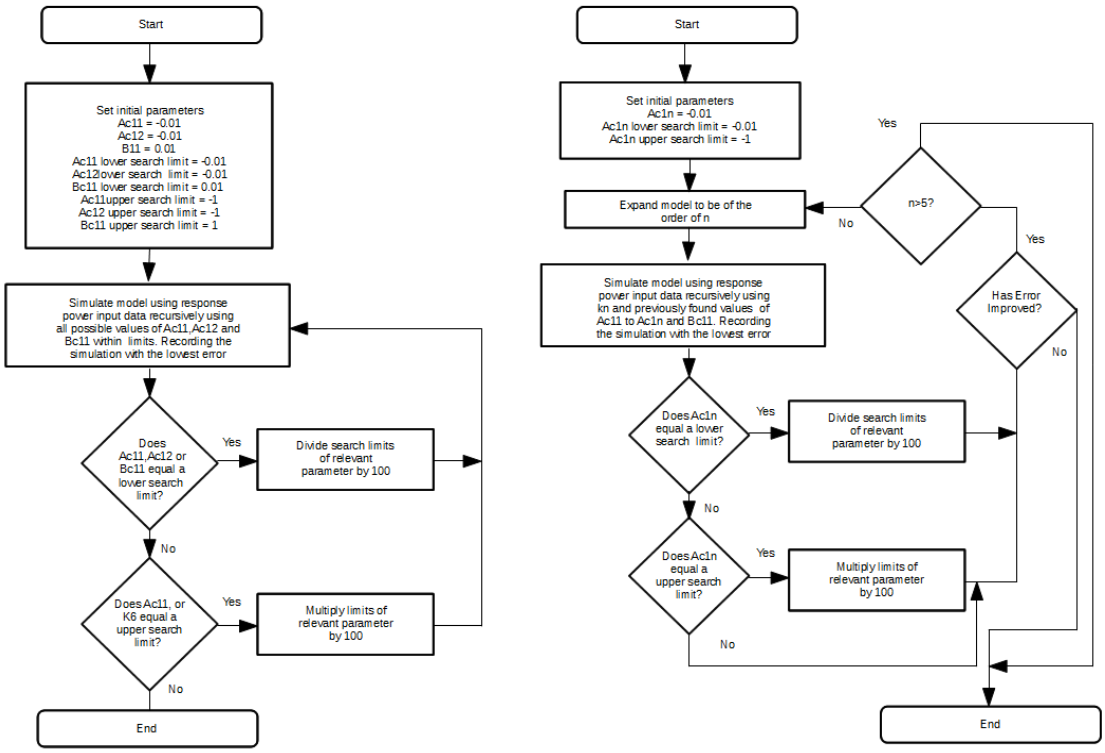

Figure II.1: Branching algorithm

Pyranometer parameter matching algorithm

This was a simplified version of the branching algorithm and employed to find equivalent circuit values to enable the calibration of the Low Cost Pyranometer (LCP).

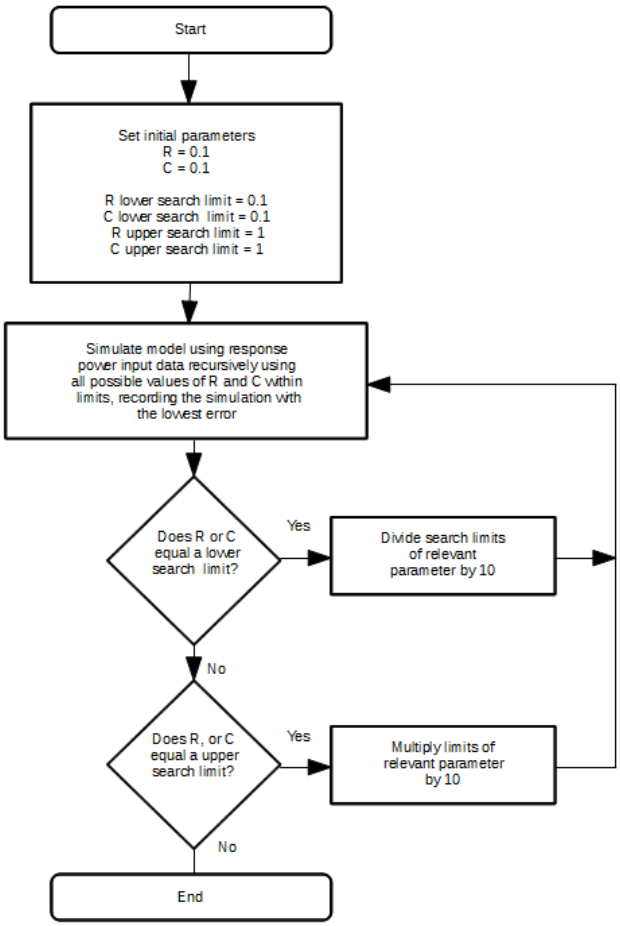

Figure II.2: Modified branching algorithm